Analytical study of methods to reduce excavation-induced movements

Aryani, Febrina

2011

Aryani, F. (2011). Analytical Study of Methods to Reduce Excavation-Induced Movements. Final year project report, Nanyang Technological University.

https://hdl.handle.net/10356/79671

ANALYTICAL STUDY OF METHODS TO REDUCE EXCAVATION-INDUCED MOVEMENTS

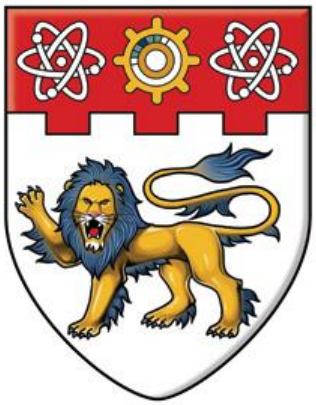

NANYANG TECHNOLOGICAL UNIVERSITY

Febrina Aryani

SCHOOL OF CIVIL AND ENVIRONMENTAL ENGINEERING

COLLEGE OF ENGINEERING

NANYANG TECHNOLOGICAL UNIVERSITY

2011

ANALYTICAL STUDY OF METHODS TO REDUCE EXCAVATION-INDUCED MOVEMENTS

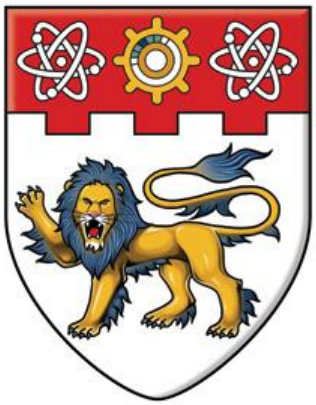

NANYANG TECHNOLOGICAL UNIVERSITY

Submitted by:

Febrina Aryani

School of Civil and Environmental Engineering

College of Engineering

Nanyang Technological University

A Final Year Project presented to the Nanyang Technological University in partial fulfillment of the requirements for the Degree of Bachelor of Engineering

2011

ABSTRACT

In this project, both two-dimensional and three-dimensional analyses were carried out using the finite element method to evaluate the performance of braced excavation systems in soft clay deposit. Wall systems of different stiffness were considered. Plane Strain Ratio (PSR) is used to compare the two-dimensional wall movement with the three-dimensional wall movement. The results show that plane strain analyses give slightly more conservative estimates of wall movement as compared to three-dimensional analyses. As the excavation length is more than four times the width of the excavation, the PSR is close to unity.

In situations where the wall movements are excessive, improvement methods are commonly used to further reduce the wall movements. In this report, two improvement methods are analyzed, namely jet grouting and cross wall system. Several arrangements of the improvement methods are modeled using PLAXIS 3D Foundation software. Eighteen three-dimensional models with varied wall stiffness are considered to find out the optimal improvement method to reduce the wall movement and the maximum strut forces.

Comparisons of the wall movements and strut forces from jet grouting and cross walls methods indicate that both improvement methods are effective in reducing both the wall movement and the strut forces. Jet grouting is observed to be more effective in the cases of low stiffness wall systems, while cross wall method is more effective for the higher stiffness wall systems. Wall-type jet grouting gives better performance than block-type jet grouting. Block-type jet grouting requires a very large improvement area to be effective and thus is not as economical. Cross walls should be installed at the right positions to restrain the wall movement effectively, i.e. around the area where the maximum wall movement is anticipated.

ACKNOWLEDGEMENT

First, The Author would like to send her gratitude to her FYP supervisor at **Nanyang Technological University, Assoc. Prof. Anthony Goh Teck Chee** for supervising her work throughout the year and helping her on the work progress. His great help and comments have led The Author to understand the topic better.

Second, The Author would like to thank **the staffs of CADD Lab II and CADD Lab IV** for making necessary arrangements for The Author to work on the FYP.

And lastly, The Author would also like to thank **her mother and father** for their supports and care during the completion of the report; to **Andri Soenoyo** for the moral support given to The Author; and to **all fellow friends** who have helped The Author in various ways.

The Author hopes that this report may be found useful and comprehensive for those who read it.

TABLE OF CONTENT

LIST OF TABLES

LIST OF FIGURES

Chapter 1

Chapter 2

Chapter 3

Chapter 4

LIST OF SYMBOLS

A (m^2)	Area
B (m)	Excavation width
c_u (kPa)	Undrained shear strength of soil
d (m)	Distance away from the excavation
E (kPa)	Young's Modulus
G (kPa)	Shear Modulus
H (m)	Depth of excavation
h_{avg} (m)	average vertical spacing of struts
I ($kg.m^2$)	Moment of inertia
I_r	Improvement ratio
K	Earth pressure coefficient
K_a	Active earth pressure coefficient
K_o	At rest earth pressure coefficient
L	Length of excavation
m	Parameter index
P (kN)	Strut force
P_c	Property of untreated soil
P_g	Property of jet grout
T (m)	Depth of hard stratum from the bottom of the excavation
z (m)	Depth below the ground level

q_u	Shear strength of jet grout
S_{eq}	Equivalent shear strength of jet grout-soil mix
S_u	Shear strength of untreated soil
γ (kN/m^3)	Unit weight of soil
δ (m)	Total deflection
δ_{max} (m)	Maximum deflection
σ_a (kPa)	Active earth pressure
σ_o (kPa)	Initial earth pressure
σ_{hp} (kPa)	Additional earth pressure
φ (degree)	Friction angle
ν	Poisson's ratio

CHAPTER 1

INTRODUCTION

1.1 Background

Nowadays, due to the limitation of land in urban environment, excavation is common to be carried out in order to create an underground space. Retaining walls are installed prior to the excavation in order to provide the earth support system and to control the ground movement during the excavation process. Some analyses using Finite Element Software are usually conducted to simulate the excavation procedures. One of the most widely used software is PLAXIS.

Two-dimensional and three-dimensional finite element software are available in the market, but excavations are usually modeled in plane strain condition, i.e. the wall is assumed to be infinitely long. However, depending on the excavation geometry, plane strain and three-dimensional analyses may not yield the same reliable result. According to Finno et. al. (2007), larger ground movements occur towards the middle of the excavation and smaller ground movements near the corner are observed in three-dimensional analyses due to the corner stiffening effect. Hence, comparisons are required to decide under what conditions the two-dimensional analyses would yield the realistic results given that most excavations have a three-dimensional geometry.

The stability of braced excavation relies on lateral supports from struts, internal bracings, or tieback anchors rather than its passive resistance. The presence of struts at certain direction may reduce the flexural stresses in the wall as well as the lateral movements. However, the reduction in wall movement provided by braced excavation may not be enough to satisfy the serviceability requirement. In this case, more advanced construction methods need to be carried out to reduce the excavation-induced movements further.

Some common methods to limit the ground movement include the use of jet grouting, cross walls, buttress walls, and berms. In this project, two methods namely jet grouting and cross walls will be analyzed and the comparisons will be carried out in terms of the reduction to the wall movement and the strut forces before and after the application of the improvement methods.

1.2 Objectives

This project involves the use of PLAXIS 2D and PLAXIS 3D finite element software. The objectives of this project are as follows:

- to compare the results of three-dimensional analysis and conventional plane strain analysis
- to analyze and compare the effectiveness of different improvement methods, i.e. jet grouting and cross wall, to reduce the excavation induced-movement for different wall stiffness systems
- to analyze and compare the strut forces from jet grouting and cross walls method for different wall stiffness systems

1.3 Scope of Work

The scope of work includes modeling of several cases of excavation using PLAXIS 2D and PLAXIS 3D. The soil conditions and the dimensions of excavation are kept unchanged, whilst the wall stiffness and additional methods to reduce wall movement are to be varied.

The excavation is 84m long, 20m wide, and 16m deep. The soil comprises of 32m soft clay layer and a 20m stiff clay layer. The wall is embedded 1m into the stiff clay layer. Five level-struts at 3m vertical spacing and 4m horizontal spacing are to be installed using a conventional excavation construction method. The details of the excavation dimension are shown in Figure 1.1(a) and Figure 1.1(b).

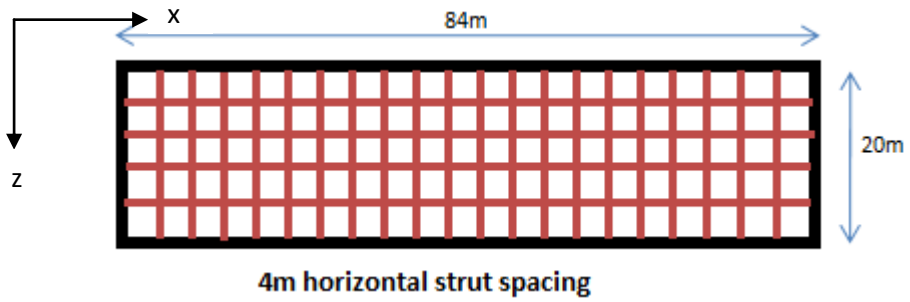

1.1.(a)

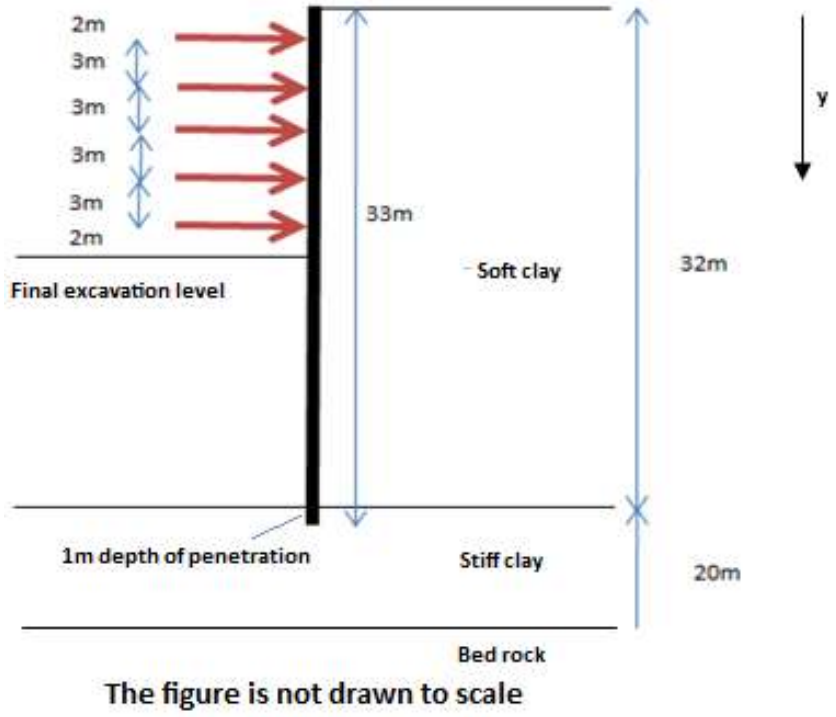

1.1. (b)

Figure 1.1 Dimensions of the Excavation in: (a) x-z plane and (b) z-y plane

Six cases are to be set up, i.e. excavation without any improvement method, excavation with wall type jet grouting, excavation with block type jet grouting, excavation with two cross walls, excavation with four cross walls, and excavation with six cross walls. In each sub-case, three models with different wall stiffness are set up. Two-dimensional analyses are also performed for comparison. The wall movements and strut forces for all the cases are then compared and analyzed.

1.4 Organization

This report is divided into 5 chapters:

- Chapter 1 highlights the background, objectives, and scopes of the project.
- Chapter 2 provides literature review of braced excavation system, including the earth pressure, strut forces, and induced wall movement, as well as the review of jet grouting and cross wall methods in reducing wall movement.

- Chapter 3 provides the methodology and assumed parameters in the braced excavation models analyzed using PLAXIS 2D and PLAXIS 3D Foundation.

- Chapter IV presents the results from two-dimensional and three-dimensional finite element study. Comparisons of the effectiveness of various methods of jet grouting and cross wall in reducing the excavation induced wall movements are also considered.

- Chapter V summarizes the project results presented in the preceding chapters and gives recommendations for future projects.

CHAPTER 2

LITERATURE REVIEW

2.1 Earth Pressure Distribution on Braced Excavation

Braced excavation relies on the passive resistance of the soil in front of the wall, as well as the additional lateral supports provided by a series of struts, as shown in Figure 2.1. The struts are connected to both sides of the excavation. The load is transferred from the strut to vertical beam, which is called a waler, before being transferred further to the embedded retaining wall and then to the soil.

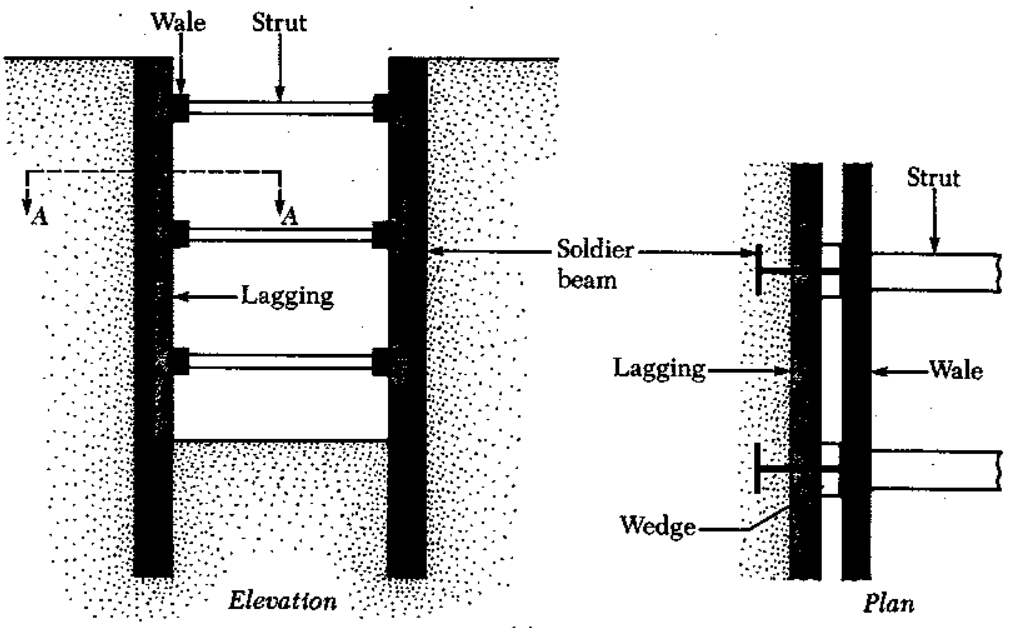

Figure 2.1: Braced Excavation Elevation View (Das, 2007)

After the retaining walls are installed, a series of soil excavation and strutting are conducted. When the open cut is made, the wall moves towards the excavation due to the pressure exerted by the soil behind the wall. Installation of the struts and walers right after the excavation prevents the wall from yielding further and pushes the wall back towards the retained soil. The strutting system exerts a lateral pressure that is larger than the active value. However, the wall is still not able to move back to its original position. Hence, the stress condition is neither at rest nor active state.

The earth pressure distribution for braced excavation cannot be predicted using Rankine's or Coulomb's theory, where the earth pressure increasing linearly from the soil surface. For the braced excavation, the wall is rotating about the top of the excavation, thus the earth pressure is somewhat parabolic and the point of application of the thrust will act at height of n_aH above the bottom of the wall. This difference is due to the arching effect, preloading, and incremental excavation and strut installation. Figure 2.2(a) shows a typical comparison between at rest earth pressure, active earth pressure, and the earth pressure in braced excavation. The earth pressure in braced excavation is not at at-rest, neither active condition, and is parabolic in shape. Figure 2.2(b) demonstrates the non-hydrostatic earth pressure distribution behind braced wall based on the laboratory experiments by Sherif and Fang (1984).

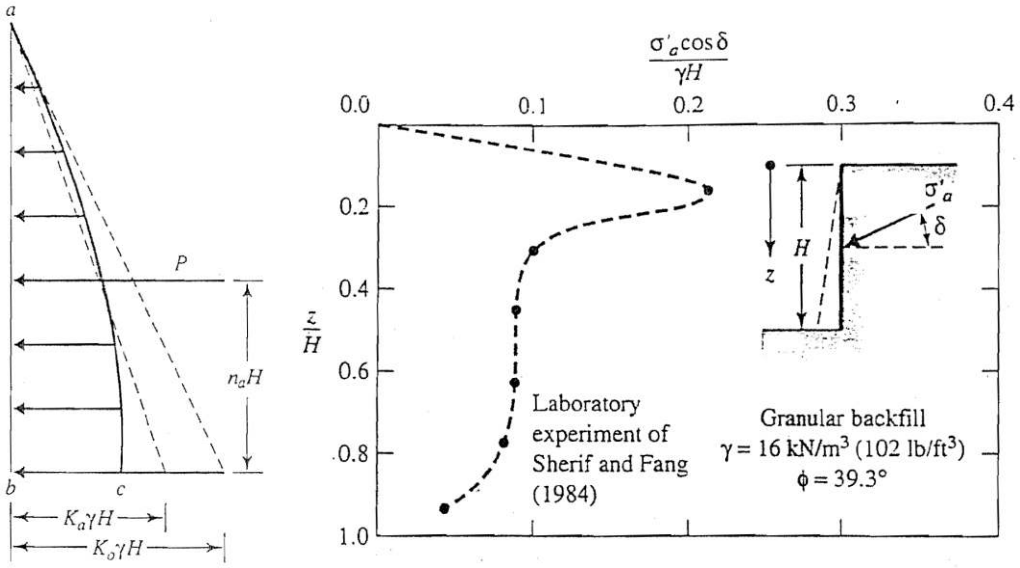

Figure 2.2(a): Earth Pressure in Braced Excavation (Das, 1999); Figure 2.2(b): Field Measurement of Earth Pressure in Braced Excavation (Sherif and Fang, 1984)

Peck (1943) and later Terzaghi and Peck (1996, 3rd ed.) proposed an empirical method to calculate the pressure distribution behind a braced excavation. A term of apparent pressure diagram was introduced, i.e. the pressure envelope of the maximum pressures that were found empirically during various projects. The struts were assumed to be hinged at each strut level.

Tschebotarioff et. al. (1973) modified the Peck pressure diagram for certain combinations of $c_u/\gamma H$ of clay since Peck's method could produce K_a=0 which was not realistic. Figure 2.3 shows the summary of Peck and Tscebotarioff's apparent pressure diagram for braced excavation.

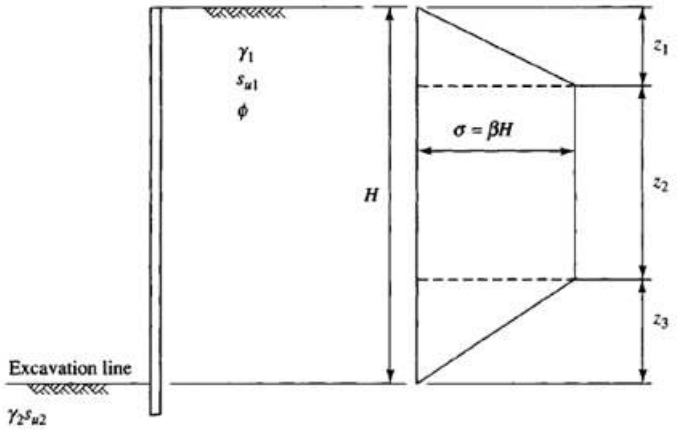

Soil Type	Author	z_1	z_2	z_3	β
Sand	P	0	1.0	0	$0.65_\lambda K_a$
Sand	T	0.	0.7	0.2	0.25_λ
Soft-to-Medium Clay	P	0.25	0.75	0	λK_{ap}*
Temp. Support Medium Clay	T	0.6	0	0.4	0.3λ
Stiff fissured Clay	P	0.25	0.50	0.25	K_{ap}†
Perm. Support Medium Clay	T	0.75	0	0.25	0.375λ

* K_{ap} = 0.4 to 1.0
† K_{ap} = 0.2 to 0.4
Source: P = Peck (1969); T = Tschebotarioff (1973).

Figure 2.3: Peck (1967) and Tschebotharioff (1973) Apparent Pressure Diagrams (Bowles, 1996)

Peck introduced a term, called stability number $\gamma H/c_{u,}$ where γ and c_u are the unit weight and undrained shear strength of the soil adjacent to the excavation. The case of soft-to-medium clay is applicable when the stability number exceeds 4, and a plastic zone is expected to develop near the bottom of the excavation. When the stability number is less than 4 and the clay is strong enough to resist the load transferred from the structure, most of the soil is in the elastic zone and the case of stiff clay is applicable. On the other hand, when the stability number is greater than 6 or 7, extensive plastic zone is developed thus producing a large ground movements.

Figure 2.4(a) shows the apparent pressure distribution for soft-to-medium clay. The pressures are usually ranged from $0.3\gamma H$ to $0.5\gamma H$ with an average of $0.39\ \gamma H$; at one cut the exceptionally high value of $0.59\ \gamma H$ was found (Terzhagi, Peck, and Mesri, 1996). The pressure coefficient, K, and the pressure, σ_a, can be obtained by these equations below,

$$K = 1 - \frac{4ms_u}{\gamma H}$$

$$\text{with } m = 0.4 \text{ to } 1 \text{ and } \sigma_a = \gamma KH \qquad \textbf{(2.1)}$$

Figure 2.4(b) shows the apparent pressure distribution in stiff clay which is trapezoidal in shape. The value of pressure σ_a can be obtained by this equation below,

$$\sigma_a = 0.2\gamma H \text{ to } 0.4\ \gamma H \qquad \textbf{(2.2)}$$

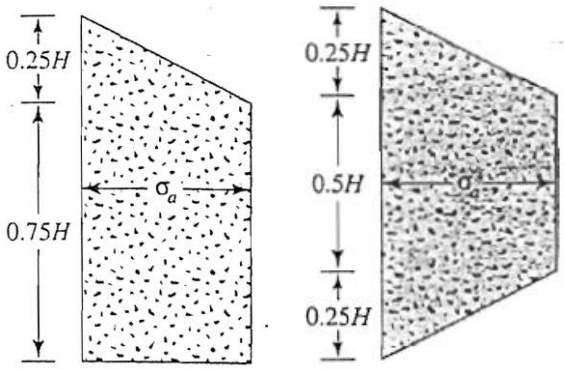

2.4(a) 2.4 (b)

Figure 2.4(a): Peck's APD for Soft Clay; Figure 2.4(b): Peck's APD for Stiff Clay

Twine and Roscoe (1999) proposed another empirical method to estimate the pressure distribution behind the wall based on 60 cases of flexible wall and 21 cases if stiff wall. The excavation depth ranged from 4m to 27m in several soil conditions, i.e. soft and firm clays, stiff and very stiff clays, and coarse grained soils. This approach takes account of the wall stiffness. Figure 2.5(a) and 2.5(b) shows the pressure diagram by Twine and Roscoe in clayey soil.

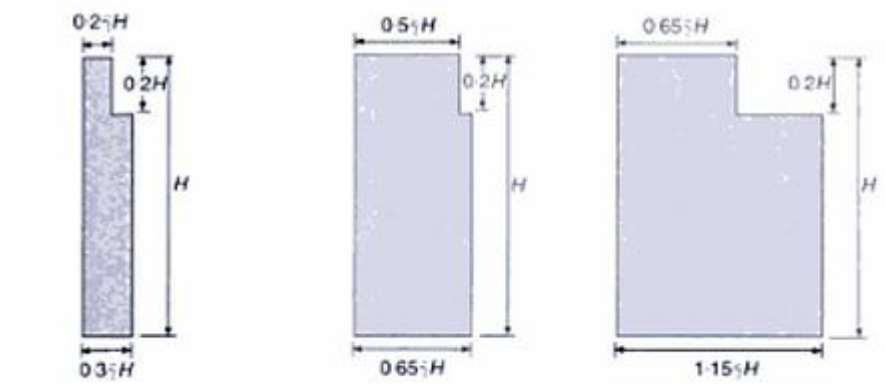

2.5 (a) Normally and slightly overconsolidated clay (soft to firm clay)

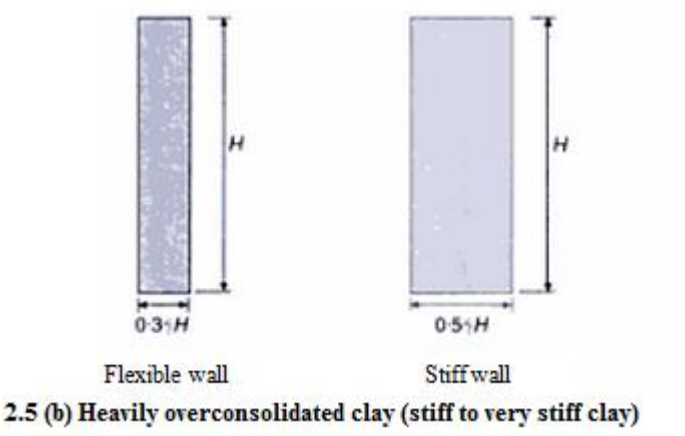

Figure 2.5: Twine and Roscoe's (1999) Earth Pressure Distribution in Clay Layer

Since the Apparent Pressure Diagram was established some time ago, when the excavation dimensions and depth were relatively smaller as compared to the cases nowadays, the reliability of apparent pressure diagram is questionable. It is suggested that the method is still useful for excavation depths not exceeding 10m, while more studies are needed for excavation depth exceeding 20 m. Moreover, Apparent Pressure Diagram concentrated on the cases of flexible wall, which were popular at that time. Nowadays, higher stiffness wall systems are being used. Thus, more study and examination are needed in using the Apparent Pressure Diagram.

2.2 Estimation of Strut Forces in Braced Excavation

The struts in braced excavation are placed horizontally to resist the earth pressure on the back of the wall by providing compression forces. I-section or circular hollow sections are usually utilized.

The distribution of pressures against the wall cannot be accurately predicted from theory. Thus, various field measurements were taken and the envelope of probable distributions was drawn through Apparent Pressure Diagram. The Apparent Pressure Diagram is actually the earth pressure diagram derived empirically from the strut load rather than from the earth pressure. Peck (1969) stated that apparent pressure diagram were not intended to represent the real distribution of the earth pressure, but instead, consisted of hypothetical pressures from which the strut loads could be calculated. The calculated strut loads might be approached but would not be exceeded in the actual cut. Thus, it can be concluded that only the strut forces can be obtained effectively from the Apparent Pressure Diagram by assuming the wall as a simply supported beam.

The strut force is calculated by assuming the load in each strut to be equal the total earth pressure acting on the sheeting over a rectangular area extending horizontally half the distance to the next vertical row of struts on each side, and vertically half the distance to the horizontal sets of struts immediately above and below (Terzhagi, Peck, and Mesri, 1996) as shown in Figure 2.6. This method is called the Tributary Area Method. It doesn't take account the effects of toe extending below the excavation level. This approach usually leads to a conservative design.

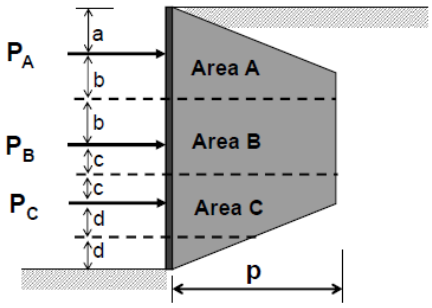

Figure 2.6: Strut Force Calculation Using Tributary Area Method

Another method to calculate the strut forces from the Apparent Pressure Diagram is using Simple Beam Method. The retaining wall is considered as a continuous beam. The strut forces are calculated by dividing the beam into several simply supported beams with the struts acting as the supports. Figure 2.7 describes Simple Beam Method. Simple equilibrium calculation is then used to obtain each strut force. However, these two methods yield slightly different results.

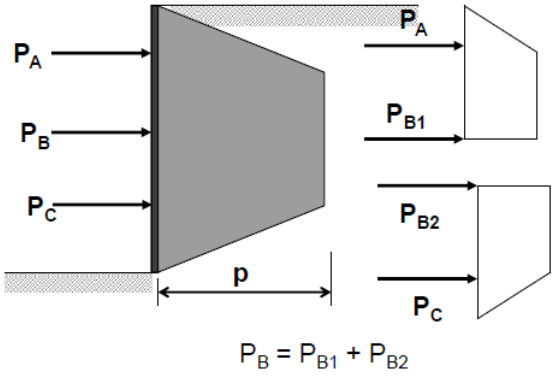

Figure 2.7: Strut Force Calculation Using Simple Beam Method

Lambe et al. (1970) and Golder et al. (1970) verified that Peck's Apparent Pressure Diagram might overestimate the strut force in normally consolidated soils up to 50% greater than the actual measured loads. However, different soil conditions may lead the error to be on the unsafe side.

The Distributed Propped Load (DPL) Method proposed by Twine and Roscoe (1999) is adopted by CIRIA to calculate the strut forces. Figure 2.5 and Figure 2.8 describe the Distributed Propped Load Method. Both Tributary Area and Simple Beam Method may be used to calculate the strut forces. This method is an update of Peck's Apparent Pressure Diagram, which doesn't consider the stiffness of the wall. It is stated that the strut forces calculated using this method provide conservative estimation to be expected in the field of normal circumstances.

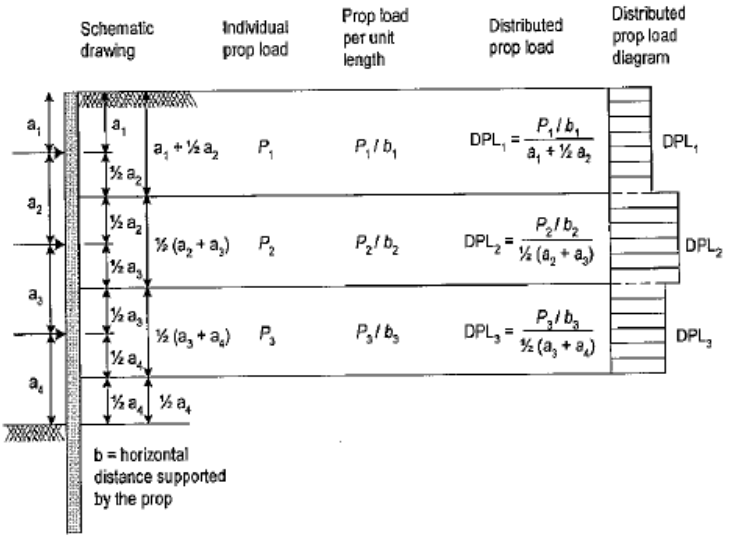

Figure 2.8: Example of Strut Force Calculation by DPL Method using Tributary Area Method (CIRIA C580)

The structural design of the struts complying with the Design Code is based on the calculation of the strut forces. However, the soil-structure interaction is not included in the empirical formula although it may model the stress redistribution more realistically. Moreover, although Apparent Pressure Diagram and Distributed Prop Load Method represent the envelopes of the strut forces throughout the entire excavation stages, the staged construction needs to be simulated in order to achieve more effective and economical design.

The maximum strut force for each strut is achieved in different excavation stages, which is difficult to assess without any finite element analyses. The maximum strut load is expected to occur close to the centre of the excavation because of the behavior of three-dimensional nature of the wall movement. This is discussed in Section 4.2, Figure 4.2.

2.3 Excavation-Induced Movement of Braced Excavation

Due to the pressure acting behind the retaining wall system for deep excavation, the wall experiences a movement towards the excavation. During the first stage of excavation, the wall acts like a cantilever wall, i.e. the free end moves towards the excavated soil side. As the construction proceeds on, the struts provide supports to the wall and hence produce less movement near the top and bottom and greater movement at the mid-depth of the wall. As the excavation proceeds, the wall movement increases with smaller movement at the strut level. The maximum value is observed at the last stage of the excavation. Figure 2.9 shows the development of wall movement due to stage-by-stage excavation.

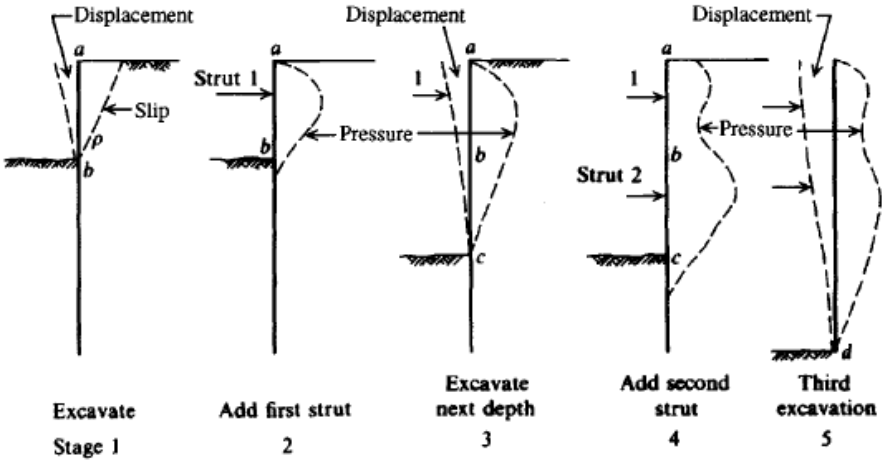

Figure 2.9: Development of Wall Movement in Braced Excavation (Bowles, 1999)

The soil behind the wall moves together with the retaining wall and causes the movement in the vertical direction, i.e. settlement. This settlement increases with the increase of the wall movement, and it can affect structures in proximity. Thus, the term of allowable wall deflection is introduced. In Singapore, the wall deflection is typically limited to 0.5%H or 100mm, whichever is less.

Mana and Clough (1981) showed that there was a strong correlation between wall deflection and the potential for basal heave as proposed by Terzaghi (1943). Clough and O'Rourke (1990) expanded the study by proposing a semi-empirical chart to estimate the wall deflection. The wall movements depend on the wall stiffness ($EI/\gamma h_{avg}^4$), depth of excavation (H), and factor of safety against the basal heave (F.S.). The higher the wall stiffness and the higher the value of factor of safety adopted, the smaller wall deflection is observed, as shown in Figure 2.10.

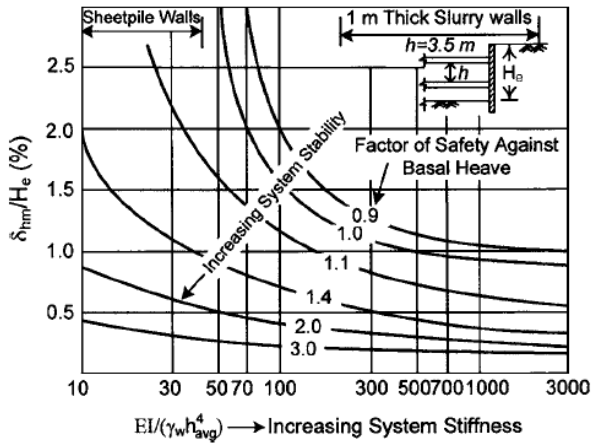

Figure 2.10: Wall Stiffness vs Wall Deflection Chart (Clough and O'Rourke, 1989)

Wong and Broms (1989) stated that the wall deflection tends to increase with the increase of the ratio of depth of the hard stratum from the bottom of the excavation to the excavation width, T/B. The lateral displacement is governed by the yielding of soil below the final excavation level, up to a depth of B/2. The wall movement is not that significant when the hard stratum is in a great depth below the critical zone, as shown in Figure 2.11.

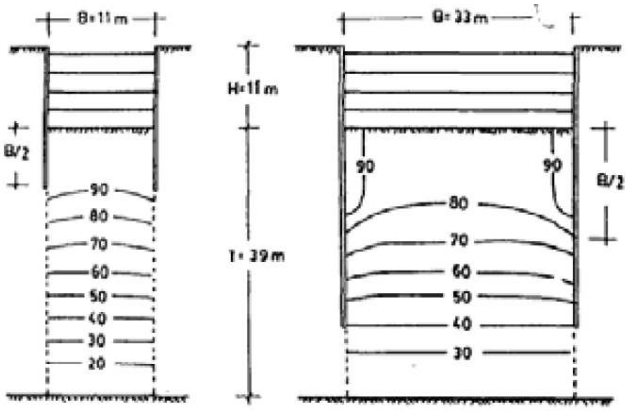

Figure 2.11: Lateral Displacement of Different Types of Soil (Wong and Broms, 1989)

It was also observed that the higher the stiffness of soil, the less excavation-induced movement is produced (Burland (1989), Atkinson (1993), Whittle et al. (1993), Hight and Higgins (1995)). Peck (1969) has also summarized a curve that showed the smaller wall movements and ground settlements in stiffer soils, as seen in Figure 2.12. A work of Tomlinson (1980) stated that the wall movement is approximately in the order of 0.25% of the excavation depth in soft clay and 0.05% in the granular soil or stiff clay.

Clough and O'Rourke (1990) found that the wider the excavation width was, the larger wall deformation was observed. On the other hand, Hashash and Whittle (1996) pointed out that the

wall deflection is nearly independent to the wall length in the case of no constraint on the toe movement.

Strutting system also plays a part in controlling the excavation induced movement. If the stiffness of the strut is low, the compression of the strut might be quite large, thereby resulting in wall movements similar to that of cantilever wall. On the other hand, smaller strut compression occurs with higher strut stiffness. Hence, smaller soil movements are observed. The stiffness of the strut can be increased by reducing the vertical strut spacing. However, the strut stiffness may be increased up to a certain extent only. Very high strut stiffness is less effective in the design and construction process.

Although Finite Element Analyses can predict both lateral wall movement and vertical ground settlement, the prediction of the latter is usually not that accurate due to the limitations in characterizing the exact soil behavior behind the wall. Some empirical and semi-empirical methods have been proposed to estimate the ground settlement based on the wall deflection, as described in this section.

There are two types of ground settlement profiles introduced, namely spandrel type and concave type. The magnitude and shape of the retaining wall deformation are responsible for the formation of these two settlement profiles.

Peck (1969) has proposed a non-dimensional curve to predict the surface settlement, as shown in Figure 2.12, based on the field measurements of wall movements and ground settlements of sheet pile and soldier pile wall. According to the curve, the surface settlement extends laterally to the distances three or four times the excavated depth H, for very soft to soft clays. The maximum value is observed to be greater than 0.2H at locations close to the wall. However, as the chart was developed based on low stiffness walls, the chart is not appropriate for stiffer wall systems. Hence, other approaches may be more accurate.

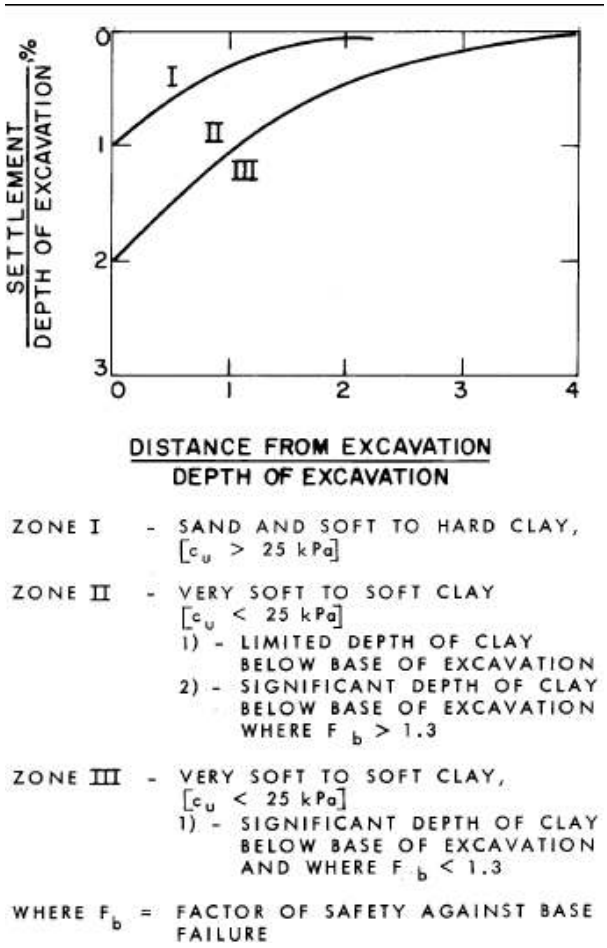

Figure 2.12: Peck's Surface Settlement Prediction Diagram (Raymond, 1997)

Settlement data for excavations supported by soldier piles and laggings in dense sand and interbedded clay were published by O'Rourke et al. (1976). It was shown that the maximum settlement might be up to 0.3% of the excavation and extends up to two times the excavation depth horizontally, as shown in Figure 2.13.

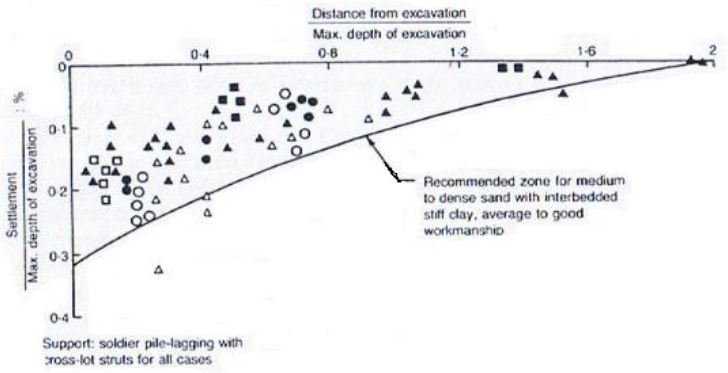

Figure 2.13: Ground Settlement Prediction Diagram (O'Rourke et al., 1976)

Clough and O'Rourke (1990) proposed a semi-empirical design chart to estimate the settlement profile for different soil type. The maximum horizontal and vertical ground movements behind the wall are typically less than 0.5% of the excavation depth. The affected zones vary from two to three times excavation depth and the ground settlement profiles may be triangular or trapezoidal, according to the soil type, as shown in Figure 2.14.

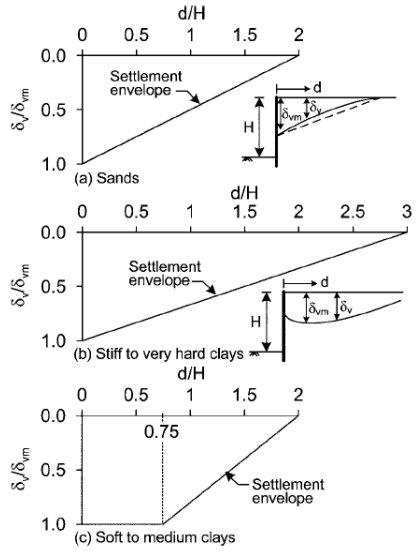

Figure 2.14: Settlement Profile Design Chart (Clough and O'Rourke, 1990)

Hsieh and Ou (1998) proposed another procedure to estimate the ground movement due to the excavation. The settlement profile is divided into primary and secondary influence zone. Figure 2.15 shows the concave settlement profile proposed by Hsieh and Ou. It was suggested that the vertical settlement, δ_v, could be predicted based on the lateral wall deflection, δ_h, in the equation of $\delta_v = R\ \delta_h$, in which R = deformation ratio = 0.5 to 1.0.

Very close to the wall, the ground settlement is not zero, but not maximum, unlike the maximum ground settlement near the wall in the spandrel profile. This is due to the contribution of wall installation process. At the distance of 0.5H away from the wall, the maximum settlement occurs before it linearly decreases to a certain value at the edge of primary influence zone, i.e. at the distance of 2H away from the wall. The settlement profile decreases further to zero at the edge of secondary influence zone.

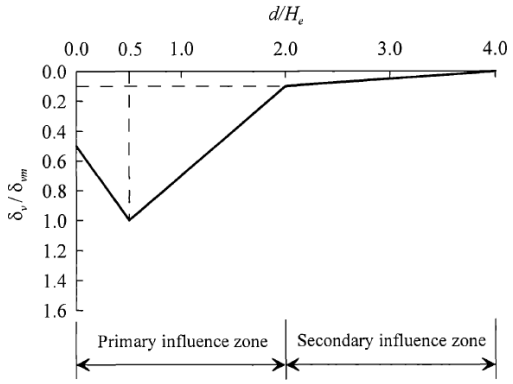

Figure 2.15: Concave Settlement Profile (Hsieh and Ou, 1998)

The accuracy of this method depends heavily on the accuracy of the lateral wall deflection obtained by other methods, e.g. Finite Element Analysis. Although more improved methods are introduced, Hsieh and Ou's method is one of the most widely used methods in estimating the settlement profile.

Based on a series of comparisons done by Ou et. al. (2000), it was concluded that Peck's method overestimated the settlement, while Clough and O'Rourke's method did not perform well. On the other hand, Hsieh and Ou's method gave results that were in line with the field measurements. Figure 2.16 shows the comparison of field measurement and prediction of ground movement in deep excavation using different methods in three cases. The first case was the excavation of TNEC (Taipei National Enterprise Centre), while the second and third cases were the excavation for buildings.

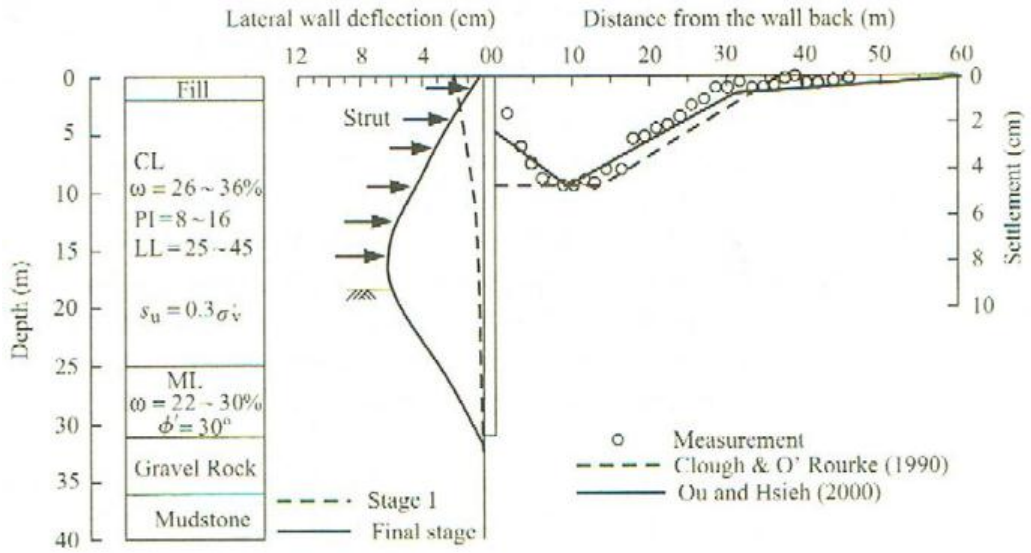

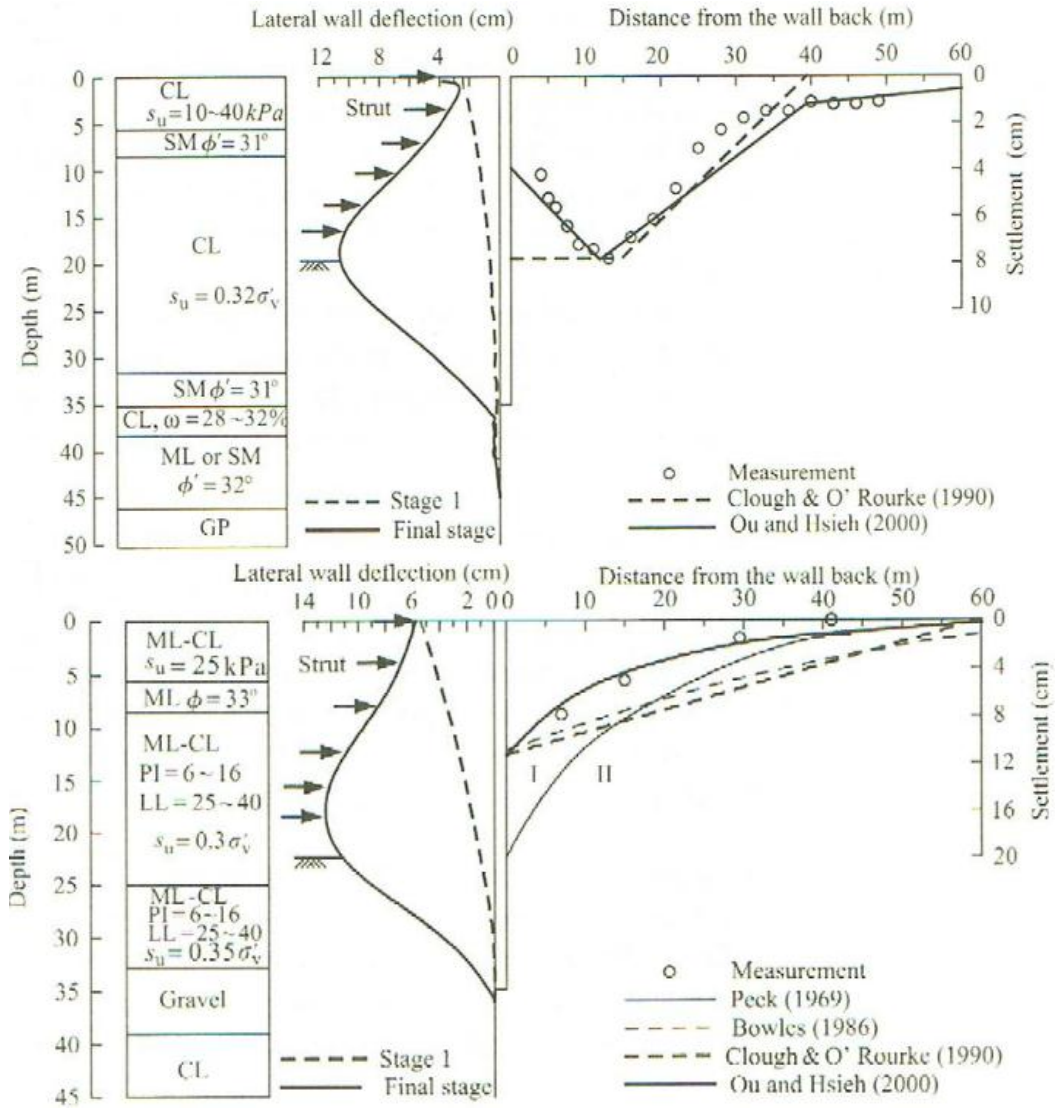

Figure 2.16: Comparison on Ground Settlement Predictions Using Several Methods in TNEC (Ou et. al., 2000)

2.4 Finite Element Analyses of Braced Excavation

For a continuous system, such as soil layer, a simple mathematical equation cannot be used to generate a very accurate result. Thus, the continuum needs to be divided into their individual elements. Each element contains nodes with certain degrees of freedom to be solved. Finite Element Method (FEM) models the stress-strain properties of the ground with the boundary conditions to realistically model the site and get accurate representations of the soil elements and within the soil element. FEM2D, SLOPE W/, ABAQUS, SAGE CRISP, and PLAXIS are some of the common software packages.

Two-dimensional and three-dimensional finite element analyses have been developed to model the systems. PLAXIS 2D is more popular than PLAXIS 3D due to its simplicity. PLAXIS 2D models a plane-strain condition where the wall is assumed to be infinitely long, while PLAXIS 3D uses x, y, and z-axis to model the actual construction. In Chapter 4, some three-dimensional finite element analyses are compared with plane strain analyses.

Ou et. Al. (1996) showed that both corrected two-dimensional and three-dimensional analyses gave very close agreement to the field measurements. However, uncorrected two-dimensional analyses yielded different results from what was observed in three-dimensional analyses. It was observed that three-dimensional analysis yielded smaller maximum wall movement in the middle of the retaining wall perpendicular to the wall compared to the plane strain analysis, as well as in the corner of the excavation. Some studies suggested that the difference was caused by corner stiffening effects.

To address the smaller wall movement at the corner of the retaining wall in three-dimensional analysis as compared to two-dimensional analysis, a value of Plane Strain Ratio (PSR) was introduced by Ou et. al. (1996)

$$PSR = \frac{\delta max\ (3D)}{\delta max\ (2D)} \qquad \textbf{(2.3)}$$

PSR can be utilized to define the conditions wherein two-dimensional results are applicable to the actual geometry and develop factors that define the stiffening effects near the corners (Finno et al., 2007).

The difference of two and three-dimensional analyses were shown by the work of Simic and French (1998). A case of an underground station box was modeled using both methods. The results showed that two-dimensional analyses were more conservative. The steel quantity should have been reduced by 25% overall because the walls near the corners were computed to be less heavily loaded.

It was also observed that the difference of the results between two-and three-dimensional analyses is dependent on several factors, such as the strut stiffness and the excavation geometry. (Lee et. al, 1998).

Based on the study conducted by Ou et al. (1996), it was agreed that the movement from three-dimensional analyses with large distance between the wall toe and the hard stratum was smaller and closely related to the field response. For the excavation with rigid layer immediately below

the bottom of excavation, both two-dimensional and three-dimensional results were similar. It was observed that the ratio of length of the wall to the excavation depth (L/H) was the most influential effect to the PSR. Two-dimensional analysis overestimated the movement in the case where the embedded depth is small (small L/H). However, when L/H is larger than 6, PSR corresponded to unity (Finno et al., 2007).

PSR value is dependent on the soil conditions, the type of the walls, and other conditions, such as loading exerted from adjacent structure and the adopted factor of safety against basal heave. Thus, the value of PSR for each case may differ significantly from what Ou has obtained. According to Ou (1996), only 3D analysis can obtain realistic results for excavation cases with soil improvement or property protection measures, such as counterfort wall or cross wall.

2.5 Methods to reduce Excavation-Induced Movement

There are several methods to reduce the wall movement and the ground settlement resulting from excavation, namely cross walls, buttress walls, berms, and jet grouting. However, only two of those methods, i.e. jet grouting and cross wall, will be discussed in this paper.

2.5.1 Jet Grouting

Terashi (2003), stated that the stability of deep excavation and the minimum wall movement could be achieved by increasing the strength of in situ clay through ground improvement. It is constructed in the excavated soil to enhance the passive resistance of the soil, which will directly restrain the wall movement.

The most popular method is jet grouting or deep mixing pile. It involves the mixing of soil or weak rock and cementing agent using a high energy jet of a fluid. A grouting machine is used to push the grouting pipe into the soil. The grouting pipe then emits high pressure grout or water in a high speed. As the result, the soil particles will be separated from the soil body and some particles will flow out of the ground while the remaining will mix with the grout forming grout-soil mixture. This process occurs under the influence of pounding, centrifugal force, and gravity. The grouting pipe is then lifted to shallower depth to repeat the same procedures, as shown in Figure 2.17.

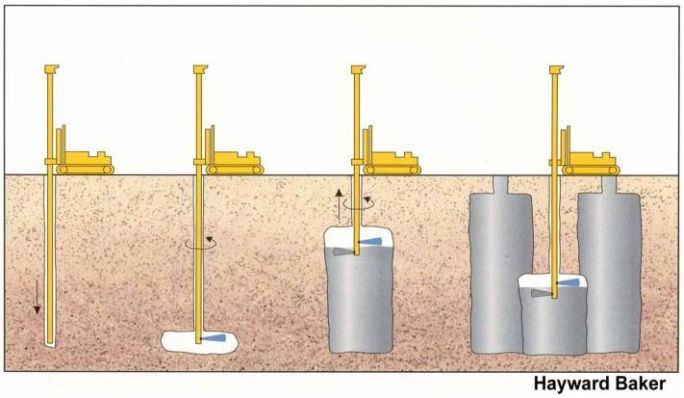

Figure 2.17: Procedures of Jet Grouting Installation

Single tube method, double tube method, and triple tube method are three commonly used methods of jet grouting. In single tube method, a special jet is attached to side of the boring rod bottom to emit high pressurized grout at about 20 MPa into the soil. With the rotation and lift of the rod, the grout and soil body will be mixed and form a column.

On the other hand, a coaxial double jet is attached to the boring rod in double tube method. The inner jet emits high pressurized grout while the outer one pumps compressed air at 0.7 MPa. The objective of introducing air to the soil is to enhance the capability to destroy and cut the soil. As the result, the column formed using this method is larger.

The triple tube method contains a jet which emits water, air, and grout simultaneously. With the additional contribution of high pressurized water, the power of destroying and cutting the soil body is enhanced even more. Smaller pressure of grout is emitted and a larger column is produced. Figure 2.18 shows these three methods.

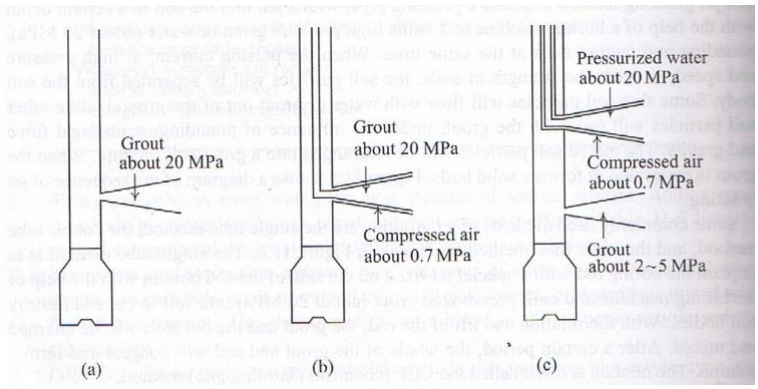

Figure 2.18: Single Tube, Double Tube, and Triple Tube Method in Jet Grouting

Three typical patterns of ground improvement are usually adopted, i.e. block type, column type, and wall type, as shown in Figure 2.19. The side friction and end bearing provides the resistance

for wall type grouting in which the lateral force caused by inward movement acts directly to the improved soil, like a counterfort wall. This pattern of improved soil can only increase the soil strength in front of the wall without raising the moment-resistance stiffness of the wall. On the other hand, in column type improvement, the lateral force acts on the untreated soil which in turn transmits it to the treated soil. The block type grouting has both the advantages of wall and column type, but a large improvement area, as well as a very high cost, is needed (Ou et. al., 1996).

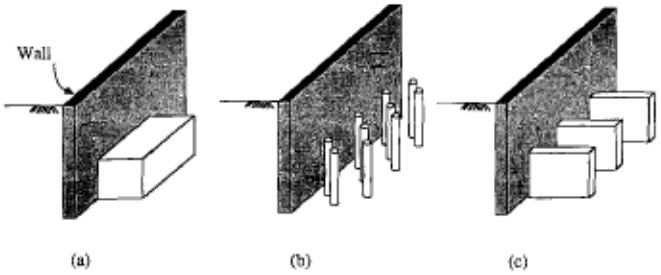

Figure 2.19(a): Block Type Grouting; Figure 2.19(b): Column Type Grouting; Figure 2.19(c): Wall Type Grouting (Ou et. al., 1996)

Hence, it is proposed that the ground improvement should be applied in a region where the ground settlement can be reduced, e.g. at a place where the building is located. According to a study conducted by Ou et. al. (2007) in Song San excavation project in Taipei, the improvement was only required in the central portion of the wall where the corner effects are absent.

The strength of the composite soil may not be easily determined and affected by several factors, i.e. the strength and layout pattern of the treated materials, the improvement ratio, and the stress path due to different loading conditions. In usual practice, an empirical formula by Hsieh et al. (2003) is used to evaluate the composite material properties such as E, Su, c, etc.

$$P_{eq} = P_g I_r^m + P_c(1-I_r^m) \qquad \textbf{(2.4)}$$

where P_g is the property of the grout, P_c is the property of untreated soil, I_r is the improvement ratio which is defined as the ratio of treated soil over the total area, and m is an equivalent parameter index which is determined based on the unconfined compressive strength of the treated soil. The design chart was developed by Ou et al. (1996) and is presented in Figure 2.20. The minimum value of m for block type and wall type is 1 where the lateral force acts directly to both treated and untreated soil. For column type, the value of m may be reduced by multiplying the index with a certain reduction factor.

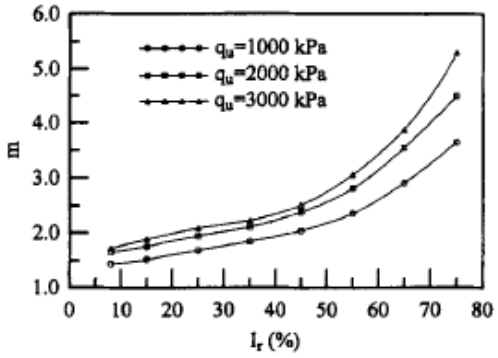

Figure 2.20: Ir vs m Diagram (Ou et al., 1996)

Another similar empirical equation of calculating the shear strength of the treated soil was established by Liao (1991), Hsieh et al. (1995), and Hsieh (2002). A reduction factor α was used instead of the parameter index m. α was determined from a field study and a value of 0.3 was adopted for column type grout while 0.4 was adopted for block and wall type grout.

$$S_{eq} = 0.5\alpha q_u I_r + S_u(1-I_r^m) \quad \textbf{(2.5)}$$

where q_u is the unconfined compression strength of the treated soil and Su is the undrained shear strength of the in-situ clay.

Although there are empirical formulas established to assess the properties of the mixture, the results need to be further verified. The required verification is due to the high anisotropy of the treated clay and may be conducted by numerical modeling. (Liao et. al., 2008)

Buttress type improvement, i.e. wall and block type, is more effective in reducing the excavation-induced wall movement. Other factors that affect the effectiveness of reducing the movement are dimension and strength of the improved soil. However, the increase in improved zone dimensions results in more significant effect rather than the increase in improved soil strength. (Hsieh et. al., 2003)

2.5.2 Cross Wall

Cross wall refers to construction of a wall that connects two retaining walls opposite to each other prior to excavation. It provides additional lateral supports to resist the inward movement of retaining wall during excavation. The construction of cross wall is similar to the construction of the retaining wall, thus this method to reduce the excavation-induced movement is less costly as compared to jet grouting. Figure 2.21 shows the plan and elevation view of cross wall.

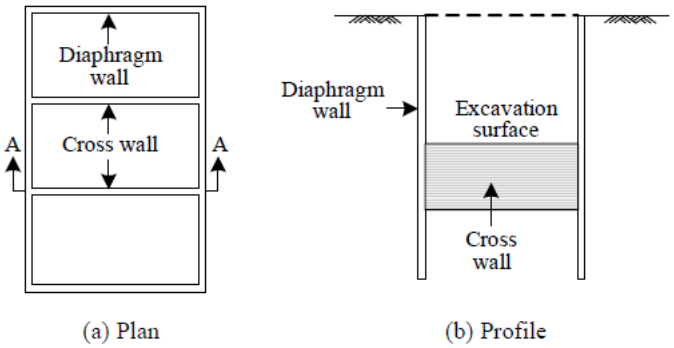

Figure 2.21: Cross Wall View

The cross wall will be removed as the excavation proceeds further, but the one below the final excavation level will remain, in order to minimize the displacement below the excavation level. The cross wall will act as a semi-rigid underground lateral support that exists before the excavation.

The movement near the cross wall will be restrained during excavation and the lateral displacement of retaining walls will decrease (Ou et. al, 2006). The efficiency of cross wall in reducing the ground movement is related to location, spacing, section size, materials, and construction quality.

The joint between the retaining wall and the cross wall should be taken into consideration for the efficacy of the cross wall. There are three types of joint, namely T-type joint, separately constructed/soft contact joint, and partition plate/clean contact joint.

T-type joint ensures rigid connection between retaining wall and cross wall, but it is poor in stability and vulnerable to collapse. Grouting is sometimes required on the corner in order to avoid the collapse. Separately constructed joint refers to the cross wall that is constructed after the retaining wall has been constructed. There's no collapse problem, but the slime between the interfaces may reach 20-30mm thick and affect the supporting functionality of the wall. Sometimes, when the cross wall and the retaining wall is constructed separately, the interconnecting part is grouted to replace the slime. In the clean contact joint, a partition plate is installed before the construction of the cross wall. The slime formed in the partition plate is removed, thus the stability problem can be avoided. Figure 2.22 describes the types of joint.

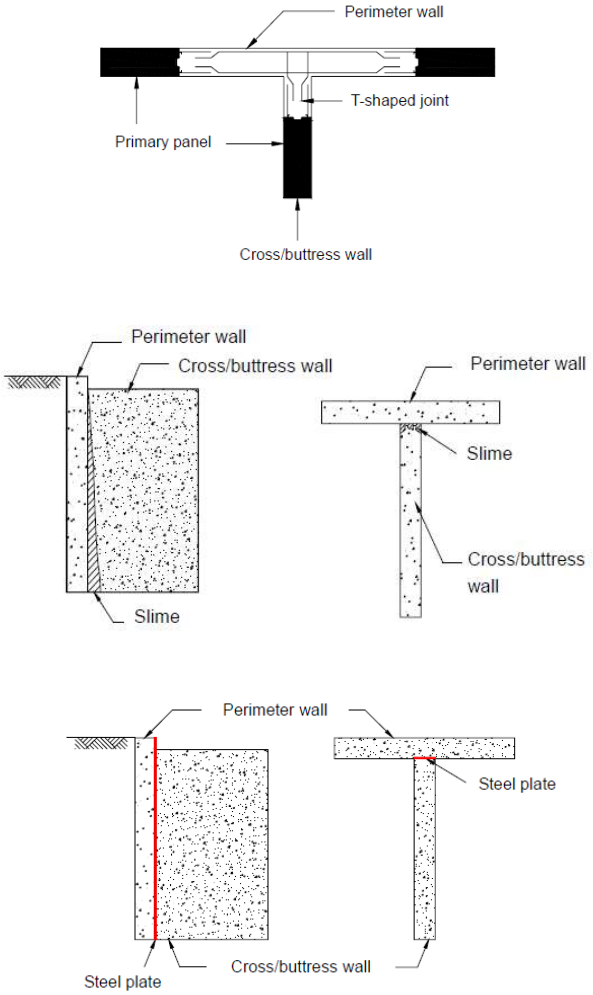

Figure 2.22(a): T-type Joint; Figure 2.22(b): Soft Contact Joint; Figure 2.22(c): Clean Contact Joint

Based on a study conducted by Hsiung et. al. (2005), the simulation of the behavior of the improved ground could be analyzed by equivalent stiffness method, horizontal-beam method, and vertical-beam method.

In equivalent stiffness method, an equation of the equivalent stiffness of the improved soil is used to replace the original soil stiffness by:

$$E_{eq} = E_{wall} \times I_r + E_{soil} \times I_r, \qquad \textbf{(2.6)}$$

where I_r is the soil improvement ratio, refers to the percentage of amount of earth replaced by cross wall.

The vertical-beam method uses several vertical beams to simulate the improved soil. On the other hand, the horizontal beams are used for horizontal-beam method. Lin (2003) suggested

that the vertical-beam method should be selected since its mechanism is adaptable to the conditions on site.

Since there are additional pressures on the wall, Hsieh et al. (2003) suggested adding additional horizontal pressure before the start of excavation. Lin et al. (2000) and Liao and Liu (1996) stated that the additional pressure, σ_{hp}, should be put horizontally at 0 to 4m above the final excavation level. σ_{hp} is computed by this equation:

$$\sigma_{hp} = 1.6\ \sigma_0 \qquad \textbf{(2.7)}$$

where σ_0 refers to the initial earth pressure at that point.

Based on a parametric studies of a 14.5 m deep excavation and 31m deep diaphragm wall conducted by Ou and Lin (1999), the best result was for the case where the cross walls were installed from the ground surface to the bottom of diaphragm wall, while the minimal effect occurred when the cross walls were installed only to the depth of excavation level.

CHAPTER 3

METHODOLOGY

3.1 Soil properties

By adopting a Mohr-Coulomb model in this project, the soil stiffness is assumed to be linear-elastic and the soil is assumed to be isotropic and homogeneous. In this model, perfect plasticity is assumed, i.e. no strain hardening/softening occurred. It only considers the variation of material strength with lateral compressive stress, but doesn't consider the variation of elastic modulus with lateral compressive stress and stress level. This model represents a first order approximation in soil and rock behavior in general until failure is reached.

Although Mohr-Coulomb model disregards the time-dependency and stress-dependency behavior of the soil, which sometimes is not realistic, this model is widely used in estimating the soil properties for a finite element analysis. It is mainly due to its relatively fast computations. There are only five required parameters to build the model, namely soil elastic modulus, E and Poisson's ratio, ν for the soil elasticity, cohesion, c and friction angle, φ for the soil plasticity, and dilatancy angle, ψ. Proper K_o value is also required to generate the initial stresses of the soil.

In this project, a total stress undrained soil condition for both soft and stiff clays is adopted. Figure 1.1 describes the excavation conditions.

The soil elastic modulus for stiff soil is higher than that for flexible soil. The Poisson's ratio and dilatancy angle for incompressible soil are taken to be 0.49 and 0 respectively. Since both the soil layers are clay and are assumed as undrained, the shear strength is represented by the undrained shear strength c_u and φ_u=0. The upper soft clay layer has increasing soil strength with depth and K_o value is assumed to be 1.0. The soil properties are summarized in Table 3.1.

Table 3.1: Soil Parameters for Finite Element Modeling

Soil parameter	Soft clay	Stiff clay
Unit weight, γ (kN/m^3)	16	20
Young's modulus, E (kPa)	$300c_u$	$500c_u$
Soil strength, c_u (kPa)	20+1.5z	200
Friction angle, φ	0	0
Poisson's ratio, ν	0.49	0.49
Earth pressure coefficient, K_o	1.0	1.0

For the computations, fine global coarseness of soil mesh with cluster refinement around the excavation is adopted for both two-dimensional and three-dimensional analyses. Figure 3.1 shows the typical two-dimensional soil mesh of the excavation, while Figure 3.2 shows the typical three-dimensional soil mesh.

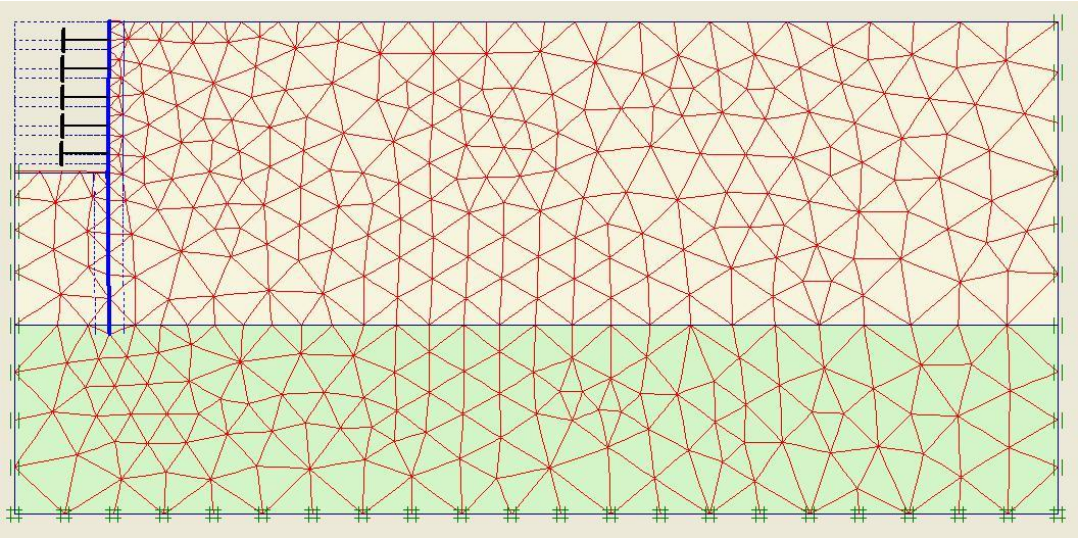

Figure 3.1 Typical Two-dimensional Soil Mesh

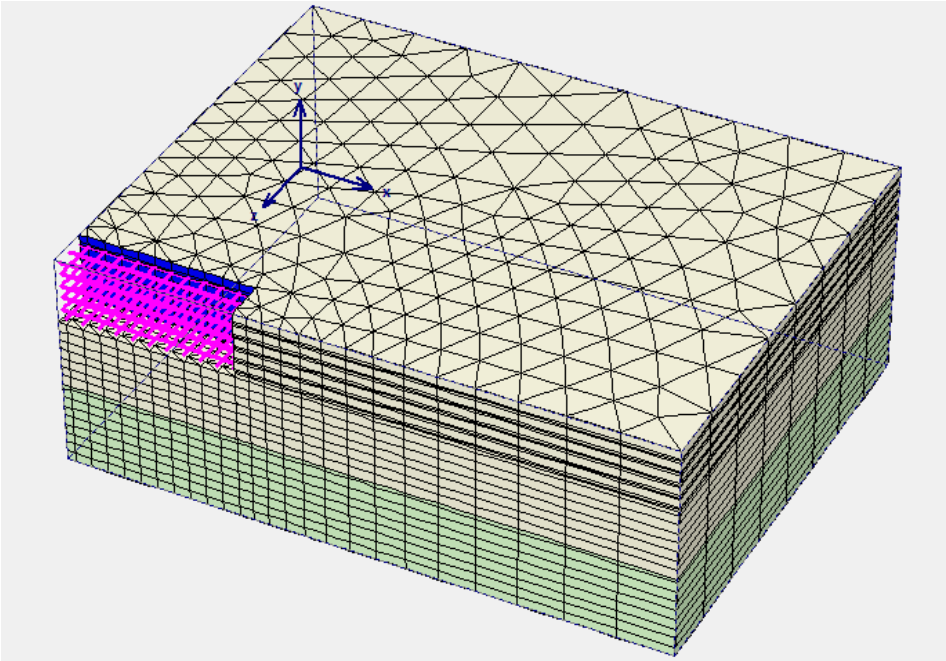

Figure3.2: Typical Three-dimensional Soil Mesh

The typical deformed mesh of soil movement can be seen in Figure 3.3 and Figure 3.4 for two-dimensional and three-dimensional model, respectively.

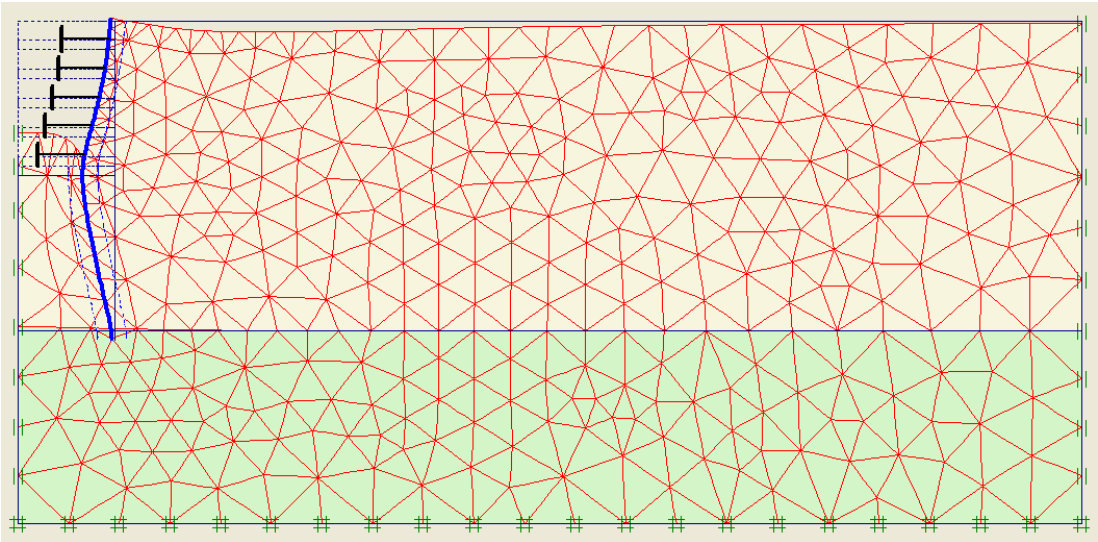

Figure 3.3: Typical Deformed Mesh of Two-dimensional Model

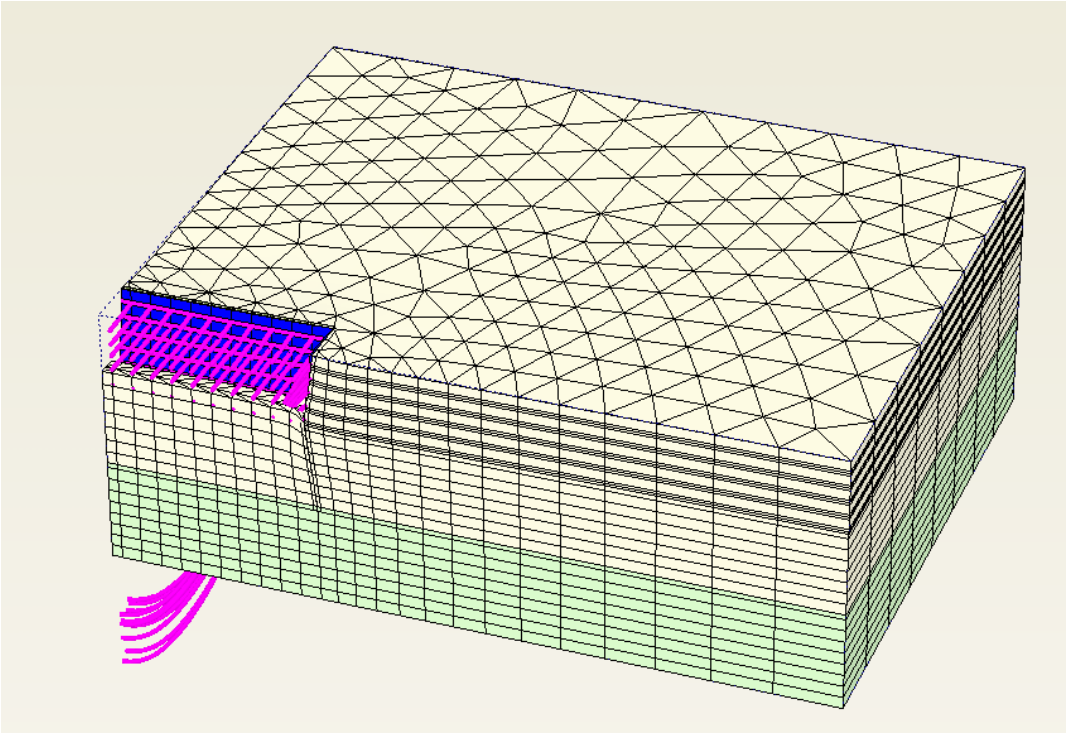

Figure 3.4: Typical Deformed Mesh of Three-dimensional Model (scaled up to 20 times)

3.2 Structural parameters

The structural parameters include the struts and wall properties. For two-dimensional analysis, the wall and the struts are assumed to be isotropic and the plane strain conditions are assumed. On the other hand, the walls and struts in three-dimensional analysis are anisotropic. The presence of walers is also simulated to represent the force transfer from the struts to the wall. The walls and the struts are installed in both x- and z-directions. Each strut level consists of primary struts and secondary struts, spaced by 0.5m vertically to represent the real construction condition. The horizontal and vertical strut spacing is 4m and 3m, respectively. The arrangement of the strutting system may be seen in Figure 3.5.

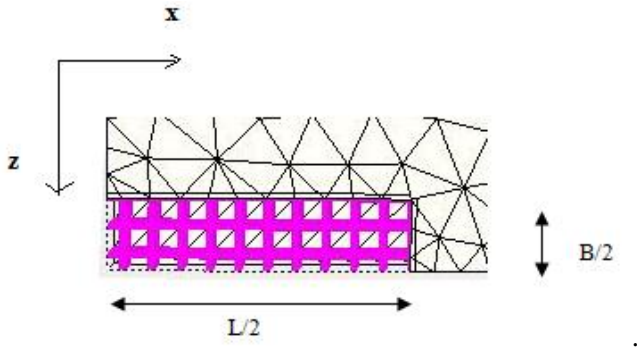

Figure 3.5: Strutting System in the Excavation

Three types of wall are used in the analysis to represent different stiffness of the wall, i.e. flexible, medium, and stiff. The system stiffness is used to represent the flexibility of the wall. The equation of system stiffness, S, is as follow:

$$S = \frac{EI}{\gamma(h_{avg})^4} \tag{3.1}$$

where EI, γ, and h_{avg} are the wall stiffness, unit weight of the soil, and vertical strut spacing, respectively.

Due to the anisotropy of the wall in three-dimensions, different values of Young's Modulus of the wall in different directions are considered to model the system stiffness. The In-plane Shear Modulus, G_{12} as well as Out-of-plane Shear modulus, G_{13} and G_{23}, are considered, as well. Table 3.2 show the properties of the wall

Table 3.2: Wall Properties for Finite Element Modeling

Parameters	Flexible wall	Medium wall	Stiff wall
2-D parameters			
System stiffness, S	32	320	3200
Bending stiffness, EI (kNm^2/m)	50400	504000	5040000
Axial stiffness, EA (kN/m)	3427000	34270000	342700000
Element thickness, d (m)	0.42	0.42	0.42
Poisson's ratio, ν	0	0	0

3-D parameters			
Young's modulus, E_1 (kPa)	8160000	81600000	816000000
E_2 (kPa)	408000	4080000	40800000
E_3 (kPa)	200000000	2000000000	20000000000
Shear modulus, G_{12} (kPa)	408000	4080000	40800000
G_{13} (kPa)	400000	4000000	40000000
G_{23} (kPa)	1330000	13300000	133000000
Poisson's ratio, ν	0	0	0
Element thickness, d (m)	0.42	0.42	0.42

Similarly for the strut and waler properties, in three-dimensional analysis, more than one input of strut moment of inertia is required. I_2 and I_3 represent the moment of inertia about y-axis and x-axis, respectively and I_{23} represents the moment of inertia against oblique bending, which is zero for symmetric beam. The strut and waler properties are shown in Table 3.3.

Table 3.3: Strut and Waler Properties for Finite Element Modeling

Parameters	Strut	Waler
Cross section area, A (m^2)	0.008682	0.022
Volumetric weight, γ (kN/m^3)	78.5	78.5
Young's modulus, E (kN/m^2)	2.1E8	2.05E8
Moment of inertia, I_3 (m^4)	1.045E-4	5.4E-4
I_2 (m^4)	3.668E-4	5.4E-4
I_{23} (m^4)	0	0

3.3 Modeling of Excavation

The excavation is modeled using finite element software, PLAXIS. Two-dimensional and three-dimensional modelings are carried out as deemed necessary. Half of the excavation is modeled in two-dimensional analyses while a quarter of the excavation is modeled using three-dimensional analyses, taking consideration of the symmetry of the soil conditions and the excavation in order to minimize the modeling and calculation time.

15-node triangular elements and 15-node wedge elements are used in PLAXIS 2D and PLAXIS 3D, respectively. These two modes provide better accuracy for the displacement and numerical integration as compared to the other element types.

The results of the modeling are analyzed, with wall movements and strut forces as the main interests. Figure 3.6 shows the plan view of the excavation in x-z plane. The primary wall, which is the longer wall, is considered. The wall movements of the primary wall are larger than for the secondary wall. The typical wall movements are shown in Figure 3.3 and Figure 3.4. The detailed analysis of the wall movements is described in the Chapter 4.

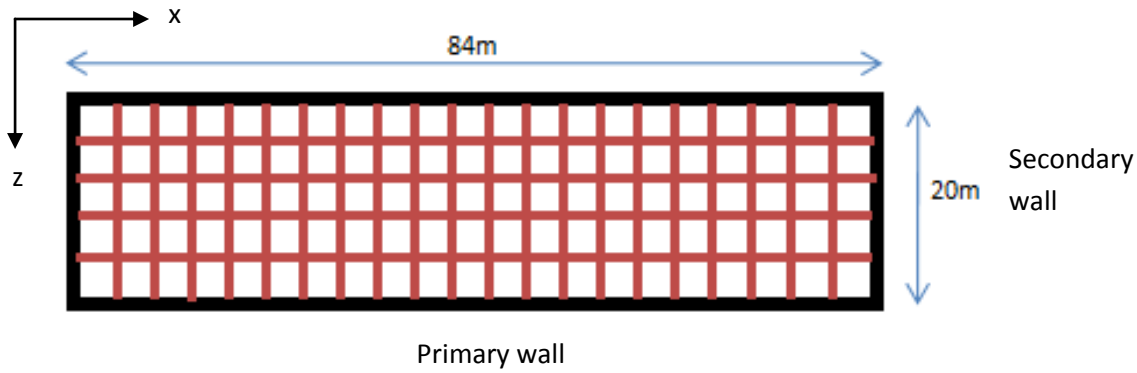

Figure 3.6: Primary Wall and Secondary Wall of the Excavation in x-z Plane (Plan View)

3.3.1 Case 1: Excavation without any improvement method

Two-dimensional and three-dimensional models are set up for this original case. The results enable comparisons of results of two-dimensional and three-dimensional analyses, and also comparisons with analyses where ground improvements are considered. A half cross section in z-y plane is modeled using PLAXIS 2D and a quarter of the excavation is modeled using PLAXIS 3D, as shown in Figure 3.7(a) and 3.7(b). Roller fixities are provided at the boundaries, which is 100m from the excavation. It is more than 5H, as recommended by Roboski (2004). Three models are set up for flexible, medium, and stiff walls.

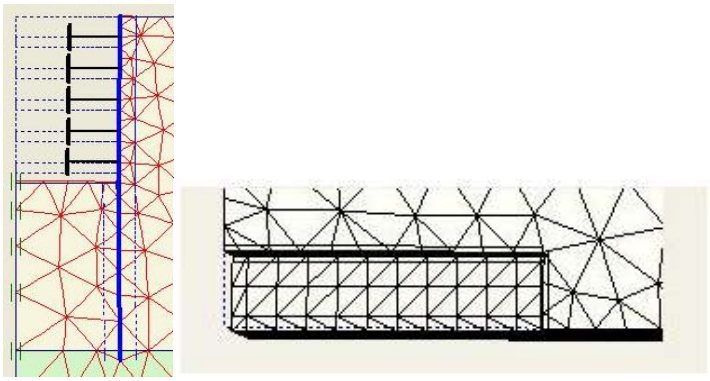

3.7 (a) 3.7 (b)

Figure 3.7: Case 1, Original Excavation Model in (a) 2D (b) 3D

3.3.2 Case 2: Excavation with jet grouting

Only three-dimensional models, with the same soil conditions, wall and strut properties, as well as the geometry as the previous case, are considered in this case. A layer of jet grout is modeled parallel to the secondary wall. The 2m thick jet grout layer is installed immediately below the final excavation level. Two sub-cases are analyzed. Case 2-1 considers a 4m wide jet grouting layer (wall type grouting) with 4m horizontal spacing as shown in Figure 3.8(a). Case 2-2 considers a block type grouting which is applied to 50% area of the excavation, as shown in Figure 3.8(b). Both wall type and block type grouting are previously described in Figure 2.19. The effectiveness of both methods are then compared. The properties of the jet grout are as follows: γ=20kN/m^3, c_u=400kPa, E=150000kPa, ν=0.495. The jet grout layers are assumed to be installed at the same time as the installation of the walls.

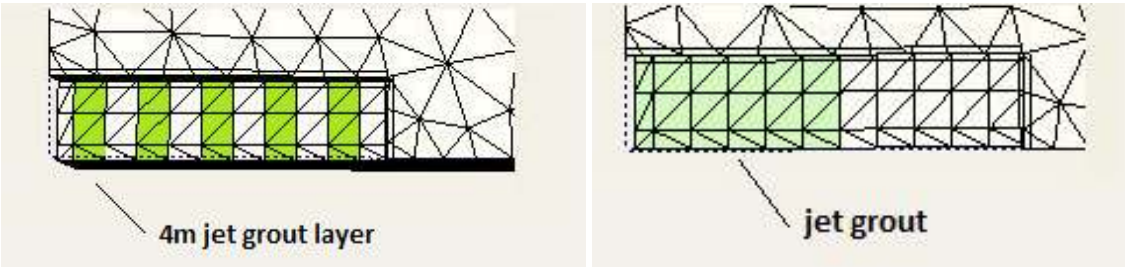

3.8 (a) 3.8 (b)

Figure 3.8: Case 2, Excavation with Jet Grouting (a) Wall Type Improvement (b) Block Type Improvement

3.3.3 Case 3: Excavation with cross walls

Only three-dimensional models are considered in this case. The cross walls are constructed in the z-direction at the same time as the installation of the retaining walls. The depth of the cross walls is 16m from the final excavation level, so that the need of hacking the wall is minimized.

Three sub-cases are considered to evaluate the most effective location for the installation of the cross walls. In Case 3-1, one cross wall is constructed 21m from the secondary wall. Case 3-2 and Case 3-3 cover the conditions where the cross walls are spaced 20m and 12m, respectively. Figure 3.9 provides the visual description of the cross wall arrangements. The cross wall is assumed to be linear elastic with unit weight of 24 kN/m^3, Young's modulus of 2.8E7 kPa, and Poisson's ratio of 0.2.

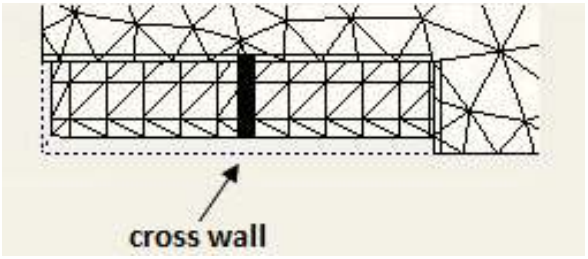

3.9 (a)

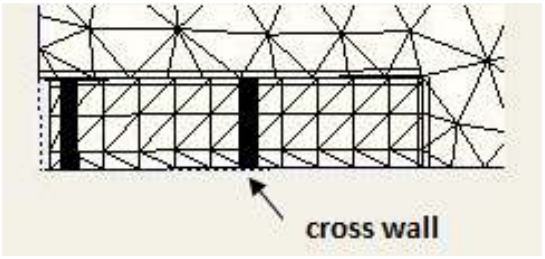

3.9 (b)

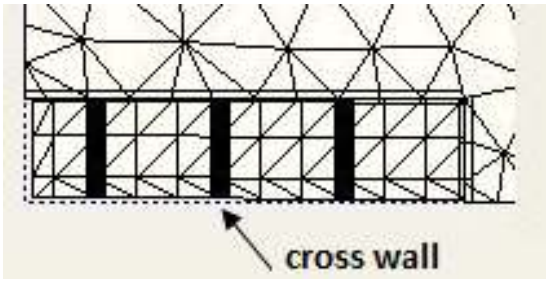

3.9 (c)

Figure 3.9: Case 3, Excavation with Cross Walls (a) 21m from the Secondary Wall (b) at 20m Spacing (c) at 12m Spacing

3.4 Excavation Stages

Staged excavation method is adopted in PLAXIS 2D and PLAXIS 3D foundation.

The stages of the excavation are as follow:

1. Install wall and/or jet grouting layer/cross walls at y=52m
2. Excavate to y=50m
3. Excavate to y=49m
4. Install strut S1 at y=50m
5. Excavate to y=47m
6. Excavate to y=46m
7. Install strut S2 at y=47m
8. Excavate to y=44m
9. Excavate to y=43m
10. Install strut S3 at y=44m
11. Excavate to y=41m
12. Excavate to y=40m
13. Install strut S4 at y=41m
14. Excavate to y=38m
15. Excavate to y=37m
16. Install strut S5 at y=38m
17. Excavate to final excavation level (FEL) at y=36m

CHAPTER 4

RESULTS AND ANALYSES

4.1 2D and 3D Analyses of Wall Movement

This section presents the results of the two-dimensional and three-dimensional analyses described in Chapter 3. The wall movement results are shown in Figure 4.1(a), 4.1(b), and 4.1(c), while the wall movements versus wall stiffness plot is shown in Figure 4.1(d)

Due to the corner stiffening effect, the plane strain analyses yield different results compared to three-dimensional analyses. In three-dimensional analyses, the struts at the corner seem to be less heavily loaded and the maximum wall movement close to the centre of the excavation is observed to be smaller.

The observations of the two-dimensional and three-dimensional models agree with the results from previous published findings. The maximum wall movement in plane strain analyses is more conservative.

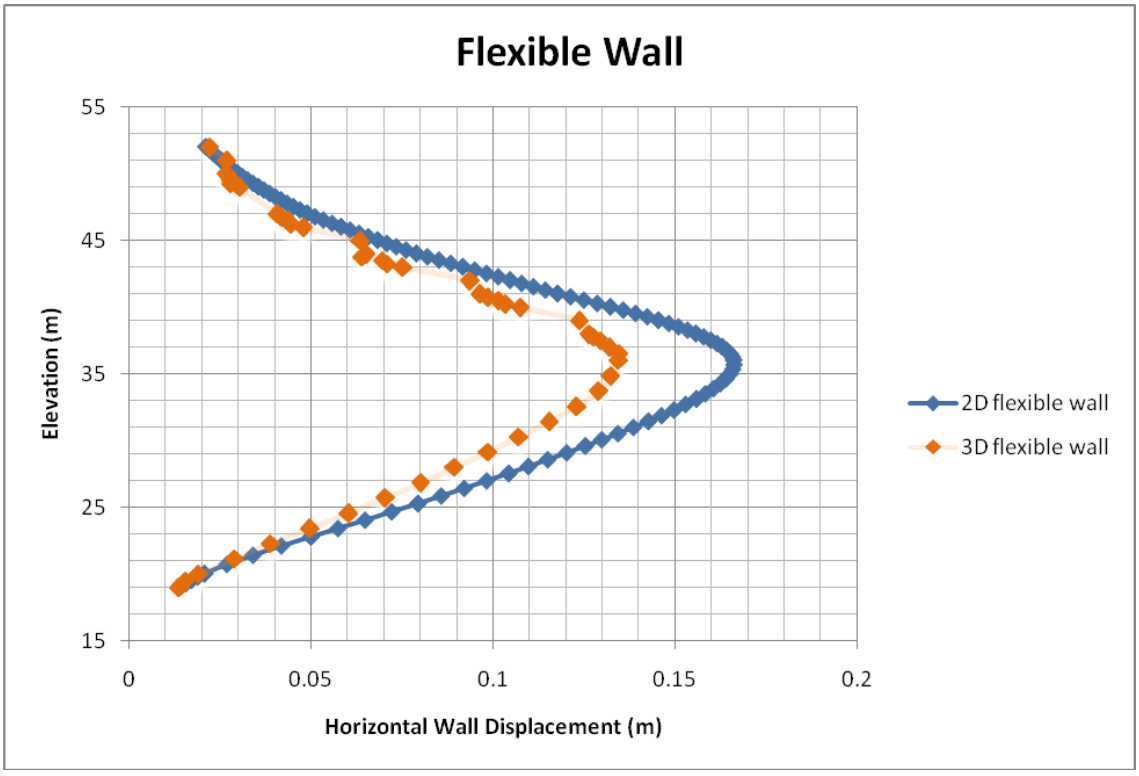

4.1 (a)

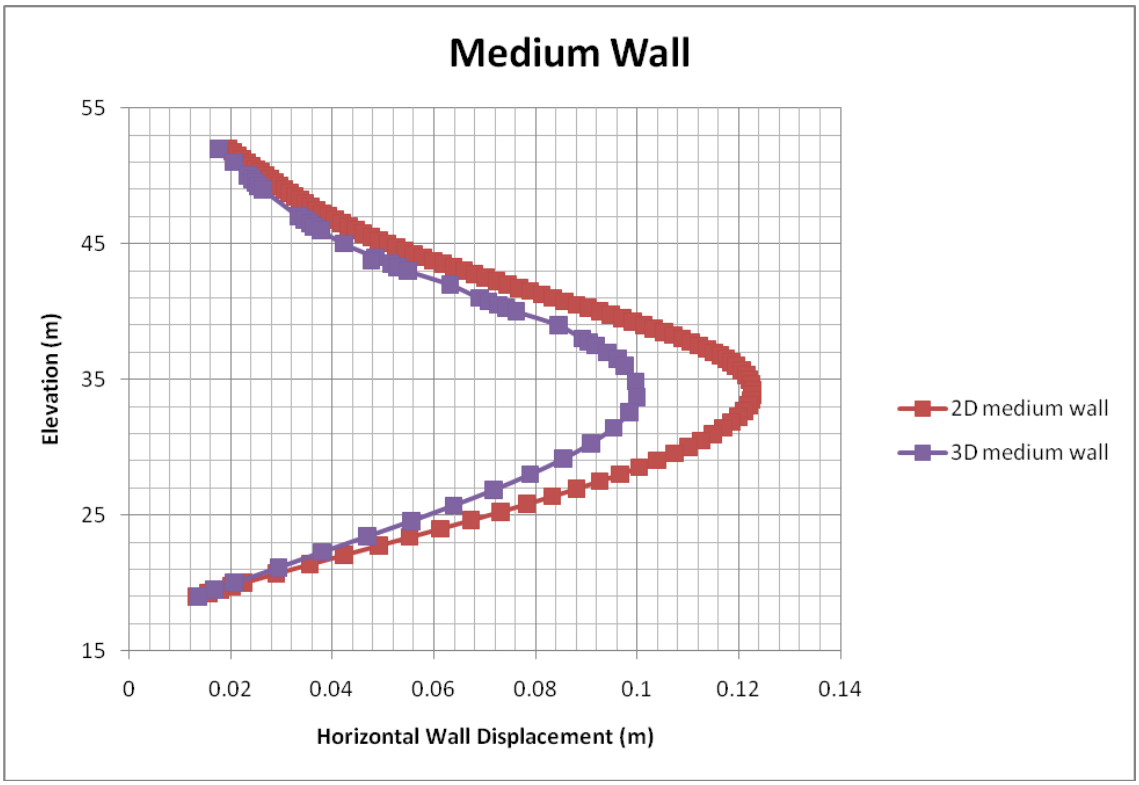
Medium Wall
55
45
35
25
15
Elevation (m)
0
0.02
0.04
0.06
0.08
0.1
0.12
0.14
Horizontal Wall Displacement (m)
2D medium wall
3D medium wall

4.1 (b)

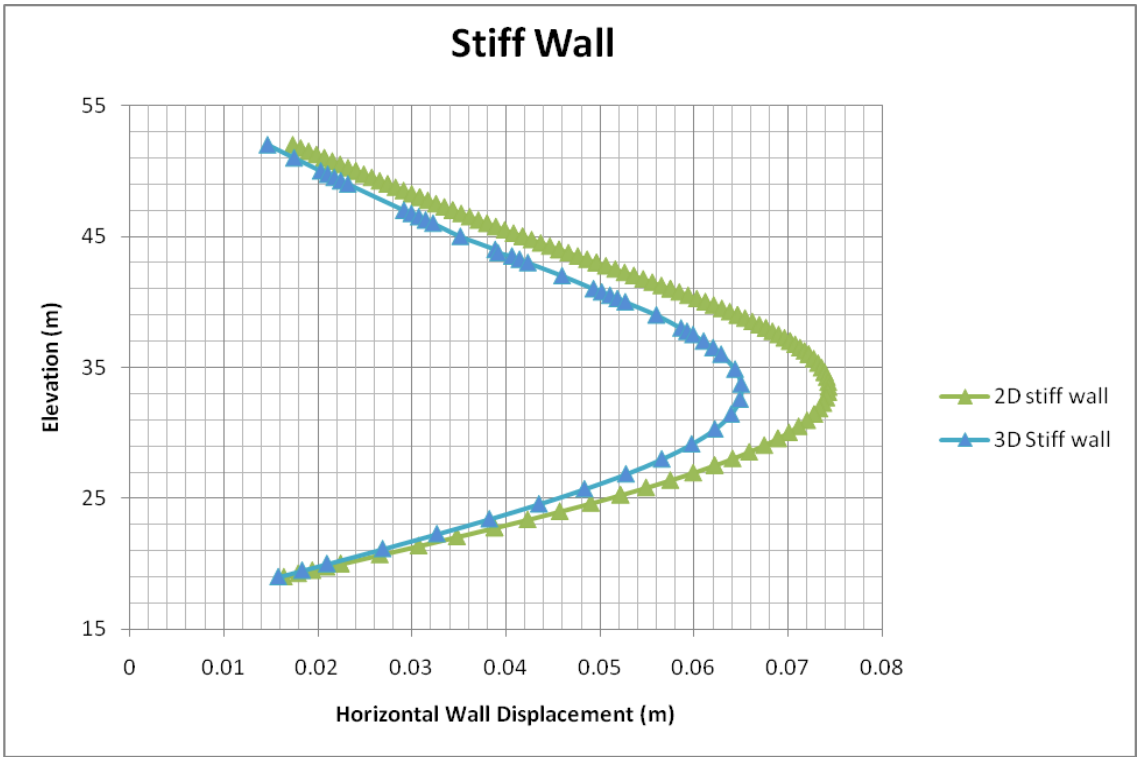
Stiff Wall
55
45
35
25
15
Elevation (m)
0
0.01
0.02
0.03
0.04
0.05
0.06
0.07
0.08
Horizontal Wall Displacement (m)
2D stiff wall
3D Stiff wall

4.1 (c)

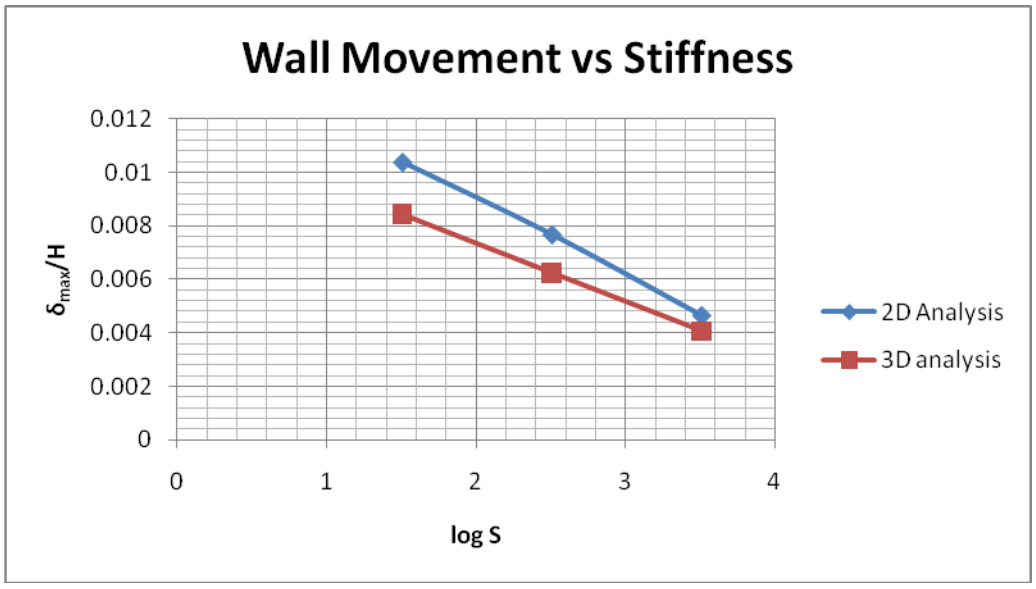

4.1 (d)

Figure 4.1: Wall Movement Profile for (a) Flexible Wall; (b) Medium Wall; (c) Stiff Wall; and (d) Wall Movement versus Stiffness Plot

From the figures above, it can be observed that both plane strain and three-dimensional models yield the same shape of wall movement profile, i.e. small at the top and bottom of the wall and maximum around the final excavation level. It is also observed in Figure 4.1(d) that the higher the wall stiffness is, the more restraint the wall provides to the lateral movement, i.e. the smaller wall movement is observed.

The results show that the plane strain analyses give more conservative results in term of wall movement. Table 4.1 summarizes the PSR of flexible, medium, and stiff wall of this project to assess the reliability of plane strain analysis as compared to three-dimensional analysis.

Table 4.1: Comparison of Two-dimensional and Three-dimensional Maximum Horizontal Wall Movements

Case	Stiffness		
	Flexible	Medium	Stiff
Maximum horizontal wall movement (2D) (mm)	166.1	122.7	74.2
Maximum horizontal wall movement (3D) (mm)	134.9	100.4	66.0
PSR	0.81	0.82	0.89

The PSRs for flexible, medium, and stiff wall are 0.82, 082, and 0.89, respectively. It shows that the plane strain analysis is higher for the high stiffness wall system. Stiff wall has relatively small movement compared to flexible and medium wall, so the corner stiffening effect is more insignificant. The results differ with the observation of Finno et. al. (2007), which showed that the PSR value reduced with the increase of the wall stiffness. Different wall depth and soil conditions in this project may be the reason of this disagreement.

However, the results agree with another finding of Finno et. al. (2007) which stated that the plane strain and three-dimensional analyses lead to the same wall movement for the value of $L/H \geq 6$. In this case, $L/H = 84/16 = 5.25$, and the PSR is approaching unity, although still less than one. The overestimation of plane strain analyses is not that significant since the wall is considered quite long.

The use of three-dimensional analyses may lead to the more economical design for the ultimate and serviceability limit state, although the modeling and computation phases take more time to complete.

4.2 Effects of improvement methods to the wall movements

The plane strain model is not able to represent the whole three-dimensional behavior of excavation with soil improvement or property protection measures. Hence, only three dimensional analyses are carried out for these cases, as shown previously in Figure 3.8 and Figure 3.9.

The movement across the excavation, either in primary or secondary wall, is not constant. The movement near the corner of the excavation is smaller to the movement around the center of the excavation because of the arching/corner stiffening effect, as shown in Figure 4.2.

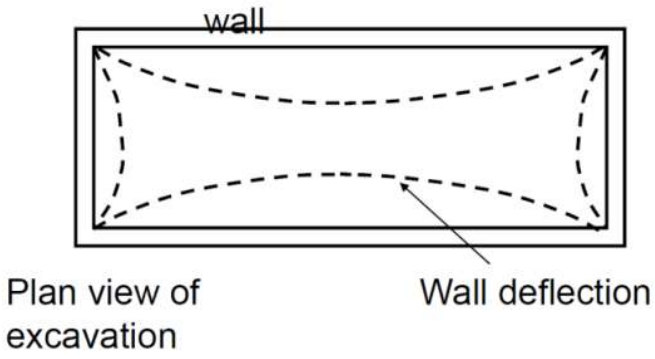

4.2 (a)

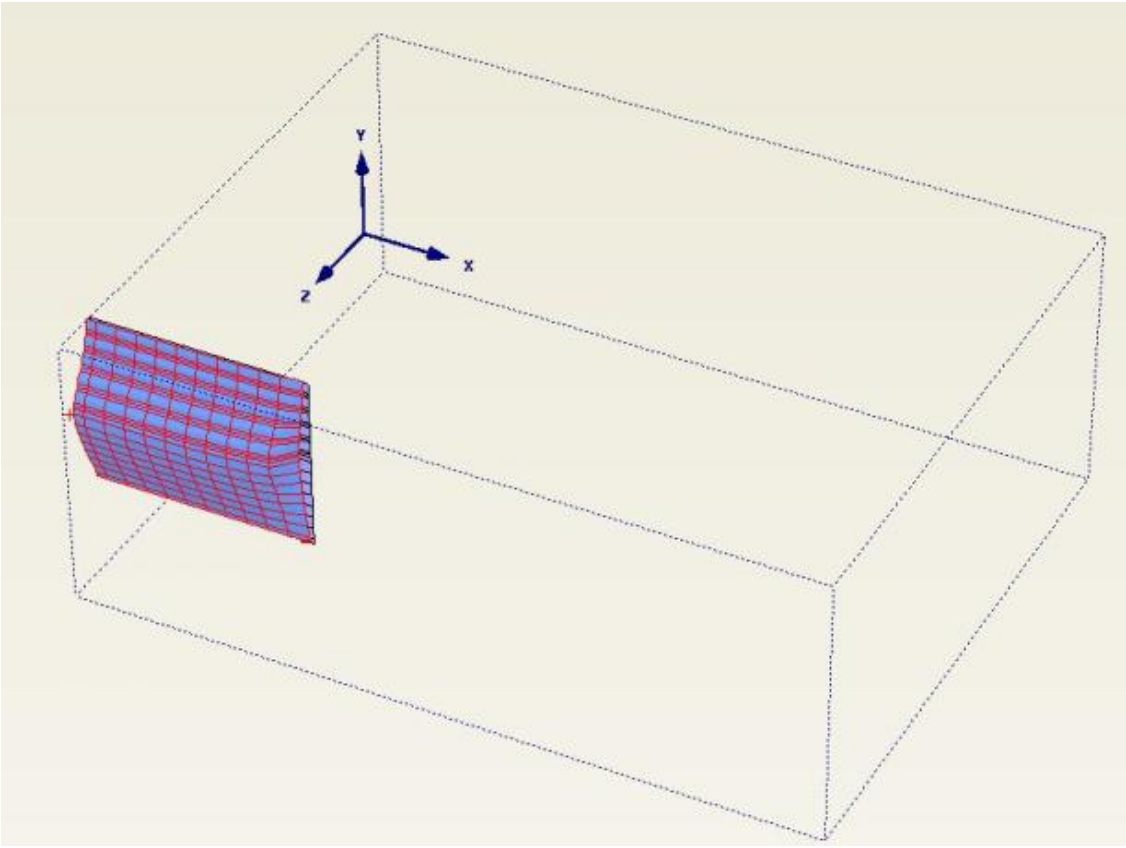

4.2 (b)

Figure 4.2: Three-dimensional Wall Movement in: (a) Plan View, (b) Three-dimensional View

The primary wall movement is expected to be bigger than secondary wall movement, thus only the results from the primary wall are analyzed and compare. The results of maximum wall movements and wall movement behaviors from various methods are presented in Table 4.2 and Figure 4.3.

Table 4.2: Maximum Horizontal Wall Movement for Different Methods

Case	Maximum horizontal wall movement (mm)		
	Flexible Wall	Medium Wall	Stiff Wall
Case 1: 3D original	134.9	100.4	66.0
Case2.1: 3D grouting	95.0 (29.6%)	68.0 (32.3%)	49.8 (24.5%)
Case 2.2.: 3D centre grouting	110.7 (17.9%)	79.3 (21.0%)	53.1 (19.5%)
Case 3.1: 3D cross wall @21m	128.0 (5.1%)	95.2 (5.2%)	63.3 (4.1%)
Case 3.2: 3D cross wall per 20m	114.3 (15.3%)	73.6 (26.7%)	45.6 (30.8%)
Case 3.3: 3D cross wall per 12m	98.8 (26.7%)	55.8 (44.4%)	25.5 (61.4)

Note: values in brackets show the percentage reduction as compared to Case 1

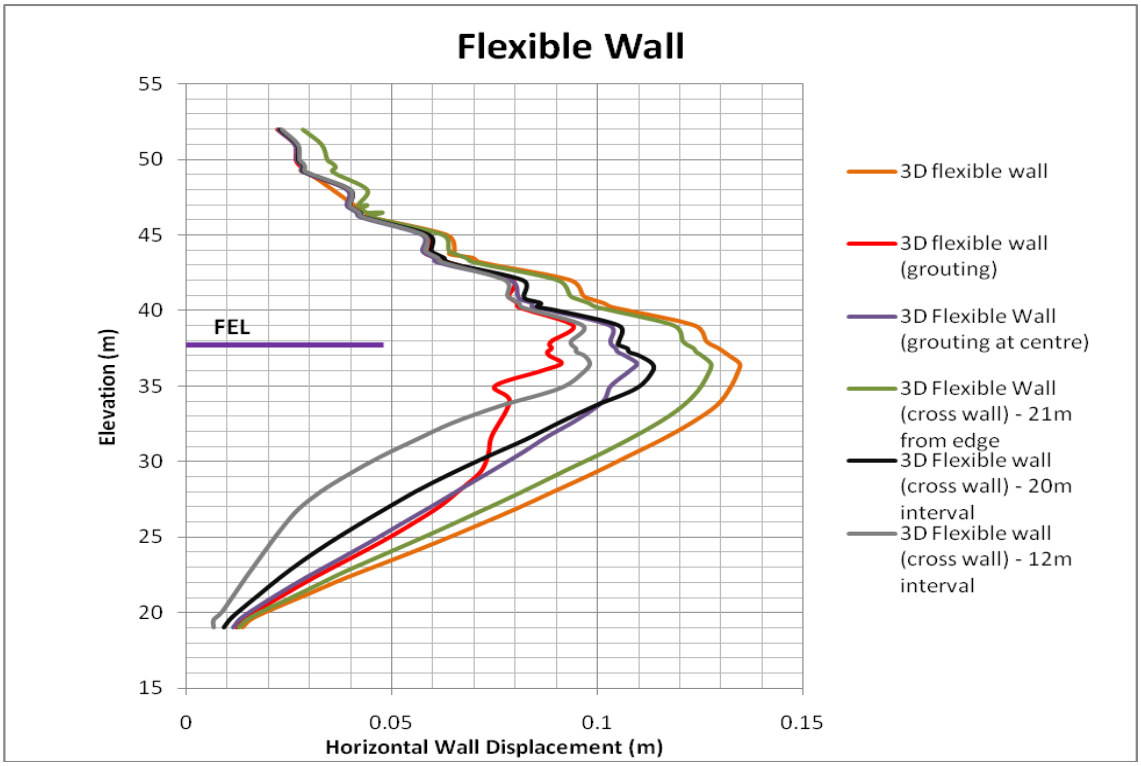
Flexible Wall
55
50
45
40
35
30
25
20
15
Elevation (m)
FEL
0
0.05
0.1
0.15
Horizontal Wall Displacement (m)
3D flexible wall
3D flexible wall (grouting)
3D Flexible Wall (grouting at centre)
3D Flexible Wall (cross wall) - 21m from edge
3D Flexible wall (cross wall) - 20m interval
3D Flexible wall (cross wall) - 12m interval

4.3 (a)

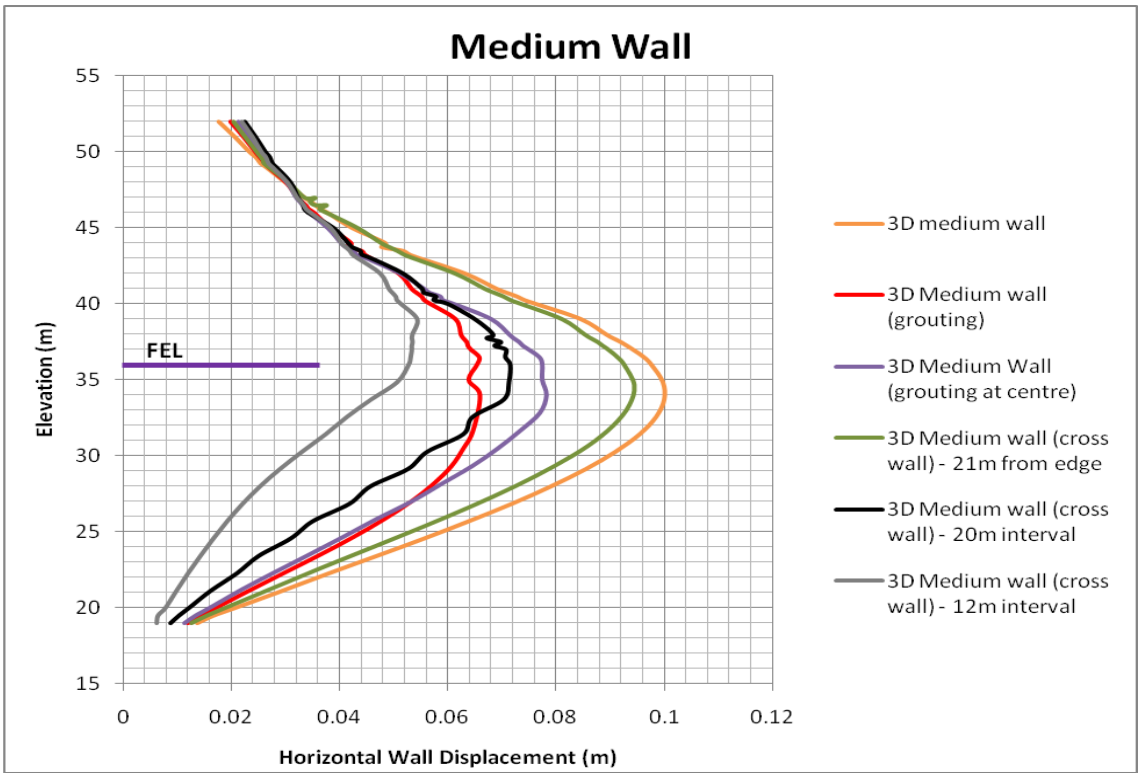
Medium Wall
55
50
45
40
35
30
25
20
15
Elevation (m)
FEL
0
0.02
0.04
0.06
0.08
0.1
0.12
Horizontal Wall Displacement (m)
3D medium wall
3D Medium wall (grouting)
3D Medium Wall (grouting at centre)
3D Medium wall (cross wall) - 21m from edge
3D Medium wall (cross wall) - 20m interval
3D Medium wall (cross wall) - 12m interval

4.3 (b)

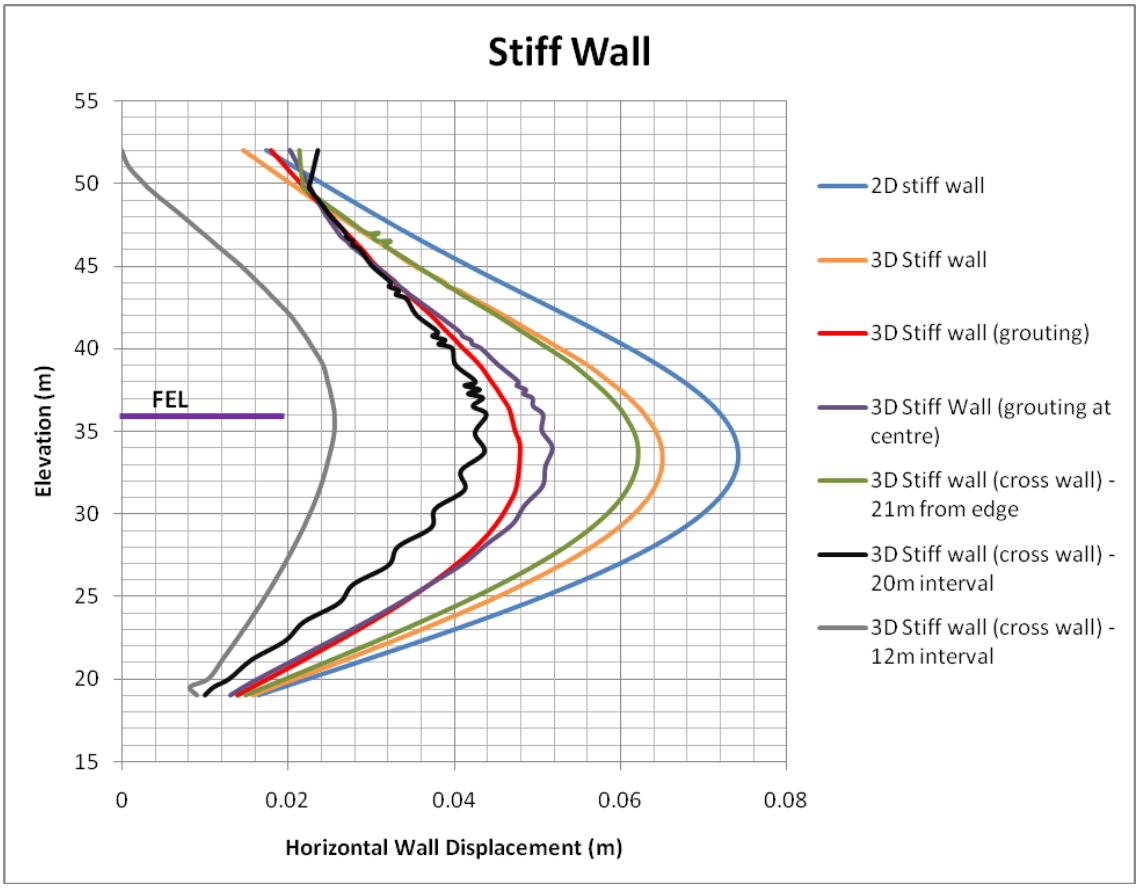

4.3 (c)

Figure 4.3: Depth vs Wall Movement from Various Improvement Method of: (a) Flexible Wall (b) Medium Wall (c) Stiff Wall

The shape of the wall movement profiles for each method is the same, i.e. small at the top and bottom of the wall and maximum around the final excavation level, regardless of the stiffness of the wall.

In the cases of the flexible wall, the wall movement is reduced to 95 mm (29.6% reduction) in Case 2-1. A sudden reduction at the depth of 36m to 35m, where the JGP layer is constructed, is observed. On the other hand, Case 2-2 gives less favorable result of maximum wall movement of 110.7mm. Case 3-1 is not effective in reducing the horizontal wall movement, i.e. only 6.9mm or 5.1% reduction. On the other hand, in Case 3-2, the maximum horizontal wall movement is observed to be 114.3mm or 15.3% smaller than what is observed in Case 1. Case 3-3 is effective in reducing the wall movement by 26.7% and the maximum wall movement observed is 98.8 mm. Case 2-1 gives similar result to what is observed in Case 3-3. 29.6% and 26.7% reduction of wall movement are observed in the former and latter, respectively.

With the increase of the wall stiffness, the maximum wall movement in the medium wall is reduced when compared to the flexible wall. The effects of different type of jet grouting are also similar to that observed in the cases of the flexible wall. Case 2-1 shows the reduction of 32.7mm or 32.3% as compared to the maximum wall movement in Case 1, while Case 2-2 reduces only 21.1mm or 21% of the wall movement. On the other hand, the effects of cross walls in medium wall are more favorable, except for the Case 3-1, where the reduction of maximum wall movement is only 5.25 mm. The maximum wall movements for Case 3-2 and Case 3-3 are 73.6mm and 55.8mm, respectively. It can be observed that the effect of wall type grouting in Case 2-1 is comparable to Case 3-2. However, the result in Case 3-3 shows that it is significantly more effective than Case 2-1 for the case of medium wall stiffness.

For high stiffness wall, the performance shown by Case 2-1 is about the same as compared to the performance shown by Case 2-2. The maximum wall movements are 49.8mm and 53.1mm, or 24.5% and 19.5% reduction, for the former and the latter respectively. For the wall with high stiffness, the jet grouting is not effective in reducing the wall movement. On the other hand, cross walls show better performances with the increase of wall stiffness, apart from Case 3-1. The other sub-cases show significant reduction of wall movement to 45.6mm and 25.5mm, which means there is 30.8% reduction in Case 3-2 and 61.4% reduction in Case 3-3. It can be observed that for the high stiffness wall, the cross wall method is more effective than jet grouting.

These two improvement methods behave in different ways for different wall stiffness. Each method is more suitable to be applied in certain cases of wall stiffness. The findings are discussed below.

4.2.1 Jet Grouting

From the data presented above, it is observed that 4m wall type grouting with 4m spacing (Case 2-1) performs better than block type grouting covering the 44m central part of the excavation (Case 2-2). In the former case, the grouting influences the whole part of the excavation, thus restraining the wall movement at the centre as well as around the corner of the excavation. In the latter case, the grouting only reduces the wall movement around the centre of the excavation, where the jet grout layer is constructed. This result agrees with the findings of Ou (1996) which stated that block type grouting needed a large improvement area to reduce the wall movement significantly.

The typical three-dimensional wall movement of Case 2 may be seen in Figure 4.4 and 4.5. The difference in the behavior of wall movement as resulted from these two types of jet grouting

may be observed. In Case 2-2, there is a jump in the wall movement at the end of the jet grout layer, which shifts the maximum wall movement to the edge of the excavation.

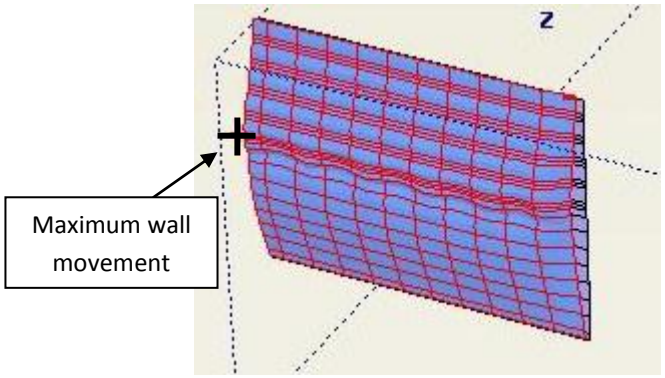

Figure 4.4: Typical Wall Movement in Case 2-1 in Flexible Wall

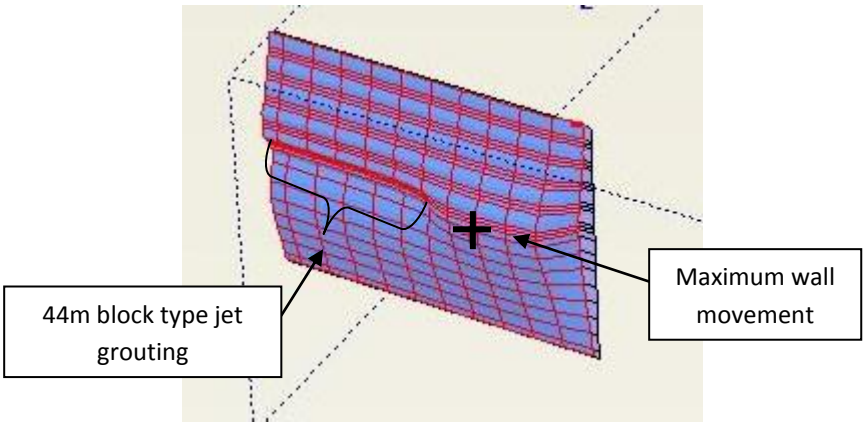

Figure 4.5: Typical Wall Movement in Case 2-2 in Flexible Wall

The installation of jet grouting to reduce of wall movement is the most effective for walls with medium stiffness. The percentage of reduction of wall movement is observed to increase as compared to the case with flexible wall. In Case 2-1, it increases from 29.6% to 32.3%. In Case 2-2, it increases from 17.9% to 21.0%. However, for the stiff wall, the effect of jet grouting is minimal in restraining the wall movement.

4.2.2 Cross Wall

The effect of cross wall installation is dependent to the positions of the cross walls. The reduction of wall movement is only effective around the area restrained by the cross wall. As the maximum wall movement is observed to be around the centre of the excavation, the cross wall should be positioned near the centre to restrain the wall movement. As shown in Figure 4.6, for Case 3-1, the cross wall only restrains the horizontal movement at the distance 21m

from the wall, but it is too far away to influence the maximum wall movement which occurs at the centre of the excavation.

In Case 3-2, where the cross walls are installed at 20m intervals, the reduction effects are quite significant. The cross wall restrains the maximum movement at the centre of the excavation, causing the maximum wall movement to shift to the area in between the two cross walls, as seen in Figure 4.7.

Case 3-3 gives even more significant reduction to the wall movements. Shorter spacing between the cross walls ensures the wall movement is restrained along the entire length of the excavation. The maximum movement is no longer observed at the centre of the excavation, i.e. it is shifted from the centre of the excavation. Typical three-dimensional wall movement of Case 3.3 is shown in Figure 4.8.

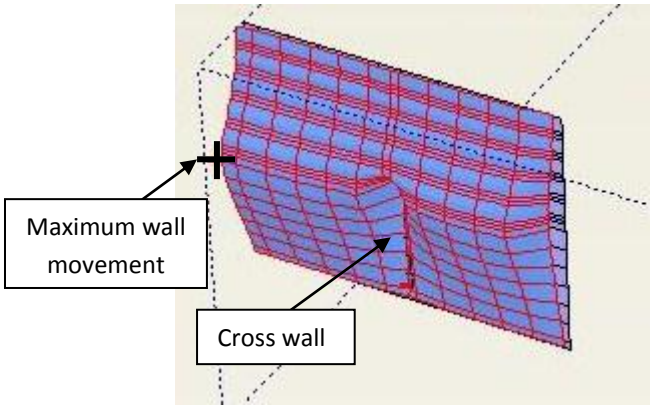

Figure 4.6: Typical Wall Movement in Case 3-1

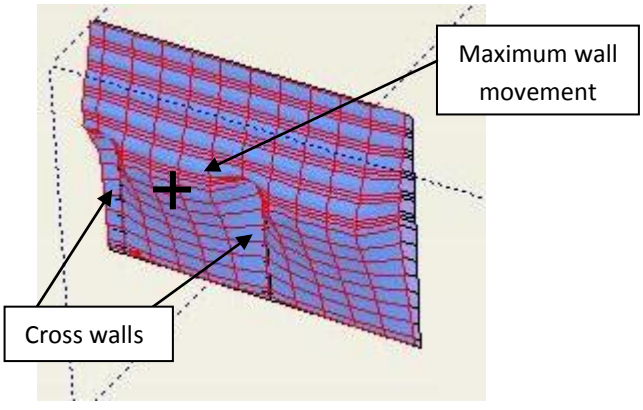

Figure 4.7: Typical Wall Movement in Case 3-2

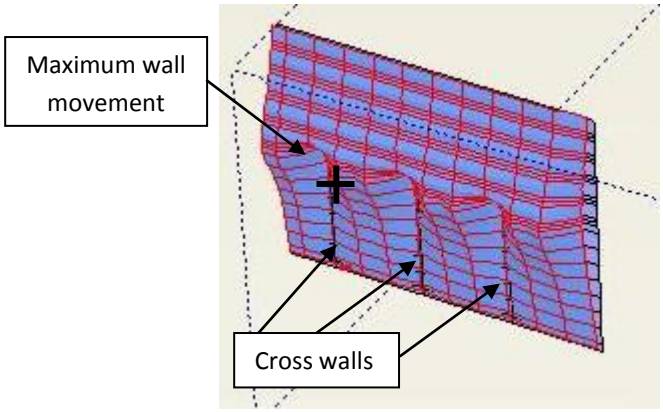

Figure 4.8: Typical Wall Movement in Case 3-3

Based on the results of this project, the effect of cross walls is more significant with increasing wall stiffness, provided that the cross walls are positioned correctly. In Case 3-1, the cross wall is not positioned well, thus the effect is insignificant for any wall stiffness. In Case 3-2, the percentage of wall movement reduction is 15.3%, 26.7%, and 30.8% for flexible, medium, and stiff wall, respectively. The same trend is also observed for Case 3-3, where the percentage of wall movement reduction is increasing from 26.7% in flexible wall, 44.4% in medium wall, to 61.4% in stiff wall.

4.3 2D and 3D Analyses of Strut Forces

The design of the strutting system is also important for any excavation projects, thus the data of strut forces are required. A safe excavation should not have any single strut overloaded. The maximum strut force is used for designing the structural properties of all the struts because the design is based on the envelope of the pressure distribution.

In plane strain analysis, the strut forces per meter run can be extracted directly. The extracted data is multiplied by the horizontal spacing of the struts, which is 4m in this case, to get the force of each strut. On the other hand, the extracted data of the strut forces in three-dimensional model are already in term of force per strut. The most heavily loaded struts are expected to be in the centre of the excavation, where the maximum wall movement occurs. Therefore, in this project, the strut forces of the centre of the excavation are considered. The maximum strut forces from each strut level are then presented in graphical form.

Besides extracting the data from Finite Element Method, the strut forces envelope may be calculated using either Peck's Apparent Pressure Diagram (APD) or Twine and Roscoe's

Distributed Propped Load (DPL), as discussed in Chapter 2. DPL is basically the updated profile of APD. The findings of Twine and Roscoe (1999) state that the strut forces calculated using this method provide conservative estimation to be expected in the field of normal circumstances. Hence, the strut forces calculated from DPL are also presented in this section. Figure 4.10(a), 4.10(b), and 4.10(c) show the strut forces computed using the two-dimensional model, three-dimensional model, and DPL Method, respectively.

According to the DPL Method, the soil classification in this project is assumed to be normally and slightly overconsolidated soft to firm clay. As seen in Figure 2.5(a), the correct diagram for this project is the middle plot, i.e. the diagram of flexible wall in the soft clay with stable base. Based on the unit weight of the soil of 16kN/m^3, the extracted DPL for this project are shown in Figure 4.9.

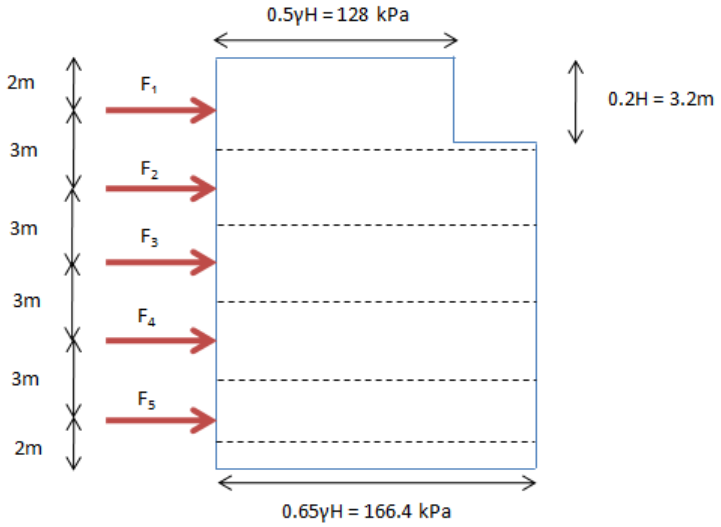

Figure 4.9: DPL of Flexible Wall

Using Tributary Area Method, as described in Chapter 2.2, each strut force is then calculated. The results for the strut forces are 1838.1kN, 1996.8kN, 1996.8kN, 1996.8kN, and 1664.0kN from top to bottom. The calculated forces are shown in Figure 4.10 and compared with the results using the Finite Element Method.

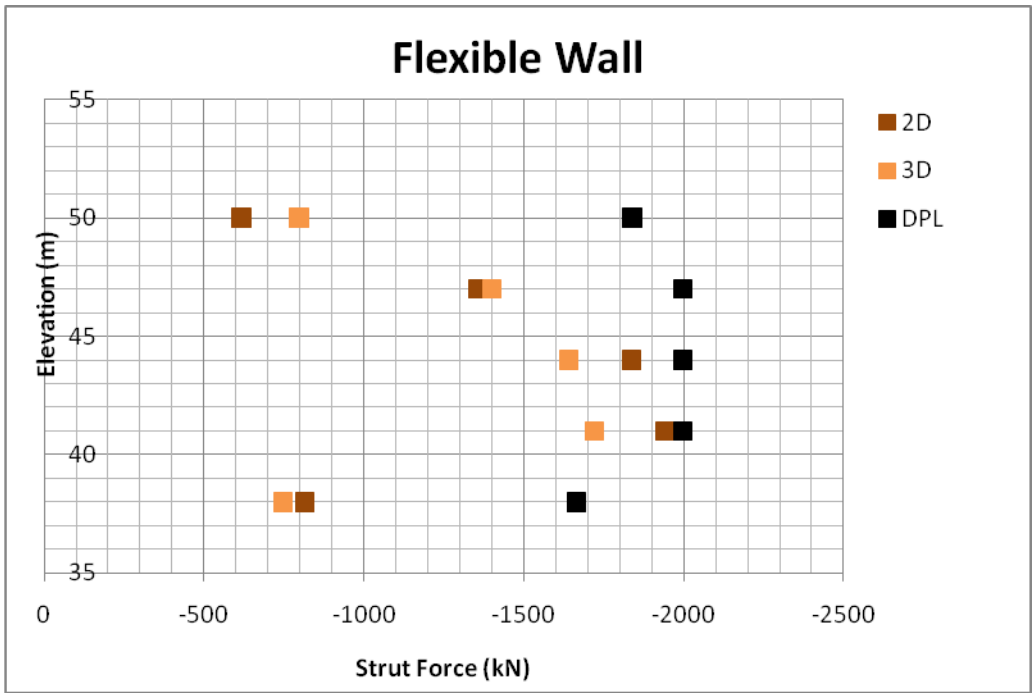
Flexible Wall
55
50
45
40
35
Elevation (m)
0
-500
-1000
-1500
-2000
-2500
Strut Force (kN)
2D
3D
DPL

4.10 (a)

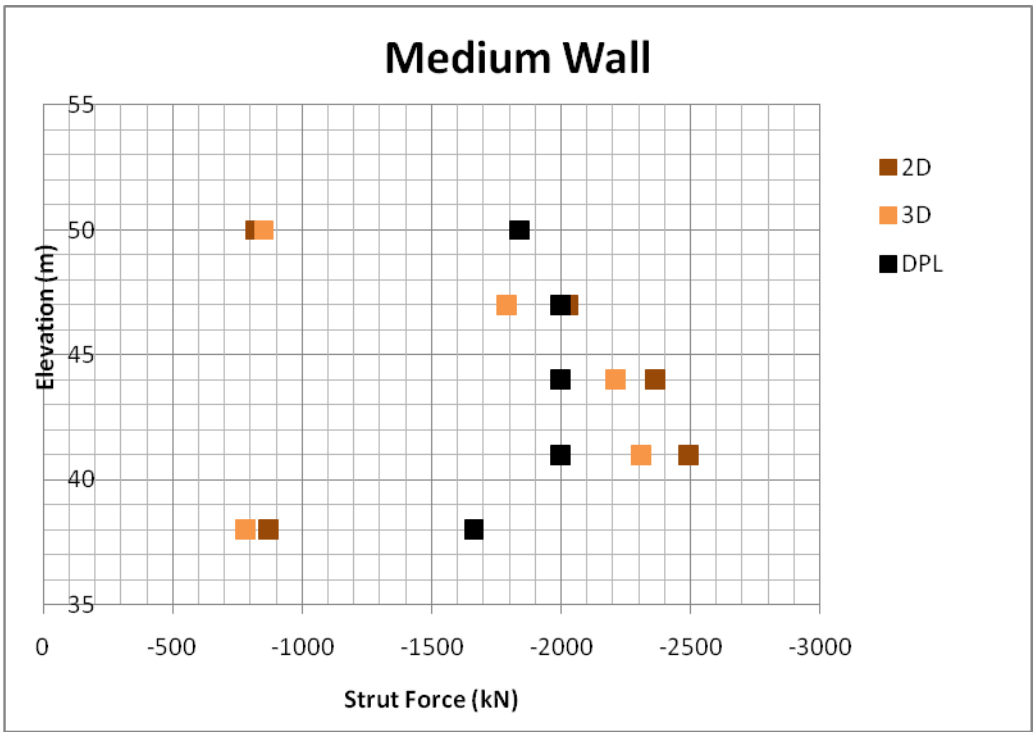
Medium Wall
55
50
45
40
35
Elevation (m)
0
-500
-1000
-1500
-2000
-2500
-3000
Strut Force (kN)
2D
3D
DPL

4.10 (b)

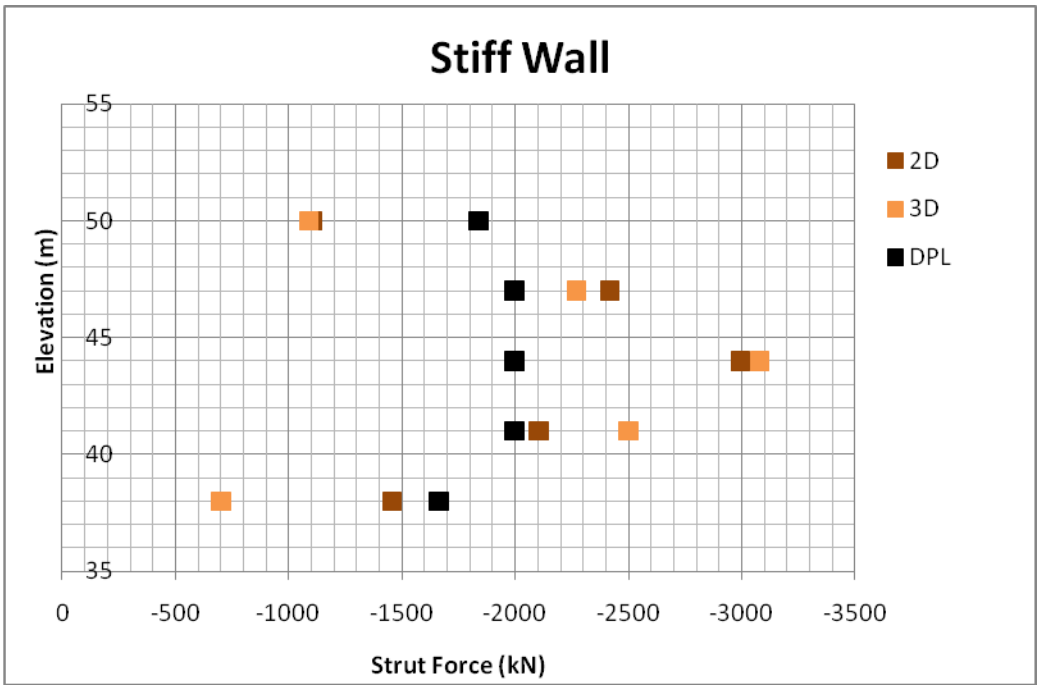

4.10 (c)

Figure 4.10: Strut Forces vs Depth of PLAXIS 2D, PLAXIS 3D, and DPL on (a) Flexible Wall, (b) Medium Wall, and (c) Stiff Wall

Generally, two-dimensional analyses result in more conservative values of strut force than three-dimensional analyses. It is similar to what is observed in the wall movement analyses. For the case of flexible and medium walls, the maximum strut force for the two-dimensional analysis is 200kN larger than for the three-dimensional analysis. However, for the high stiffness wall, both two-dimensional and three-dimensional analyses give similar maximum strut force, i.e. about 3000kN. The insignificant cornering effect, shown by higher PSR in Table 4.1, may be the reason of the similar maximum strut forces.

Terzaghi, Peck, and Mesri (1996) stated that the strut forces derived from APD and DPL would result in conservative design. The findings in this project show that this statement is only true for the case of flexible walls.

In the case of the flexible wall, the overestimation of the strut forces is more significant for the first and last struts. In the DPL, the earth pressure diagram is rectangular with reduced pressure at the top part of the excavation. However, the finite element results indicate that the earth pressure diagram, as well as the strut forces diagram, is trapezoidal.

The DPL Method overestimates by about 56% the forces at the top and bottom struts when being compared with both two-dimensional and three-dimensional analyses. For the second, third, and fourth strut, the overestimation from DPL method is not as significant, namely about 30%, 18%, and 14%, respectively, for three dimensional analysis. The DPL calculated strut forces result in smaller overestimation for plane strain analysis, i.e. only 30%, 8%, and 3% for the three middle struts.

As mentioned in Chapter 2.1, since there are no recommendations of DPL for higher stiffness wall, engineers commonly assume the same DPL for medium and stiff wall. However this approach can be unconservative. As observed in Figure 4.10, the strut forces increase with the increasing wall stiffness. The less flexibility of the wall results in the less arching effect and higher strut forces. Thus, in the cases considered, using the DPL of flexible wall for higher stiffness wall leads to underestimation of the maximum strut forces and unsafe design of the strutting system.

The underestimation of strut forces may be seen in Figure 4.10(b) and Figure 4.10(c) for medium and stiff walls, respectively. In the medium wall, the finite element computed maximum strut force exceeds the maximum force from DPL by up to 25% in three-dimensional analysis and 15% in plane strain analysis. For the high stiffness wall, about 35% underestimation from DPL is observed to occur for both two-dimensional and three-dimensional analyses.

The results from this project indicate that the DPL Method can serve as a good estimation for the struts design. However, this approach may be used for high flexibility walls only. Further analyses are required to ensure the effectiveness of the struts design.

4.4 Effects of improvement methods to the strut forces

Since the strut forces in staged excavation can vary, i.e. the maximum force doesn't necessarily occur at the end of the final excavation, the maximum forces of each strut are compiled in Figure 4.11(a) for flexible wall, 4.11(b) for medium wall, and 4.11(c) for stiff wall to be compared.

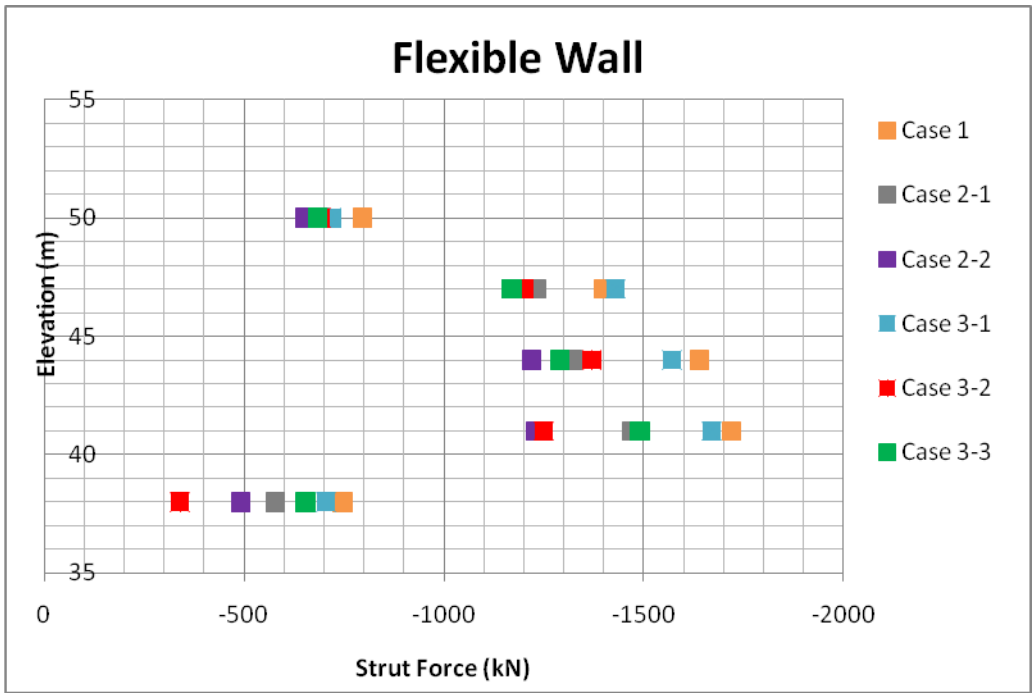
Flexible Wall
55
50
45
40
35
Elevation (m)
0
-500
-1000
-1500
-2000
Strut Force (kN)
Case 1
Case 2-1
Case 2-2
Case 3-1
Case 3-2
Case 3-3

4.11 (a)

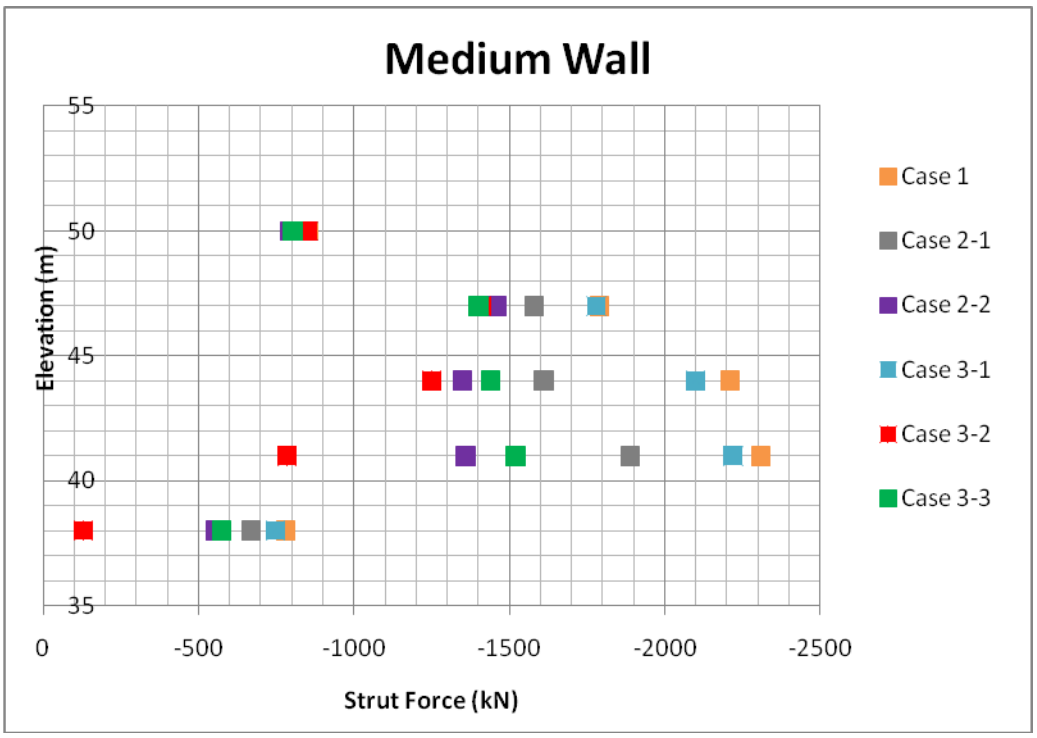
Medium Wall
55
50
45
40
35
Elevation (m)
0
-500
-1000
-1500
-2000
-2500
Strut Force (kN)
Case 1
Case 2-1
Case 2-2
Case 3-1
Case 3-2
Case 3-3

4.11 (b)

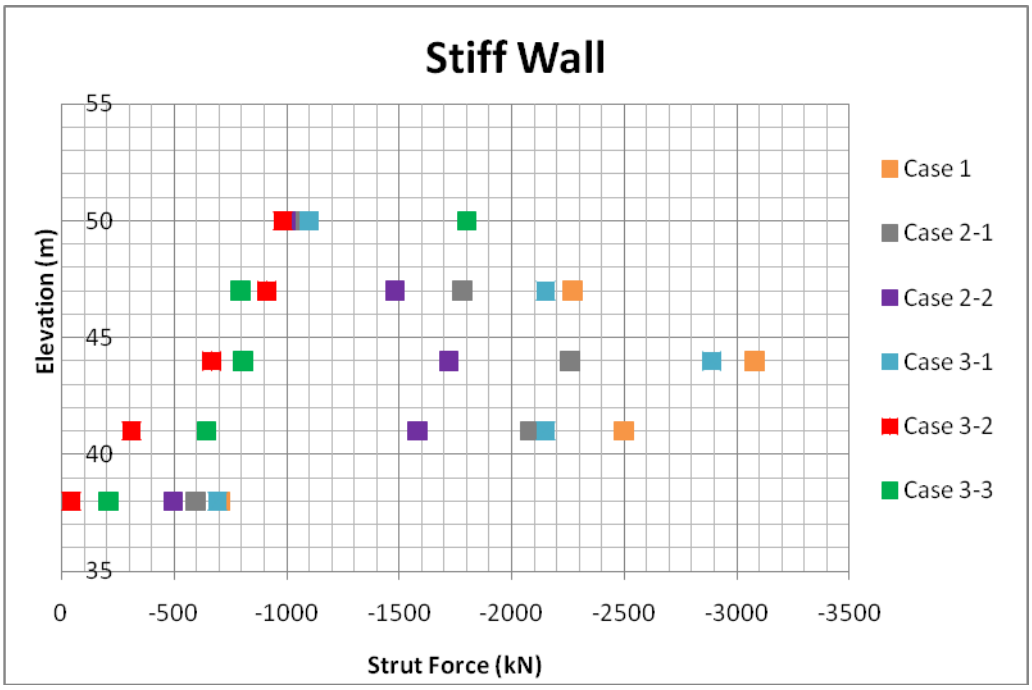

4.11 (c)

Figure 4.11: Strut Force vs Depth of Various Cases on: (a) Flexible Wall, (b) Medium Wall, and (c) Stiff Wall

The plot shows that the strut forces increase with the increase of the wall stiffness. More restraint to the wall movement, which is provided by higher stiffness wall, results in larger earth pressures, thereby affecting the distribution of the strut forces. However, by applying the improvement methods, i.e. jet grouting and cross wall, the strut forces are observed to decrease. The earth pressure is distributed not only to the struts, but also to the jet grout layer or cross walls.

In the cases of the flexible wall, Case 2-2 gives the best performance in reducing the maximum strut force, namely from 1750kN to 1200kN. Case 2-1 and Case 3-3 show similar reductions to 1500kN, while Case 3-2 shows a reduction to 1400kN. For Case 3-1, the change in the maximum strut forces is negligible.

For the medium wall, Case 2-2 gives a significant reduction in strut forces, from 2400kN to 1500kN, while Case 2-1 shows about 500kN reduction to 1900kN. The largest reduction is for Case 3-2, i.e. to 1400kN. Case 3-3 shows the maximum strut force of 1600kN and Case 3-1 shows that the reduction of the maximum strut force is negligible.

For high stiffness wall, Case 3-2 gives the best performance of reducing the maximum strut force from 3100kN to 1000kN. The reduction of Case 3-3 is not significant although it successfully reduces the wall movement by more than 50%. The maximum strut force for this case is 1800kN. The strut forces reduction of wall type jet grouting in Case 2-1 and block type jet grouting in Case 2-2 are similar. The former reduces the maximum strut forces to 2300kN while the latter reduces it slightly more to 1700kN. As observed in the previous cases, Case 3-1 gives negligible reduction.

As stated before, the strut forces distribution is difficult to predict. The best improvement method for the serviceability limit state (displacement) doesn't guarantee the best performance in reducing the strut forces, although the poor performance in reducing the wall movement will result in the same poor results in reducing the strut forces. Thus, an empirical observation is needed for judging the better methods for designing the strutting system. Smaller maximum strut force gives the benefit of having smaller section of struts. Hence, for this typical soil condition, it is clear that either jet grouting or cross wall gives structural efficiency in the design of the struts. Jet grouting performs better in flexible wall, but the installation of cross wall is better in reducing the strut force for the higher stiffness wall.

CHAPTER 5

CONCLUSIONS AND RECOMMENDATIONS

5.1 Conclusion

The objective of this project is to highlight the effectiveness of three-dimensional analyses in simulating and analyzing the excavation and to compare several improvement methods to reduce the excavation-induced wall movement. Three two-dimensional analysis and eighteen three-dimensional analyses have been carried out with different wall stiffness and improvement methods.

The following conclusion can be drawn in this project:

- Three-dimensional analysis gives less conservative results of ultimate and serviceability limit state, thus leads to more economical design of the excavation system.
- In this project, as the wall stiffness increases, the Plain Strain Ratio (PSR) decreases due to less significant cornering effect experienced.
- The improvement methods may be used to reduce the wall deflection as well as the strut forces.
- Wall-type jet grouting performs better in reducing the wall movement as compared to the block-type jet grouting. However, the latter performs better in reducing the strut forces.
- Cross walls should be positioned correctly in order to restrain the wall movement and strut forces effectively, i.e. around the centre of the excavation where the movement is the largest.
- Jet grouting is better in reducing the wall movement and strut forces for flexible wall, but cross walls system performs better for higher stiffness wall.
- Semi empirical method, such as Distributed Propped Load (DPL) Method, overestimates the maximum strut force for flexible wall, but underestimates the maximum strut force for medium and stiff wall.

5.2 Recommendation

The findings presented in this report showed that improvement methods could effectively limit the excavation-induced wall movement and strut forces. However, the improvement methods described here were limited to jet grouting and cross walls system. There are still more methods to be considered. Thus, more methods, such as buttress walls system and berm, should be analyzed and compared as well. Column type ground improvement may be assessed as well as a further study to the jet grouting method.

The study can be extended by introducing various thicknesses of jet grout layer and the depths of the cross walls. The results may then be compared with current findings. The purpose is to assess the effect of the embedment depth of jet grout and cross walls in reducing the wall movement and strut forces.

The properties of the jet grout and the cross walls may be changed as well, in order to assess the significance of the stiffness over geometry to reduce the wall movement and strut forces.

REFERENCES

Atkinson, J.H., 1993. *An Introduction to the Mechanics of Soils and Foundations: Through Critical State of Soil Mechanics*, McGraw-Hill, New York.

Bowles, J.E., 1996. *Foundation Analysis and Design*. 5th ed, McGraw-Hill, New York.

Burland, J.N., 1989. Ninth Laurits Bjerrum Memorial Lecture: Small is Beautiful – The Stiffness of Soils at Small Strain. *Canadian Geotechnical Journal*, Vol. 26, No. 4, pp 499-516.

Clough, G.W. and O'Rourke, T.D., 1990. Construction Induced Movements of In Situ Walls. *Proceeding to Design and Performance of Earth Retaining Structure*, Geotechnical Special Publication No. 25, ASCE, pp 439-470.

Craig, R.F., 2004. *Craig's Soil Mechanics*. 7th ed, Spon Press, New York.

Das, M.B., 1999. *Principles of Geotechnical Engineering*. 6th ed, Thomson Learning, Canada.

Das, M.B., 2007. *Principles of Foundation Engineering*. 6th ed. Thomson Learning, Canada.

Finno, R.J., Blackburn, J.T. and Roboski, J.F., 2007. Three-Dimensional Effects for Supported Excavations in Clay. *Journal of Geotechnical and Geoenvironmental Engineering*, Vol. 133, No. 1, January, pp 30-36.

Gaba, A.R., Simpson, B., Powrie, W. and Beadman, D.R., 2003. *Embedded Retaining Walls – Guidance for Economic Design C580*. CIRIA, London.

Golder, H.Q., Gould, J.P., Lambe, T.W., Tschebotarioff, G.P. and Wilson, S.D., 1970. Predicted Performance of Braced Excavation. *Journal of the Soil Mechanics and Foundation Division*, Vol. 96, No. 3, May, pp 801-815.

Hashash, Y. M. A. and Whittle, A. J., 1996. Ground Movement prediction for Deep Excavations in Soft Clay. *Journal of Geotechnical Engineering*, Vol. 122, No. 6, pp 474-486.

Hight, D.W. and Higgins, k.G., 1995. An Approach to the Prediction of Ground Movements in Engineering Practice: Background and Application. *International Symposium on prefailure Deformation Characteristics of Geomaterials*, Vol. 2, Balkema, Rotterdam, The Netherlands, pp 909-945.

Hsieh, H.S. and Ou, C.Y., 1998. Shape of Ground Surface Settlement Profiles Caused by Excavation. *Canada Geotechnical Journal*, Vol. 35, No. 6, pp 1004-1017.

Hsieh, H.S., Wang, C.C. and Ou, C.Y., 2003. Use of Jet Grouting to Limit Diapraghm Wall Displacement of a Deep Excavation. *Journal of Geotechnical and Geoenvironmental Engineering*, Vol. 129, No. 2, February, pp 146-157.

Hsieh, H.S., Lu, Y.C. and Lin, T.M., 2008. Effects of Joint Details on the Behavior of Cross Walls. *Journal of geoEngineering*, Vol. 3, No. 2, August, pp 55-60.

Hsiung, B.C.B., Lin, H.D. and Lin, W.B., 2005. Influences of Use of Pile-Type Cross-Walls on Deep Excavations. *Journal of Taylor and Francis Group*, pp 803-808.

Kung, G.T.C., Juang, C.H., Hsiao, E. C. LO. and Hashhash, Y.M.A., 2007. Simplified Model for Wall Deflection and Ground Surface Settlement Caused by Braced Excavation in Clays. *Journal of Geotechnical and Geoenvironmental Engineering*, Vol. 133, No. 6, June, pp 731-734.

Lambe et. al., 1970. Measured Performance of Braced Excavation. *JSMFD, ASCE*, Vol. 96, No. 3, May, pp 817-836.

Lee, F.H., Yong, K.Y., Quan, K.C.N. and Chee, K.T., 1998. Effect of Corners in Strutted Excavations: Field Monitoring and Case Histories. *Journal of Geotechnical and Geoenvironmental Engineering*, Vol. 124, No. 4, pp 339-349.

Liao, H.J. and Liu, C.H., 1996. The Influence of High-pressure jetted Grouting on Silty Clay. *Journal of Chinese Institute of Civil and Hydraulic Engineering*, Vol. 8, No. 2, pp 171-182.

Liao, H.J., Lin, C.C. and Huang, C.J., 2008. Modeling the Effect of Ground Improvement on Reducing Movement during Bermed Excavation in Clay. *Journal of the Chinese Institute of Engineers*, Vol. 31, No. 1, January, pp 81-93.

Lin, Y.K., Sun, Y.H., Lu, F.C. and Huang, C.H., 2000. A Note on Application of Ground Improvement in Deep Excavation in Soft Clay. *SinoGeotechnique*, Vol. 78, pp 104-112.

Lin, W.B., 2003. Analysis of Deep Excavation Behavior of Clay Improved by Pile-Type Cross Wall. *MSc Thesis*, National Taiwan University of Science and Technology, Taipei.

Mana, A. I. and Clough, G.W., 1981. Prediction of Movements for Braced Cuts in Clay. *Journal of the Geotechnical Engineering Division*, Vol. 107, No. 6, June, pp 759-777.

Ou, C.Y., Chiou, D.C. and Wu, T.S., 1996. Three-Dimensional Finite Element Analysis of Deep Excavation. *Journal of Geotechnical Engineering*, Vol. 122, No. 5, September, pp 337-345

Ou, C.Y., Wu, T.S. and Hsieh, H.S., 1996. Analysis of Deep Excavation with Column Type of ground Improvement in Soft Clay. *Journal of Geotechnical and Engineering*, Vol. 122, No. 9, September, pp 709-716.

Ou, C.Y., Shiau, B.Y. and Wang, I.W., 2000. Three-Dimensional Deformation of the Taipei National Enterprise Centre (TNEC) Excavation Case History. Canada Geotechnical Journal, Vol. 37, No. 2, pp 438-448.

Ou, C.Y., Lin, Y.L. and Hsieh, P.G., 2006. Case Record of An Excavation with Cross Walls and Buttress Walls. *Journal of GeoEngineering*, Vol, 1, No. 2, December, pp 79-86.

Ou, C.Y., Teng, F.C. and Wang, I.W., 2007. Analysis and Design of partial ground Improvement in Deep Excavations. *Computers and Geotechnics*, Vol 35, No. 4, July, pp 576-584.

Peck, R.B., 1943. Earth Pressure Measurements in Open Cuts. Trans. ASCE, Vol. 108, pp 1008-1058.

Puller, M., 1996. *Deep Excavation: A Practical Manual*. Thomas Telford, London.

Raymond, G.P., 1997. Braced and Strutted Excavations. *Lecture on Geotechnical Engineering*.

Roboski, M.A., 1974. Three-Dimensional Performance and Analysis of Deep Excavations. *PhD Thesis*, Northwestern University, Illinois.

Sherif, M.A. and Fang, Y.S., 1984. Dynamic Earth Pressure on Walls Rotating About the Top. *Soils and Foundations*, Vol. 24, No. 4, December, pp 109-117.

Simic, M. and French, D.J., 1998. Three-Dimensional Analysis of Deep Underground Station. *Proceeding to Conference Value of Geotechnics in Construction*, Institution of Civil Engineering, London.

Simpson, B. and Powrie, W., 2001. Embedded Retaining Walls: Theory, Practice, and Understanding. *Perspective Lecture on 15th International Conference on Soil Mechanics and Geotechnical Engineering*, Istanbul.

Terashi, M., 2003. The State of Practice in Deep Mixing Methods. *Proceedings of the International Conference of Geotechnical Centrifuge Modeling – Centrifuge 88*, Paris, France, pp 233-242.

Terzaghi, K., Peck, R.B. and Mesri, G., 1996. *Soil Mechanics in Engineering Practice*. 3rd ed, John Wiley and Sons, New York.

Tomlinson, M.J., 1980. *Foundation Design and Construction*, 4th ed, Pitman, London.

Tschebotarioff, G.P., 1973. *Foundations Retaining and Earth Structures*, 2nd ed, Mcgraw-Hill, New York.

Twine, D. and Roscoe, H., 1999. *Temporary Propping of Deep Excavation - Guidance on Design Publication C517*. CIRIA, London.

Whittle, A.J., Hashash, Y.M.A. and Whitman, R.V., 1993. Analysis of Deep Excavation in Boston. *Journal of Geotechnical Engineering*, Vol. 119, No. 1, pp 69-90.

Wong, K.S. and Broms, B.B., 1989. Lateral Wall Deflections of Braced Excavations in Clay. *Journal of Geotechnical Engineering*, Vol. 115, No. 6, pp 853-870.

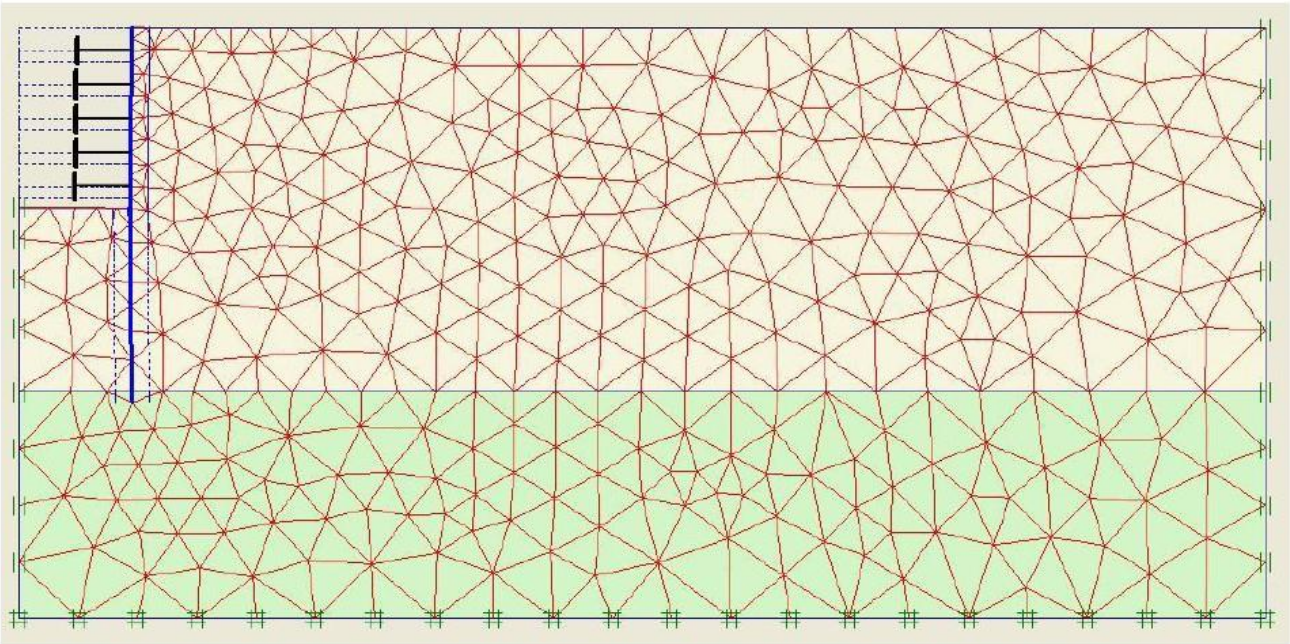

NANYANG TECHNOLOGICAL UNIVERSITY

Appendix A1: Two-dimensional PLAXIS Model of Case 1

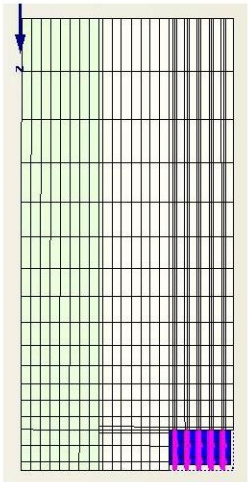

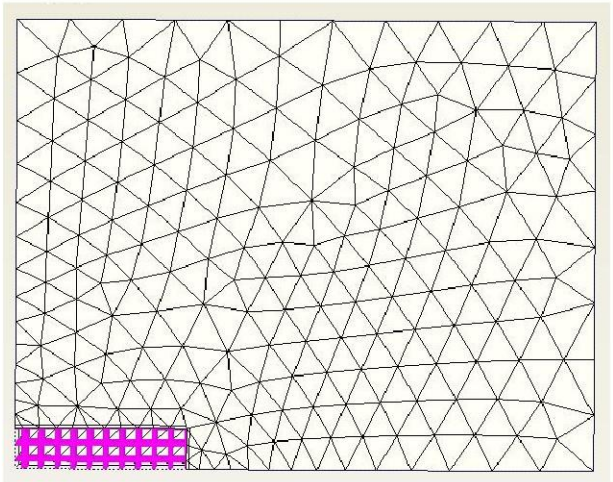

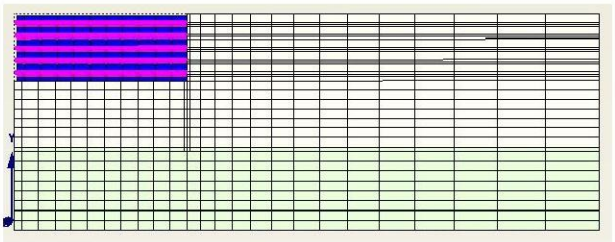

NANYANG TECHNOLOGICAL UNIVERSITY

Appendix A2: Three-dimensional PLAXIS Model of Case 1

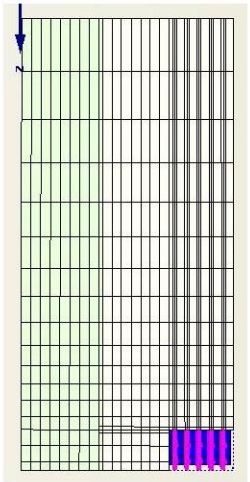

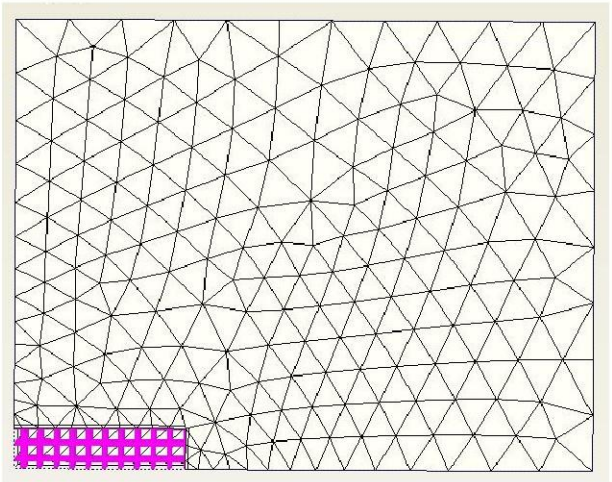

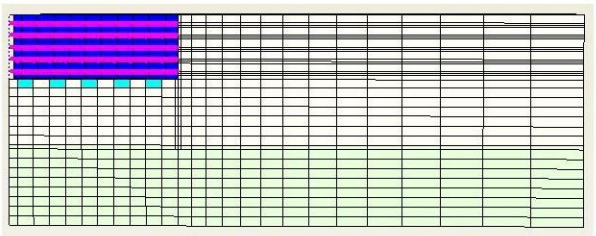

NANYANG TECHNOLOGICAL UNIVERSITY

Appendix B: Three-dimensional PLAXIS Model of Case 2

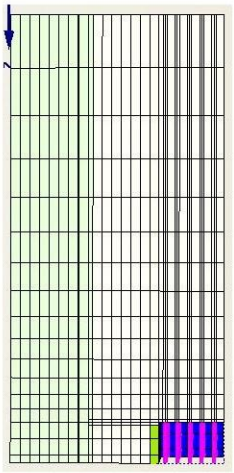

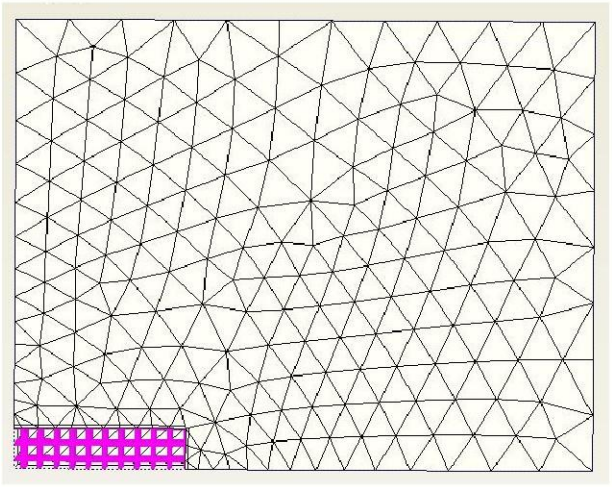

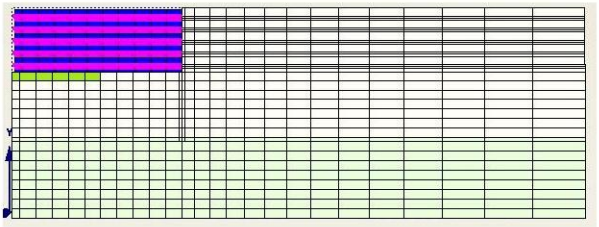

NANYANG TECHNOLOGICAL UNIVERSITY

Appendix B2: Three-dimensional PLAXIS Model of Case 2-2

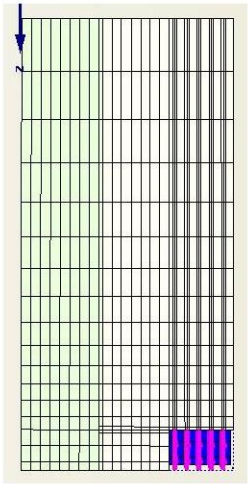

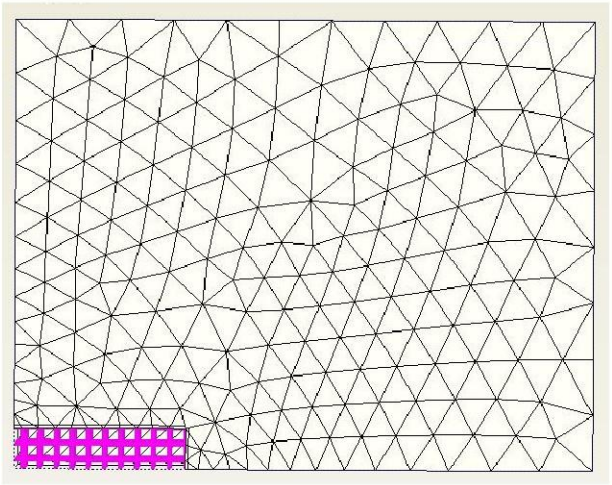

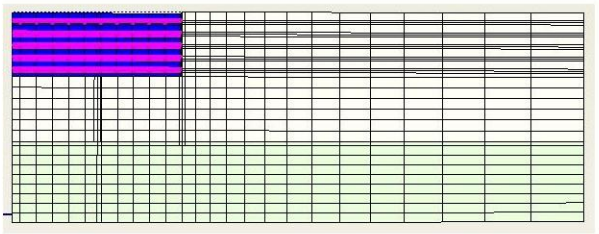

NANYANG TECHNOLOGICAL UNIVERSITY

Appendix C1: Three-dimensional PLAXIS Model of Case 3-1

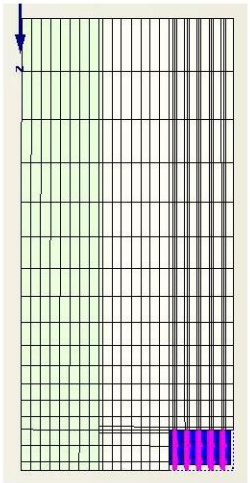

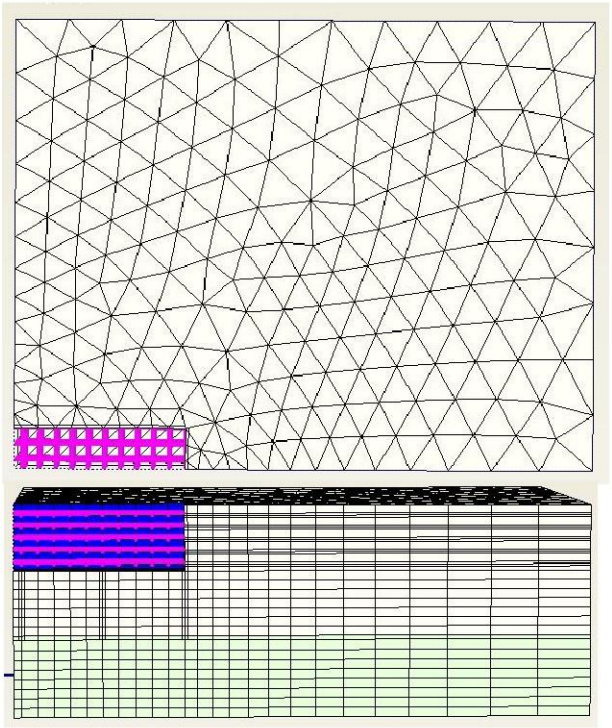

NANYANG TECHNOLOGICAL UNIVERSITY

Appendix C2: Three-dimensional PLAXIS Model of Case 3-2

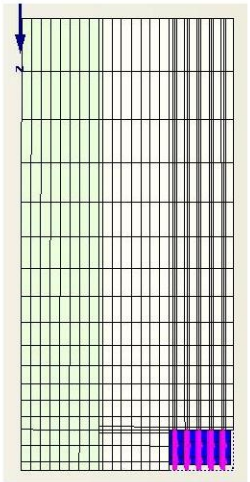

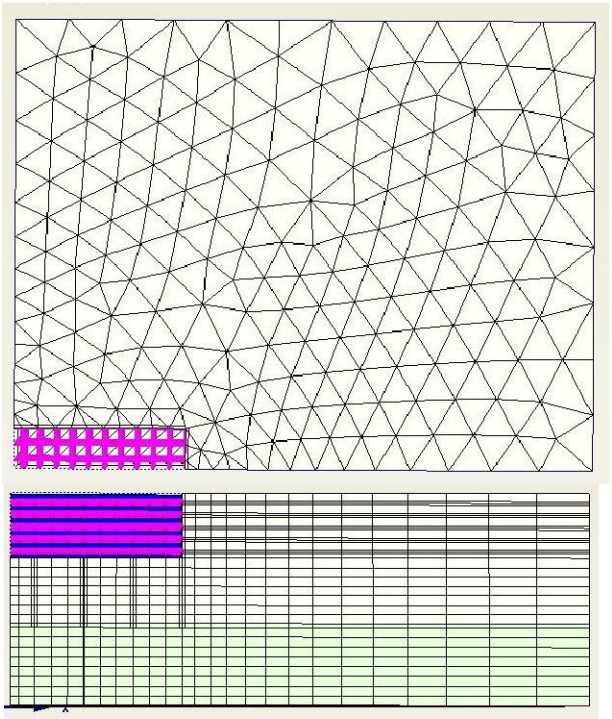

NANYANG TECHNOLOGICAL UNIVERSITY

Appendix C3: Three-dimensional PLAXIS Model of Case 3-3

Appendix D: Plane Strain Simulation Results

Flexible Wall		Medium Wall		Stiff Wall	
Depth (m)	Wall Movement (m)	Depth (m)	Wall Movement (m)	Depth (m)	Wall Movement (m)
52	0.020997	52	0.019561	52	0.017302
51.75	0.022031	51.75	0.020468	51.75	0.018141
51.5	0.023066	51.5	0.021375	51.5	0.018979
51.25	0.024106	51.25	0.022282	51.25	0.019817
51	0.025159	51	0.023191	51	0.020655
51	0.025159	51	0.023191	51	0.020655
50.75	0.026235	50.75	0.0241	50.75	0.021494
50.5	0.027347	50.5	0.025013	50.5	0.022332
50.25	0.02851	50.25	0.025928	50.25	0.023171
50	0.029744	50	0.026849	50	0.024011
50	0.029744	50	0.026849	50	0.024011
49.75	0.031087	49.75	0.027775	49.75	0.02485
49.5	0.032498	49.5	0.02871	49.5	0.025691
49.25	0.033959	49.25	0.029654	49.25	0.026533
49	0.035453	49	0.030611	49	0.027377
49	0.035453	49	0.030611	49	0.027377
48.75	0.036974	48.75	0.031585	48.75	0.028225
48.5	0.038516	48.5	0.032577	48.5	0.029075
48.25	0.040083	48.25	0.033593	48.25	0.02993
48	0.041683	48	0.034636	48	0.03079
48	0.041683	48	0.034636	48	0.03079
47.75	0.04333	47.75	0.035713	47.75	0.031656
47.5	0.045047	47.5	0.036828	47.5	0.032529
47.25	0.046863	47.25	0.037988	47.25	0.033409
47	0.048817	47	0.039201	47	0.034299
47	0.048817	47	0.039201	47	0.034299
46.75	0.050994	46.75	0.040478	46.75	0.035198
46.5	0.053302	46.5	0.041811	46.5	0.036106
46.25	0.0557	46.25	0.043197	46.25	0.037024

46	0.058153	46	0.044632	46	0.037949
46	0.058153	46	0.044632	46	0.037949
45.75	0.060638	45.75	0.046116	45.75	0.038881
45.5	0.06314	45.5	0.047647	45.5	0.039821
45.25	0.065652	45.25	0.049226	45.25	0.040768
45	0.068178	45	0.050853	45	0.041722
45	0.068178	45	0.050853	45	0.041722
44.75	0.070732	44.75	0.05253	44.75	0.042682
44.5	0.073337	44.5	0.054261	44.5	0.043649
44.25	0.076026	44.25	0.05605	44.25	0.044622
44	0.078844	44	0.0579	44	0.045603
44	0.078844	44	0.0579	44	0.045603
43.75	0.081896	43.75	0.059825	43.75	0.046591
43.5	0.08507	43.5	0.061808	43.5	0.047585
43.25	0.088315	43.25	0.063841	43.25	0.048582
43	0.09159	43	0.065915	43	0.04958
43	0.09159	43	0.065915	43	0.04958
42.75	0.094868	42.75	0.068025	42.75	0.050578
42.5	0.098129	42.5	0.070163	42.5	0.051574
42.25	0.101366	42.25	0.072327	42.25	0.052567
42	0.104581	42	0.074512	42	0.053555
42	0.104581	42	0.074512	42	0.053555
41.75	0.107788	41.75	0.076718	41.75	0.054537
41.5	0.111011	41.5	0.078941	41.5	0.055511
41.25	0.114284	41.25	0.081184	41.25	0.056478
41	0.117654	41	0.083447	41	0.057436
41	0.117654	41	0.083447	41	0.057436
40.75	0.121233	40.75	0.085741	40.75	0.058384
40.5	0.124887	40.5	0.088042	40.5	0.05932
40.25	0.128551	40.25	0.090336	40.25	0.060242
40	0.132168	40	0.09261	40	0.061148
40	0.132168	40	0.09261	40	0.061148
39.75	0.135691	39.75	0.094852	39.75	0.062035
39.5	0.139083	39.5	0.097051	39.5	0.062901
39.25	0.142315	39.25	0.099197	39.25	0.063746

39	0.145367	39	0.101282	39	0.064568
39	0.145367	39	0.101282	39	0.064568
38.75	0.148227	38.75	0.103299	38.75	0.065365
38.5	0.15089	38.5	0.105241	38.5	0.066135
38.25	0.15336	38.25	0.107105	38.25	0.066878
38	0.155648	38	0.108884	38	0.067593
38	0.155648	38	0.108884	38	0.067593
37.75	0.157798	37.75	0.110581	37.75	0.068279
37.5	0.159746	37.5	0.112184	37.5	0.068935
37.25	0.161463	37.25	0.113685	37.25	0.069557
37	0.162926	37	0.115079	37	0.070146
37	0.162926	37	0.115079	37	0.070146
36.75	0.164119	36.75	0.116361	36.75	0.070698
36.5	0.165035	36.5	0.117528	36.5	0.071214
36.25	0.165673	36.25	0.118577	36.25	0.071692
36	0.166039	36	0.119507	36	0.07213
36	0.166039	36	0.119507	36	0.07213
35.65538	0.16613	35.65538	0.120593	35.65538	0.07267
35.31077	0.165786	35.31077	0.121455	35.31077	0.073132
34.96615	0.165048	34.96615	0.122096	34.96615	0.073515
34.62154	0.163956	34.62154	0.122518	34.62154	0.073818
34.62154	0.163956	34.62154	0.122518	34.62154	0.073818
34.24105	0.162386	34.24105	0.122736	34.24105	0.074059
33.86056	0.160478	33.86056	0.1227	33.86056	0.0742
33.48007	0.158274	33.48007	0.122418	33.48007	0.07424
33.09959	0.155813	33.09959	0.121898	33.09959	0.074179
33.09959	0.155813	33.09959	0.121898	33.09959	0.074179
32.6795	0.152838	32.6795	0.121058	32.6795	0.073995
32.2594	0.149628	32.2594	0.11995	32.2594	0.073687
31.83931	0.146217	31.83931	0.118587	31.83931	0.073257
31.41922	0.142634	31.41922	0.116981	31.41922	0.072706
31.41922	0.142634	31.41922	0.116981	31.41922	0.072706
30.9554	0.138507	30.9554	0.114942	30.9554	0.071958
30.49158	0.134226	30.49158	0.112639	30.49158	0.071066
30.02776	0.129813	30.02776	0.11009	30.02776	0.070032

29.56394	0.125287	29.56394	0.10731	29.56394	0.068861
29.56394	0.125287	29.56394	0.10731	29.56394	0.068861
29.05185	0.120175	29.05185	0.103991	29.05185	0.06741
28.53975	0.114957	28.53975	0.100431	28.53975	0.065801
28.02765	0.109642	28.02765	0.09665	28.02765	0.064039
27.51555	0.104237	27.51555	0.092666	27.51555	0.062129
27.51555	0.104237	27.51555	0.092666	27.51555	0.062129
26.95015	0.098168	26.95015	0.088053	26.95015	0.059859
26.38475	0.09199	26.38475	0.083239	26.38475	0.057427
25.81935	0.085699	25.81935	0.078247	25.81935	0.054844
25.25395	0.079291	25.25395	0.0731	25.25395	0.052122
25.25395	0.079291	25.25395	0.0731	25.25395	0.052122
24.62969	0.072083	24.62969	0.067266	24.62969	0.048968
24.00544	0.064746	24.00544	0.061303	24.00544	0.045673
23.38118	0.05732	23.38118	0.055247	23.38118	0.042256
22.75693	0.049873	22.75693	0.049133	22.75693	0.038732
22.75693	0.049873	22.75693	0.049133	22.75693	0.038732
22.0677	0.04176	22.0677	0.042363	22.0677	0.034742
21.37847	0.033975	21.37847	0.035625	21.37847	0.03067
20.68923	0.026813	20.68923	0.028976	20.68923	0.026543
20	0.02065	20	0.022476	20	0.022387
20	0.02065	20	0.022476	20	0.022387
19.75	0.018764	19.75	0.020168	19.75	0.020877
19.5	0.017072	19.5	0.017887	19.5	0.019368
19.25	0.015515	19.25	0.015627	19.25	0.017859
19	0.014019	19	0.013376	19	0.01635
	0.16613		0.122736		0.07424

Appendix E: Three-dimensional Simulation Results

Case 1					
Flexible Wall		Medium Wall		Stiff Wall	
Depth (m)	Wall Movement (m)	Depth (m)	Wall Movement (m)	Depth (m)	Wall Movement (m)
5.20E+01	2.22E-02	5.20E+01	1.76E-02	5.20E+01	1.46E-02
5.10E+01	2.69E-02	5.10E+01	2.06E-02	5.10E+01	1.75E-02
5.00E+01	2.67E-02	5.00E+01	2.33E-02	5.00E+01	2.03E-02
4.98E+01	2.76E-02	4.98E+01	2.42E-02	4.98E+01	2.10E-02
4.95E+01	2.81E-02	4.95E+01	2.49E-02	4.95E+01	2.17E-02
4.93E+01	2.80E-02	4.93E+01	2.54E-02	4.93E+01	2.24E-02
4.90E+01	3.04E-02	4.90E+01	2.64E-02	4.90E+01	2.32E-02
4.70E+01	4.08E-02	4.70E+01	3.35E-02	4.70E+01	2.91E-02
4.68E+01	4.20E-02	4.68E+01	3.45E-02	4.68E+01	2.99E-02
4.65E+01	4.37E-02	4.65E+01	3.56E-02	4.65E+01	3.07E-02
4.63E+01	4.44E-02	4.63E+01	3.64E-02	4.63E+01	3.15E-02
4.60E+01	4.79E-02	4.60E+01	3.78E-02	4.60E+01	3.23E-02
4.50E+01	6.35E-02	4.50E+01	4.23E-02	4.50E+01	3.52E-02
4.40E+01	6.52E-02	4.40E+01	4.84E-02	4.40E+01	3.89E-02
4.38E+01	6.40E-02	4.38E+01	4.77E-02	4.38E+01	3.92E-02
4.35E+01	6.96E-02	4.35E+01	5.16E-02	4.35E+01	4.06E-02
4.33E+01	7.10E-02	4.33E+01	5.29E-02	4.33E+01	4.14E-02
4.30E+01	7.52E-02	4.30E+01	5.48E-02	4.30E+01	4.23E-02
4.20E+01	9.37E-02	4.20E+01	6.32E-02	4.20E+01	4.60E-02
4.10E+01	9.66E-02	4.10E+01	6.90E-02	4.10E+01	4.93E-02
4.08E+01	9.86E-02	4.08E+01	7.08E-02	4.08E+01	5.02E-02
4.05E+01	1.02E-01	4.05E+01	7.27E-02	4.05E+01	5.11E-02
4.03E+01	1.03E-01	4.03E+01	7.42E-02	4.03E+01	5.19E-02
4.00E+01	1.08E-01	4.00E+01	7.63E-02	4.00E+01	5.27E-02
3.90E+01	1.24E-01	3.90E+01	8.46E-02	3.90E+01	5.60E-02
3.80E+01	1.26E-01	3.80E+01	8.92E-02	3.80E+01	5.86E-02
3.78E+01	1.28E-01	3.78E+01	9.04E-02	3.78E+01	5.93E-02
3.75E+01	1.30E-01	3.75E+01	9.19E-02	3.75E+01	5.99E-02

3.70E+01	1.32E-01	3.70E+01	9.41E-02	3.70E+01	6.10E-02
3.65E+01	1.35E-01	3.65E+01	9.62E-02	3.65E+01	6.20E-02
3.60E+01	1.34E-01	3.60E+01	9.76E-02	3.60E+01	6.29E-02
3.49E+01	1.32E-01	3.49E+01	9.97E-02	3.49E+01	6.44E-02
3.37E+01	1.29E-01	3.37E+01	9.99E-02	3.37E+01	6.50E-02
3.26E+01	1.23E-01	3.26E+01	9.84E-02	3.26E+01	6.49E-02
3.14E+01	1.16E-01	3.14E+01	9.54E-02	3.14E+01	6.40E-02
3.03E+01	1.07E-01	3.03E+01	9.09E-02	3.03E+01	6.22E-02
2.91E+01	9.85E-02	2.91E+01	8.54E-02	2.91E+01	5.98E-02
2.80E+01	8.93E-02	2.80E+01	7.90E-02	2.80E+01	5.66E-02
2.69E+01	8.02E-02	2.69E+01	7.18E-02	2.69E+01	5.28E-02
2.57E+01	7.04E-02	2.57E+01	6.39E-02	2.57E+01	4.84E-02
2.46E+01	6.03E-02	2.46E+01	5.56E-02	2.46E+01	4.35E-02
2.34E+01	4.97E-02	2.34E+01	4.68E-02	2.34E+01	3.82E-02
2.23E+01	3.88E-02	2.23E+01	3.80E-02	2.23E+01	3.27E-02
2.11E+01	2.90E-02	2.11E+01	2.95E-02	2.11E+01	2.69E-02
2.00E+01	1.92E-02	2.00E+01	2.06E-02	2.00E+01	2.10E-02
1.95E+01	1.55E-02	1.95E+01	1.67E-02	1.95E+01	1.83E-02
1.90E+01	1.37E-02	1.90E+01	1.37E-02	1.90E+01	1.58E-02

Case 2-1					
Flexible Wall		Medium Wall		Stiff Wall	
Depth (m)	Wall Movement (m)	Depth (m)	Wall Movement (m)	Depth (m)	Wall Movement (m)
5.20E+01	2.22E-02	5.20E+01	1.99E-02	5.20E+01	1.79E-02
5.10E+01	2.64E-02	5.10E+01	2.23E-02	5.10E+01	1.97E-02
5.00E+01	2.66E-02	5.00E+01	2.45E-02	5.00E+01	2.14E-02
4.95E+01	2.80E-02	4.95E+01	2.57E-02	4.95E+01	2.23E-02
4.90E+01	3.00E-02	4.90E+01	2.69E-02	4.90E+01	2.32E-02
4.80E+01	3.95E-02	4.80E+01	3.01E-02	4.80E+01	2.51E-02
4.70E+01	3.94E-02	4.70E+01	3.23E-02	4.70E+01	2.70E-02
4.65E+01	4.20E-02	4.65E+01	3.38E-02	4.65E+01	2.79E-02
4.63E+01	4.25E-02	4.63E+01	3.43E-02	4.63E+01	2.84E-02

4.60E+01	4.56E-02	4.60E+01	3.53E-02	4.60E+01	2.89E-02
4.50E+01	5.86E-02	4.50E+01	3.83E-02	4.50E+01	3.06E-02
4.40E+01	5.93E-02	4.40E+01	4.21E-02	4.40E+01	3.29E-02
4.38E+01	5.83E-02	4.38E+01	4.12E-02	4.38E+01	3.29E-02
4.35E+01	6.24E-02	4.35E+01	4.40E-02	4.35E+01	3.40E-02
4.33E+01	6.32E-02	4.33E+01	4.46E-02	4.33E+01	3.45E-02
4.30E+01	6.63E-02	4.30E+01	4.58E-02	4.30E+01	3.50E-02
4.20E+01	7.94E-02	4.20E+01	5.09E-02	4.20E+01	3.72E-02
4.10E+01	7.84E-02	4.10E+01	5.33E-02	4.10E+01	3.91E-02
4.08E+01	7.92E-02	4.08E+01	5.41E-02	4.08E+01	3.96E-02
4.05E+01	8.06E-02	4.05E+01	5.51E-02	4.05E+01	4.02E-02
4.03E+01	8.08E-02	4.03E+01	5.56E-02	4.03E+01	4.06E-02
4.00E+01	8.34E-02	4.00E+01	5.68E-02	4.00E+01	4.11E-02
3.90E+01	9.42E-02	3.90E+01	6.14E-02	3.90E+01	4.30E-02
3.80E+01	8.90E-02	3.80E+01	6.24E-02	3.80E+01	4.45E-02
3.78E+01	8.84E-02	3.78E+01	6.28E-02	3.78E+01	4.48E-02
3.75E+01	8.89E-02	3.75E+01	6.34E-02	3.75E+01	4.52E-02
3.73E+01	8.78E-02	3.73E+01	6.36E-02	3.73E+01	4.55E-02
3.70E+01	8.84E-02	3.70E+01	6.42E-02	3.70E+01	4.58E-02
3.65E+01	9.13E-02	3.65E+01	6.58E-02	3.65E+01	4.65E-02
3.60E+01	8.64E-02	3.60E+01	6.53E-02	3.60E+01	4.68E-02
3.50E+01	7.51E-02	3.50E+01	6.38E-02	3.50E+01	4.73E-02
3.40E+01	7.87E-02	3.40E+01	6.59E-02	3.40E+01	4.79E-02
3.17E+01	7.43E-02	3.17E+01	6.46E-02	3.17E+01	4.75E-02
3.05E+01	7.35E-02	3.05E+01	6.28E-02	3.05E+01	4.65E-02
2.93E+01	7.17E-02	2.93E+01	6.06E-02	2.93E+01	4.50E-02
2.82E+01	6.68E-02	2.82E+01	5.73E-02	2.82E+01	4.30E-02
2.70E+01	6.15E-02	2.70E+01	5.32E-02	2.70E+01	4.04E-02
2.58E+01	5.48E-02	2.58E+01	4.82E-02	2.58E+01	3.74E-02
2.47E+01	4.74E-02	2.47E+01	4.26E-02	2.47E+01	3.40E-02
2.35E+01	3.94E-02	2.35E+01	3.64E-02	2.35E+01	3.02E-02
2.23E+01	3.12E-02	2.23E+01	2.99E-02	2.23E+01	2.62E-02
2.12E+01	2.37E-02	2.12E+01	2.35E-02	2.12E+01	2.19E-02
2.00E+01	1.64E-02	2.00E+01	1.71E-02	2.00E+01	1.76E-02
1.95E+01	1.37E-02	1.95E+01	1.43E-02	1.95E+01	1.57E-02

1.90E+01	1.22E-02	1.90E+01	1.20E-02	1.90E+01	1.38E-02

Case 2-2					
Flexible Wall		Medium Wall		Stiff Wall	
Depth (m)	Wall Movement (m)	Depth (m)	Wall Movement (m)	Depth (m)	Wall Movement (m)
5.20E+01	2.24E-02	5.20E+01	2.13E-02	5.20E+01	2.02E-02
5.10E+01	2.64E-02	5.10E+01	2.34E-02	5.10E+01	2.12E-02
5.00E+01	2.68E-02	5.00E+01	2.54E-02	5.00E+01	2.23E-02
4.98E+01	2.78E-02	4.98E+01	2.60E-02	4.98E+01	2.26E-02
4.95E+01	2.82E-02	4.95E+01	2.64E-02	4.95E+01	2.29E-02
4.93E+01	2.80E-02	4.93E+01	2.67E-02	4.93E+01	2.31E-02
4.90E+01	3.02E-02	4.90E+01	2.75E-02	4.90E+01	2.34E-02
4.80E+01	3.91E-02	4.80E+01	3.03E-02	4.80E+01	2.46E-02
4.70E+01	3.90E-02	4.70E+01	3.20E-02	4.70E+01	2.60E-02
4.68E+01	4.01E-02	4.68E+01	3.27E-02	4.68E+01	2.64E-02
4.65E+01	4.14E-02	4.65E+01	3.33E-02	4.65E+01	2.70E-02
4.63E+01	4.19E-02	4.63E+01	3.36E-02	4.63E+01	2.74E-02
4.60E+01	4.48E-02	4.60E+01	3.45E-02	4.60E+01	2.81E-02
4.50E+01	5.74E-02	4.50E+01	3.79E-02	4.50E+01	3.05E-02
4.40E+01	5.74E-02	4.40E+01	4.04E-02	4.40E+01	3.28E-02
4.38E+01	5.84E-02	4.38E+01	4.12E-02	4.38E+01	3.34E-02
4.35E+01	6.02E-02	4.35E+01	4.27E-02	4.35E+01	3.40E-02
4.33E+01	6.06E-02	4.33E+01	4.32E-02	4.33E+01	3.46E-02
4.30E+01	6.39E-02	4.30E+01	4.50E-02	4.30E+01	3.53E-02
4.20E+01	7.89E-02	4.20E+01	5.13E-02	4.20E+01	3.80E-02
4.10E+01	8.05E-02	4.10E+01	5.57E-02	4.10E+01	4.07E-02
4.08E+01	8.11E-02	4.08E+01	5.66E-02	4.08E+01	4.10E-02
4.05E+01	8.40E-02	4.05E+01	5.87E-02	4.05E+01	4.20E-02
4.03E+01	8.41E-02	4.03E+01	5.92E-02	4.03E+01	4.21E-02
4.00E+01	8.86E-02	4.00E+01	6.13E-02	4.00E+01	4.32E-02
3.90E+01	1.03E-01	3.90E+01	6.82E-02	3.90E+01	4.53E-02
3.80E+01	1.03E-01	3.80E+01	7.14E-02	3.80E+01	4.77E-02

3.78E+01	1.03E-01	3.78E+01	7.23E-02	3.78E+01	4.75E-02
3.75E+01	1.04E-01	3.75E+01	7.33E-02	3.75E+01	4.86E-02
3.73E+01	1.05E-01	3.73E+01	7.40E-02	3.73E+01	4.83E-02
3.70E+01	1.07E-01	3.70E+01	7.51E-02	3.70E+01	4.94E-02
3.65E+01	1.09E-01	3.65E+01	7.70E-02	3.65E+01	4.95E-02
3.60E+01	1.08E-01	3.60E+01	7.76E-02	3.60E+01	5.07E-02
3.50E+01	1.03E-01	3.50E+01	7.76E-02	3.50E+01	5.05E-02
3.40E+01	1.01E-01	3.40E+01	7.83E-02	3.40E+01	5.18E-02
3.28E+01	9.54E-02	3.28E+01	7.71E-02	3.28E+01	5.10E-02
3.17E+01	8.78E-02	3.17E+01	7.35E-02	3.17E+01	5.06E-02
3.05E+01	8.11E-02	3.05E+01	6.94E-02	3.05E+01	4.85E-02
2.93E+01	7.39E-02	2.93E+01	6.46E-02	2.93E+01	4.70E-02
2.82E+01	6.66E-02	2.82E+01	5.89E-02	2.82E+01	4.39E-02
2.70E+01	5.95E-02	2.70E+01	5.33E-02	2.70E+01	4.11E-02
2.58E+01	5.21E-02	2.58E+01	4.68E-02	2.58E+01	3.75E-02
2.47E+01	4.47E-02	2.47E+01	4.07E-02	2.47E+01	3.37E-02
2.35E+01	3.71E-02	2.35E+01	3.44E-02	2.35E+01	2.96E-02
2.23E+01	2.93E-02	2.23E+01	2.79E-02	2.23E+01	2.53E-02
2.12E+01	2.21E-02	2.12E+01	2.17E-02	2.12E+01	2.08E-02
2.00E+01	1.53E-02	2.00E+01	1.60E-02	2.00E+01	1.64E-02
1.95E+01	1.29E-02	1.95E+01	1.34E-02	1.95E+01	1.46E-02
1.90E+01	1.14E-02	1.90E+01	1.14E-02	1.90E+01	1.30E-02

Case 3-1					
Flexible Wall		Medium Wall		Stiff Wall	
Depth (m)	Wall Movement (m)	Depth (m)	Wall Movement (m)	Depth (m)	Wall Movement (m)
5.20E+01	2.84E-02	5.20E+01	2.04E-02	5.20E+01	2.13E-02
5.10E+01	3.30E-02	5.10E+01	2.26E-02	5.10E+01	2.15E-02
5.00E+01	3.44E-02	5.00E+01	2.47E-02	5.00E+01	2.17E-02
4.98E+01	3.56E-02	4.98E+01	2.53E-02	4.98E+01	2.18E-02
4.95E+01	3.64E-02	4.95E+01	2.58E-02	4.95E+01	2.25E-02
4.93E+01	3.55E-02	4.93E+01	2.61E-02	4.93E+01	2.31E-02
4.90E+01	3.69E-02	4.90E+01	2.69E-02	4.90E+01	2.38E-02

4.80E+01	4.41E-02	4.80E+01	3.06E-02	4.80E+01	2.66E-02
4.70E+01	4.19E-02	4.70E+01	3.36E-02	4.70E+01	2.94E-02
4.70E+01	4.40E-02	4.70E+01	3.55E-02	4.70E+01	3.09E-02
4.68E+01	4.27E-02	4.68E+01	3.46E-02	4.68E+01	3.01E-02
4.65E+01	4.40E-02	4.65E+01	3.55E-02	4.65E+01	3.09E-02
4.65E+01	4.77E-02	4.65E+01	3.76E-02	4.65E+01	3.23E-02
4.63E+01	4.45E-02	4.63E+01	3.63E-02	4.63E+01	3.16E-02
4.60E+01	4.77E-02	4.60E+01	3.76E-02	4.60E+01	3.23E-02
4.50E+01	6.26E-02	4.50E+01	4.34E-02	4.50E+01	3.54E-02
4.40E+01	6.39E-02	4.40E+01	4.77E-02	4.40E+01	3.85E-02
4.38E+01	6.56E-02	4.38E+01	4.92E-02	4.38E+01	3.93E-02
4.35E+01	6.81E-02	4.35E+01	5.07E-02	4.35E+01	4.01E-02
4.33E+01	6.94E-02	4.33E+01	5.19E-02	4.33E+01	4.09E-02
4.30E+01	7.34E-02	4.30E+01	5.37E-02	4.30E+01	4.17E-02
4.20E+01	9.05E-02	4.20E+01	6.14E-02	4.20E+01	4.51E-02
4.10E+01	9.34E-02	4.10E+01	6.69E-02	4.10E+01	4.82E-02
4.08E+01	9.53E-02	4.08E+01	6.85E-02	4.08E+01	4.90E-02
4.05E+01	9.79E-02	4.05E+01	7.03E-02	4.05E+01	4.98E-02
4.03E+01	9.96E-02	4.03E+01	7.17E-02	4.03E+01	5.05E-02
4.00E+01	1.04E-01	4.00E+01	7.36E-02	4.00E+01	5.13E-02
3.90E+01	1.19E-01	3.90E+01	8.11E-02	3.90E+01	5.43E-02
3.80E+01	1.21E-01	3.80E+01	8.53E-02	3.80E+01	5.66E-02
3.78E+01	1.22E-01	3.78E+01	8.64E-02	3.78E+01	5.72E-02
3.75E+01	1.23E-01	3.75E+01	8.77E-02	3.75E+01	5.78E-02
3.73E+01	1.24E-01	3.73E+01	8.86E-02	3.73E+01	5.83E-02
3.70E+01	1.26E-01	3.70E+01	8.97E-02	3.70E+01	5.88E-02
3.65E+01	1.28E-01	3.65E+01	9.14E-02	3.65E+01	5.97E-02
3.60E+01	1.27E-01	3.60E+01	9.26E-02	3.60E+01	6.04E-02
3.47E+01	1.24E-01	3.47E+01	9.45E-02	3.47E+01	6.18E-02
3.33E+01	1.19E-01	3.33E+01	9.35E-02	3.33E+01	6.21E-02
3.20E+01	1.11E-01	3.20E+01	9.06E-02	3.20E+01	6.13E-02
3.07E+01	1.02E-01	3.07E+01	8.59E-02	3.07E+01	5.96E-02
2.93E+01	9.17E-02	2.93E+01	7.97E-02	2.93E+01	5.69E-02
2.80E+01	8.18E-02	2.80E+01	7.24E-02	2.80E+01	5.34E-02
2.67E+01	7.13E-02	2.67E+01	6.42E-02	2.67E+01	4.90E-02

2.53E+01	6.07E-02	2.53E+01	5.54E-02	2.53E+01	4.40E-02
2.40E+01	4.95E-02	2.40E+01	4.62E-02	2.40E+01	3.84E-02
2.27E+01	3.84E-02	2.27E+01	3.68E-02	2.27E+01	3.24E-02
2.13E+01	2.83E-02	2.13E+01	2.78E-02	2.13E+01	2.62E-02
2.00E+01	1.80E-02	2.00E+01	1.89E-02	2.00E+01	1.97E-02
1.95E+01	1.48E-02	1.95E+01	1.55E-02	1.95E+01	1.73E-02
1.90E+01	1.29E-02	1.90E+01	1.27E-02	1.90E+01	1.49E-02

Case 3-2					
Flexible Wall		Medium Wall		Stiff Wall	
Depth (m)	Wall Movement (m)	Depth (m)	Wall Movement (m)	Depth (m)	Wall Movement (m)
5.20E+01	2.29E-02	5.20E+01	2.25E-02	5.20E+01	2.36E-02
5.10E+01	2.70E-02	5.10E+01	2.45E-02	5.10E+01	2.31E-02
5.00E+01	2.73E-02	5.00E+01	2.63E-02	5.00E+01	2.27E-02
4.98E+01	2.83E-02	4.98E+01	2.70E-02	4.98E+01	2.25E-02
4.95E+01	2.87E-02	4.95E+01	2.73E-02	4.95E+01	2.29E-02
4.93E+01	2.85E-02	4.93E+01	2.76E-02	4.93E+01	2.32E-02
4.90E+01	3.07E-02	4.90E+01	2.83E-02	4.90E+01	2.37E-02
4.80E+01	4.00E-02	4.80E+01	3.10E-02	4.80E+01	2.52E-02
4.70E+01	3.98E-02	4.70E+01	3.24E-02	4.70E+01	2.69E-02
4.68E+01	4.09E-02	4.68E+01	3.29E-02	4.68E+01	2.70E-02
4.65E+01	4.23E-02	4.65E+01	3.33E-02	4.65E+01	2.78E-02
4.63E+01	4.29E-02	4.63E+01	3.35E-02	4.63E+01	2.78E-02
4.60E+01	4.59E-02	4.60E+01	3.43E-02	4.60E+01	2.87E-02
4.50E+01	5.92E-02	4.50E+01	3.89E-02	4.50E+01	3.01E-02
4.40E+01	5.96E-02	4.40E+01	4.16E-02	4.40E+01	3.24E-02
4.38E+01	6.09E-02	4.38E+01	4.23E-02	4.38E+01	3.21E-02
4.35E+01	6.27E-02	4.35E+01	4.38E-02	4.35E+01	3.33E-02
4.33E+01	6.34E-02	4.33E+01	4.41E-02	4.33E+01	3.30E-02
4.30E+01	6.64E-02	4.30E+01	4.59E-02	4.30E+01	3.43E-02
4.20E+01	8.20E-02	4.20E+01	5.18E-02	4.20E+01	3.55E-02
4.10E+01	8.22E-02	4.10E+01	5.53E-02	4.10E+01	3.80E-02
4.08E+01	8.27E-02	4.08E+01	5.56E-02	4.08E+01	3.74E-02

4.05E+01	8.63E-02	4.05E+01	5.78E-02	4.05E+01	3.89E-02
4.03E+01	8.55E-02	4.03E+01	5.75E-02	4.03E+01	3.81E-02
4.00E+01	9.03E-02	4.00E+01	6.01E-02	4.00E+01	3.98E-02
3.90E+01	1.05E-01	3.90E+01	6.51E-02	3.90E+01	4.02E-02
3.80E+01	1.05E-01	3.80E+01	6.84E-02	3.80E+01	4.26E-02
3.78E+01	1.05E-01	3.78E+01	6.73E-02	3.78E+01	4.13E-02
3.75E+01	1.07E-01	3.75E+01	6.99E-02	3.75E+01	4.31E-02
3.73E+01	1.08E-01	3.73E+01	6.87E-02	3.73E+01	4.17E-02
3.70E+01	1.10E-01	3.70E+01	7.08E-02	3.70E+01	4.35E-02
3.65E+01	1.13E-01	3.65E+01	7.07E-02	3.65E+01	4.23E-02
3.60E+01	1.14E-01	3.60E+01	7.16E-02	3.60E+01	4.39E-02
3.49E+01	1.10E-01	3.49E+01	7.14E-02	3.49E+01	4.25E-02
3.37E+01	9.96E-02	3.37E+01	7.04E-02	3.37E+01	4.37E-02
3.26E+01	9.07E-02	3.26E+01	6.46E-02	3.26E+01	4.08E-02
3.14E+01	8.24E-02	3.14E+01	6.29E-02	3.14E+01	4.13E-02
3.03E+01	7.29E-02	3.03E+01	5.63E-02	3.03E+01	3.77E-02
2.91E+01	6.40E-02	2.91E+01	5.27E-02	2.91E+01	3.72E-02
2.80E+01	5.58E-02	2.80E+01	4.57E-02	2.80E+01	3.33E-02
2.69E+01	4.85E-02	2.69E+01	4.19E-02	2.69E+01	3.21E-02
2.57E+01	4.14E-02	2.57E+01	3.51E-02	2.57E+01	2.79E-02
2.46E+01	3.47E-02	2.46E+01	3.10E-02	2.46E+01	2.61E-02
2.34E+01	2.84E-02	2.34E+01	2.51E-02	2.34E+01	2.19E-02
2.23E+01	2.28E-02	2.23E+01	2.11E-02	2.23E+01	1.97E-02
2.11E+01	1.76E-02	2.11E+01	1.62E-02	2.11E+01	1.56E-02
2.00E+01	1.25E-02	2.00E+01	1.22E-02	2.00E+01	1.30E-02
1.95E+01	1.06E-02	1.95E+01	1.03E-02	1.95E+01	1.11E-02
1.90E+01	9.23E-03	1.90E+01	8.76E-03	1.90E+01	1.00E-02

Case 3-3					
Flexible Wall		Medium Wall		Stiff Wall	
Depth (m)	Wall Movement (m)	Depth (m)	Wall Movement (m)	Depth (m)	Wall Movement (m)
5.20E+01	2.33E-02	5.20E+01	2.20E-02	5.20E+01	-2.16E-05
5.10E+01	2.72E-02	5.10E+01	2.39E-02	5.10E+01	8.44E-04

5.00E+01	2.76E-02	5.00E+01	2.56E-02	5.00E+01	2.65E-03
4.98E+01	2.85E-02	4.98E+01	2.62E-02	4.98E+01	3.09E-03
4.95E+01	2.89E-02	4.95E+01	2.66E-02	4.95E+01	3.69E-03
4.93E+01	2.87E-02	4.93E+01	2.69E-02	4.93E+01	4.25E-03
4.90E+01	3.09E-02	4.90E+01	2.76E-02	4.90E+01	4.86E-03
4.80E+01	3.98E-02	4.80E+01	3.04E-02	4.80E+01	7.32E-03
4.70E+01	3.97E-02	4.70E+01	3.21E-02	4.70E+01	9.64E-03
4.68E+01	4.07E-02	4.68E+01	3.28E-02	4.68E+01	1.02E-02
4.65E+01	4.21E-02	4.65E+01	3.34E-02	4.65E+01	1.08E-02
4.63E+01	4.25E-02	4.63E+01	3.38E-02	4.63E+01	1.14E-02
4.60E+01	4.54E-02	4.60E+01	3.47E-02	4.60E+01	1.20E-02
4.50E+01	5.79E-02	4.50E+01	3.84E-02	4.50E+01	1.43E-02
4.40E+01	5.81E-02	4.40E+01	4.04E-02	4.40E+01	1.64E-02
4.38E+01	5.93E-02	4.38E+01	4.11E-02	4.38E+01	1.69E-02
4.35E+01	6.11E-02	4.35E+01	4.19E-02	4.35E+01	1.74E-02
4.33E+01	6.18E-02	4.33E+01	4.24E-02	4.33E+01	1.78E-02
4.30E+01	6.48E-02	4.30E+01	4.34E-02	4.30E+01	1.83E-02
4.20E+01	7.76E-02	4.20E+01	4.76E-02	4.20E+01	2.02E-02
4.10E+01	7.80E-02	4.10E+01	4.91E-02	4.10E+01	2.17E-02
4.08E+01	7.92E-02	4.08E+01	4.98E-02	4.08E+01	2.20E-02
4.05E+01	8.09E-02	4.05E+01	5.04E-02	4.05E+01	2.24E-02
4.03E+01	8.14E-02	4.03E+01	5.06E-02	4.03E+01	2.27E-02
4.00E+01	8.43E-02	4.00E+01	5.14E-02	4.00E+01	2.30E-02
3.90E+01	9.64E-02	3.90E+01	5.44E-02	3.90E+01	2.42E-02
3.80E+01	9.35E-02	3.80E+01	5.35E-02	3.80E+01	2.47E-02
3.78E+01	9.35E-02	3.78E+01	5.34E-02	3.78E+01	2.48E-02
3.75E+01	9.46E-02	3.75E+01	5.35E-02	3.75E+01	2.50E-02
3.73E+01	9.48E-02	3.73E+01	5.34E-02	3.73E+01	2.51E-02
3.70E+01	9.68E-02	3.70E+01	5.34E-02	3.70E+01	2.52E-02
3.65E+01	9.80E-02	3.65E+01	5.32E-02	3.65E+01	2.54E-02
3.60E+01	9.68E-02	3.60E+01	5.28E-02	3.60E+01	2.55E-02
3.49E+01	9.08E-02	3.49E+01	5.07E-02	3.49E+01	2.55E-02
3.37E+01	7.66E-02	3.37E+01	4.58E-02	3.37E+01	2.50E-02
3.26E+01	6.48E-02	3.26E+01	4.14E-02	3.26E+01	2.44E-02
3.14E+01	5.57E-02	3.14E+01	3.74E-02	3.14E+01	2.37E-02

3.03E+01	4.70E-02	3.03E+01	3.31E-02	3.03E+01	2.28E-02
2.91E+01	3.94E-02	2.91E+01	2.90E-02	2.91E+01	2.18E-02
2.80E+01	3.27E-02	2.80E+01	2.53E-02	2.80E+01	2.07E-02
2.69E+01	2.74E-02	2.69E+01	2.21E-02	2.69E+01	1.95E-02
2.57E+01	2.37E-02	2.57E+01	1.93E-02	2.57E+01	1.81E-02
2.46E+01	2.05E-02	2.46E+01	1.67E-02	2.46E+01	1.67E-02
2.34E+01	1.75E-02	2.34E+01	1.43E-02	2.34E+01	1.53E-02
2.23E+01	1.45E-02	2.23E+01	1.20E-02	2.23E+01	1.37E-02
2.11E+01	1.16E-02	2.11E+01	9.90E-03	2.11E+01	1.21E-02
2.00E+01	8.66E-03	2.00E+01	7.83E-03	2.00E+01	1.04E-02
1.95E+01	6.73E-03	1.95E+01	6.47E-03	1.95E+01	8.20E-03
1.90E+01	6.73E-03	1.90E+01	6.22E-03	1.90E+01	9.02E-03

Appendix F: Calculation of Strut Forces from Distributed Propped Load Method

H = 16m

γ = 16kN/m^3

s = 4m

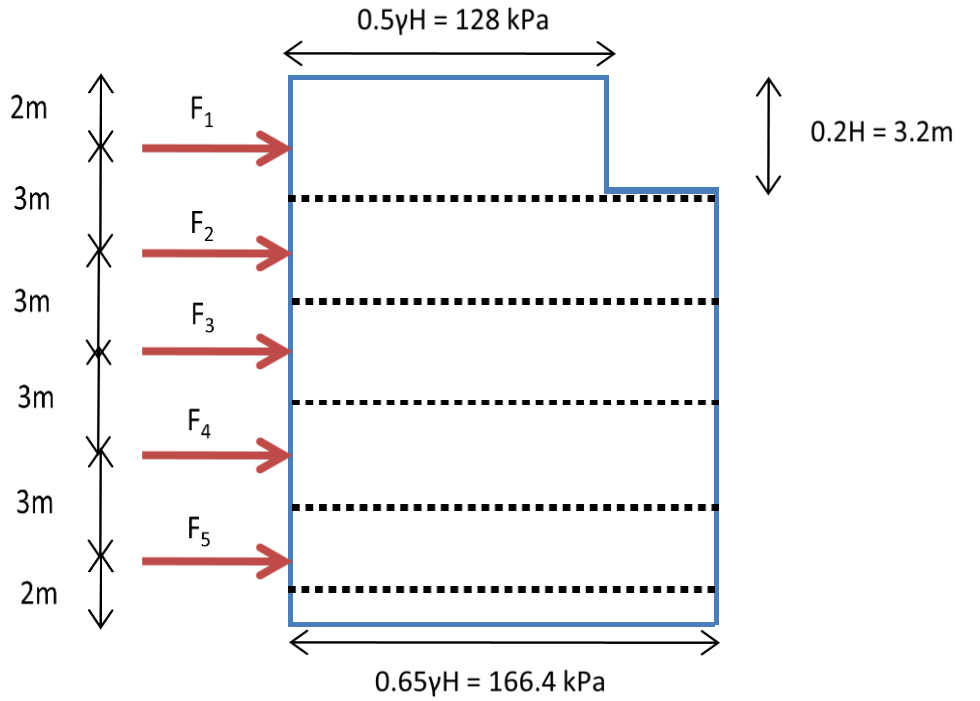

Tributary Area Method

F_1 = [3.2×128 + (2+1.5-3.2)×166.4] × 4 = 1838.08 kN

F_2 = [(1.5+1.5)×166.4] × 4 = 1996.8 kN

F_3 = [(1.5+1.5)×166.4] × 4 = 1996.8 kN

F_4 = [(1.5+1.5)×166.4] × 4 = 1996.8 kN

F_5 = [(1.5+1)×166.4] × 4 = 1664 kN

Appendix G: Extracted Strut Forces of Excavation

Flexible wall								
Strut	Wall depth (m)	Strut forces (kN)						
		2D	Case 1	Case 2-1	Case 2-2	Case 3-1	Case 3-2	Case 3-3
S1	50	-616.4	-796.46	-688.07	-652.23	-719.31	-691.71	-684.26
S2	47	-1357.2	-1400	-1230	-1170	-1430	-1200	-1170
S3	44	-1837.2	-1640	-1320	-1220	-1570	-1370	-1290
S4	41	-1941.2	-1720	-1470	-1230	-1670	-1250	-1490
S5	38	-815.2	-747.6	-578.76	-491.54	-704.83	-339.95	-654.56

Medium Wall								
Strut	Wall depth (m)	Strut forces (kN)						
		2D	Case 1	Case 2-1	Case 2-2	Case 3-1	Case 3-2	Case 3-3
S1	35	-821.2	-853.04	-814.7	-794.5	-853.41	-852.01	-803.35
S2	32	-2026.4	-1790	-1580	-1460	-1780	-1410	-1400
S3	29	-2364	-2210	-1610	-1350	-2100	-1250	-1440
S4	26	-2492.4	-2310	-1890	-1360	-2220	-785.09	-1520
S5	23	-870	-780.88	-668.88	-554.18	-748.1	-128.47	-573.79

Stiff Wall								
Strut	Wall depth (m)	Strut forces (kN)						
		2D	Case 1	Case 2-1	Case 2-2	Case 3-1	Case 3-2	Case 3-3
S1	20	-1103.2	-1090	-1020	-994.99	-1100	-983.26	-1800
S2	17	-2418.4	-2270	-1780	-1480	-2150	-912.36	-792.88
S3	14	-2994.4	-3080	-2260	-1720	-2890	-665.71	-806.57
S4	11	-2103.2	-2500	-2080	-1580	-2150	-310.81	-644.2
S5	8	-1456	-702.77	-596.04	-494.8	-690.73	-41.28	-206.46